This is to certify that the

thesis entitled

THE POWER DISK PERFORMANCE EVALUATION

- DISK TRAJECTORY SIMULATION AND SIDE FORCE STUDY

presented by

HAIBO GUO

has been accepted towards fulfillment
of the requirements for

M. S. degree in AGR. ENG.

Thomas H Burkhardt
Major professor

Date 12/23/87

THE POWER DISK PERFORMANCE EVALUATION
– DISK TRAJECTORY SIMULATION AND SIDE FORCE STUDY

By

Haibo Guo

A THESIS

Submitted to
Michigan State University
in partial fulfillment of the requirements
for the degree of

MASTER OF SCIENCE

in

Agricultural Engineering

Department of Agricultural Engineering

1987

THE POWER DISK PERFORMANCE EVALUATION
– DISK TRAJECTORY SIMULATION AND SIDE FORCE STUDY

By

Haibo Guo

APPROVED BY:

MAJOR PROFESSOR: Thomas H Burkhardt 12/22/1987
Thomas H Burkhardt

DEPARTMENT CHAIRMAN: Donald M Edwards 12/22/1987
Donald M Edwards

ABSTRACT

THE POWER DISK PERFORMANCE EVALUATION
-- DISK TRAJECTORY SIMULATION AND SIDE FORCE STUDY

By

Haibo Guo

Primary tillage is a basic requirement in agricultural production. The power disk, as an alternative tillage implement, needs to be evaluated both theoretically and experimentally. The computer simulation method was employed to simulate the disk blade trajectories and a predeveloped data acquisition system was used to collect field test data. The side force, rear furrow wheel vertical force, ground speed, tillage depth and soil moisture content were measured.

The theoretical simulation results showed that the power disk worked in the slipping condition. Given the gang angles of 26° to 34° and the ground speeds of 2 to 8 km/hr, the disk slippages were between 52.79% and 89.11%. The absolute velocity of the disk blade, with the amplitudes between 1.098V and 2.835V, was always greater than the implement ground speed (V).

The experimental and statistical analyses indicated that there was a linear relationship between the side force and the ground speed. The simple linear model could be used to express this relationship. The rear vertical force increased as the ground speed increased. The gang angle had little effect on either the side force or the rear vertical force.

This work is dedicated to the memory of my father.

I miss him very much.

ACKNOWLEDGEMENTS

The author wishes to sincerely thank Dr. Thomas H Burkhardt for serving as his major professor and for helping him to develop the skill and confidence to meet the challenge of the future.

Special thanks go to Dr. Robert H Wilkinson, committee member, for his timely and critical advice throughout the research and Dr. Larry J Segerlind, committee member, for his guidance during the author's graduate study in the department.

The author extends his appreciation to Suzanne NeSmith for her help in the preperation of this text, Milton Mah for his assistance during the research and Kiyohide Aiba for his cooperation of the study.

Many thanks are due to the faculty, staff and graduate students of the Department of Agricultural Engineering for their help of the graduate study, Albert H Case center for the use of their computer facility and Toyosha Company, Ltd, Japan for their financial support of this study.

The author wishes to express his gratitute to the people and the government of the People's Republic of China for the opportunity and the support to pursue further studies.

Finally, thanks to his mother and other family members for their love and their great encouragement.

TABLE OF CONTENTS

LIST OF TABLES

LIST OF FIGURES

FIGURE PAGE

CHAPTER 1

INTRODUCTION

Machinery plays an important role in the agricultural production system. Among all implements used in tillage, planting, harvesting and transportation, tillage machines require the highest tractor drawbar power. It is well known that the tractor engine can do more than pull. It has a relatively low efficiency of 60-65% considering the power transmission between tires and soil (Soehne, 1963). A power rotary tiller, as an alternative tillage implement, transfers the engine power directly through the PTO shaft and an insignificant transmission loss occurs.

The power driven rotary tiller is capable of performing the tillage work because of (Soehne, 1963):

1. the mixing of organic matter and manure into the soil;
2. the preparation of a seedbed for vegetables;
3. the breaking of meadows; and
4. spring tillage on heavy soils to avoid many after-tillage operations.

Nartov (1966) said that disk implements easily overcame different types of obstacles in the forms of stumps, roots, stones and fallen timber residuals. The disk rarely clogged with grass and sod-bush plants, and soil did not stick to it.

Three aspects of tillage operations are of increasing importance on today's farms (Young, 1976). They are the need for increasing farmer productivity, the need for better utilization of energy and the increasing importance of environmental aspects of tillage operations. The power disk has potential to meet the needs of increasing the productivity in terms of reducing the number of tillage operations required and for better utilizing energy in terms of reducing the energy loss in direct transmissions.

Even though the power disk has many advantages, it has not been widely marketed (Abernathy, 1976). The main problem is that its working quality can not be always guaranteed. "The disk poorly inverts the slice" (Nartov, 1966). Therefore the quantitive performance evaluation is necessary. The best disk working parameters need to be determined. Whether it will be economically feasible must be figured out.

A joint research effort with Mr. Kiyohide Aiba was initiated. The ultimate goal of this joint research was to evaluate the power disk field performance, investigate the power requirement and study the side force on the implement. The author focused on the side force and Mr. Aiba emphasized the power requirement. The hitch forces, PTO torque, ground speed, engine speed and side force were measured with the aid of an in-field microcomputer-based data acquisition system.

CHAPTER 2

LITERATURE REVIEW

Many researchers have contributed to the power disk studies. This chapter provides a review of the more pertinent literature which covers the past efforts on the experimental and theoretical works.

2.1 SIDE FORCE

The side force (lateral force) has been a special problem in disk tiller studies. A considerable amount of attention was given to the draft forces although the side force was measured and discussed. Taylor (1967) developed the trailed rig for measuring a single plow disk forces in three dimensions. The instrumented disk was carried on an L-shaped subframe which was connected to the main frame by six links with each link had a strain gauge on it. Six force components, depth, distance travelled and time elapsed were measured in an instrument van which followed the rig and was connected to it by cable. Using this instrument, he designed the factorial experiment to study the forces with four variables of gang angle (α), tilt angle (β), ground speed (V) and furrow width (W) on two different kinds of soil. The major effects on the side force were due to β, V and W. They formed a quadratic relationship between the side force and the disk angle. Some linear inteaction effects, such as Wβ, WV and Vα on the side force were shown.

Harrison (1977) conducted split-plot experiment tests. He concluded that the main effects of disk angle, depth and soil type were significant for the draft, vertical and lateral reactions. The main effect of speed was significant only for the lateral reaction. The first order interaction of the soil type-depth was significant for draft and lateral reaction. The difference in the draft and the lateral reaction for the soil types was large. The increase of the tillage depth increased the draft and the lateral reaction.

At the National Tillage Machinery Laboratory, Gill (1980-1982) conducted a series of investigations on various parameter effects on disk forces. He used the dynamometer car to control the disk in order to change one variable continuously while all other variables were held constant. The data acquisition system was employed to measure and record the forces, forward speed, rotational velocity and disk angle. His results showed that there were nonlinear effects of width of cut, depth, disk curvature and gang angle on the side forces. The ground speed was linear with the side force.

A dynamometric trolly was constructed by Nartov (1985) to determine the reactive forces acting on the disk in a soil bin. It was a carriage with a moving part and a mechanism to control the carriage. The suspended disk blade and base carriage were connected by six force transducers. Each of the transducers sensed a force particularly in the longitudinal, the transverse or the vertical direction. The disk force in any direction was calculated from the sum of the sensed forces in the same direction. The data suggested that the maximum value of the lateral force occured at the disk angle between 30 degrees and 35 degrees. A sharp reduction in the lateral force at small disk angles took place due to the counter pressure exerted by the furrow wall on the rear side of the disk. At large disk angles, the force was reduced as a result of decrease in the transverse component of normal pressure of the slice on the disk. Also with increases in the radius of curvature and a reduction in disk diameter, the lateral force increased marginally.

2.2 MOTION TRAJECTORIES OF THE CUTTER

The power driven rotary disk cutter was described as a tool with the positive drive by Klenin et al (1985). It performed complex motions. The cutter rotated about its own axis due to the positive drive from the PTO shaft or the axle of the driving wheels of the machine while it had the translatory motion with the machine. The simple generalized cutter rotated in the plane coinciding with the direction of implement travel and its trajectory equations for a point on the cutter were

$$X = R\left(\frac{\phi}{\lambda} + \cos\phi\right) \tag{2.2.1}$$

$$Y = R\sin\phi \tag{2.2.2}$$

where

X -- displacement of a point in the X axis;

Y -- displacement of a point in the Y axis;

R -- radial distance from the rotation axis;

ϕ -- rotating angle;

$$\phi = \omega t \tag{2.2.3}$$

ω -- angular velocity;

t -- time interval;

λ -- ratio of tangential velocity and machine ground speed, that is

$$\lambda = \frac{u}{V} \tag{2.2.4}$$

u -- cutter tangential velocity;

V -- implement travel speed.

The trajectory was a cycloid. The shape of the cycloid was governed by the ratio λ. If $\lambda<1$, the cycloid did not have loops, that is, a shortened cycloid. If $\lambda>1$, the trajectory was represented by an elongated cycloid.

Nartov (1985) developed a set of equations to describe the unpowered disk blade movement in three dimensions. These equations are given as Equations 5.2.7, 5.2.8 and 5.2.9 in Chapter 5. When the equations were differentiated with respect to t, the velocity of motion for a point on the spherical disk surface in three axis directions was determined. Nartov gave the expressions as

$$V_x = V - p\theta(\sin\beta\sin\alpha\sin\theta + \cos\alpha\cos\theta) \tag{2.2.5}$$

$$V_y = p\theta(\sin\alpha\cos\theta - \sin\beta\cos\alpha\sin\theta) \tag{2.2.6}$$

$$V_z = p\theta\cos\beta\sin\theta \tag{2.2.7}$$

where

V_x, V_y and V_z -- velocity components in X, Y and Z directions;

V -- assembly ground speed;

p -- radial distance from the rotation axis;

θ -- rotating angle;

α -- disk gang angle;

β -- tilt angle.

The absolute velocity was the sum of the three velocity vectors in X, Y and Z directions. The absolute velocity was studied by Nartov. He concluded that the absolute velocity was minimum at the lowest position of the disk blade. The maximum velocity occured at the top position with the amplitude of 1.95V. With an increase in disk angle and with a decrease in the radius, the velocity amplitude decreased.

CHAPTER 3

OBJECTIVES

The side force is one of the important factors that affect the performance of a power disk. The research on the single disk using specially developed equipment did not show the side force problem that occurred during real operations. A full study of the side force on the implement helped to find good working parameters for the implement under various ground speeds and gang angles.

In today's technology, a computer is a powerful tool for calculation, modeling and simulation. The dynamic behavior of a real motion or process can be approximately simulated. This technique was employed to study the disk moving trajectories and the velocities.

Specifically the objectives of this research were to study the relationship of the side force, ground speed and gang angle, and to simulate the disk motion trajectories and velocity distributions. The following parameters were measured:

1. side force;
2. vertical force on the rear wheel;
3. ground speed;

4. engine speed;

5. tractor front and rear wheel rotation speeds;

6. tillage depth and width; and

7. soil data (moisture and cone index).

CHAPTER 4

IMPLEMENT, INSTRUMENTATION AND EXPERIMENT

4.1 IMPLEMENT

The implement used in this research was a PTO driven disk tiller, called a power disk. Power is transferred from the PTO shaft to the disk blades through a centrally located bevel gear box, followed by a roller chain drive. The disk blades have a spherical surface. The lower part of the disk blade cuts the soil, deforms it and then throws the soil in a particular way.

Based on a previous study (Tembo, 1986), the light model F-800 power disk had some penetration problems. Therefore, the heavy model F-2806 was used in this research. Specifications of the F-2806 disk are listed in Appendix A.

4.2 INSTRUMENTATION

A predeveloped computer on-board data acquisition system (Aiba, 1987; Tembo, 1986) was used, and the sensors on the rear furrow wheel shaft of the power disk for measuring side and rear vertical forces (see Chapter 6 for details) were added in this research.

All instruments were powered from a 12V DC-120V AC, 60HZ, 500 watt sinusoidal voltage converter, inputted by a 12V DC battery. Force sensors were strain gauges with four arm bridges. A commercially available Dickey-john Tractor Performance Monitor II (DjTPMII) was employed to measure the engine speed, ground speed and tractor front and rear wheel rotation speeds. A torquemeter between the PTO shaft and the implement was used to measure the torque in the PTO shaft.

Once the transducer sensed a signal, it was amplified and sent to an analog-to-digital converter. A computer (Apple IIe) collected all the digits in its memory first and then saved them on a floppy disk after one set of data was collected. As shown in Figure 4.2.1, 12 channels were used. Six hundred data points were collected on each channel at a frequency of 10 data points per second.

4.3 EXPERIMENT

The experiment was conducted in the field to measure draft forces, vertical forces, side forces, PTO torque and rpm, ground speed and tractor front and rear wheel rotation speeds in November, 1986 and September and October, 1987.

4.3.1 EXPERIMENT DESIGN

There were two factors that could be varied on the tractor implement assembly: gang angle and ground speed. The treatments had five gang angle (26, 28, 30, 32 and 34 degrees) and four ground speed (2, 4, 6 and 8 km/hr) combinations so that there would be a possibility of 20 field tests without replications. Unfortunately tests for some combinations of ground speeds and gang angles were not possible because of excessive side force. For the 32 degree gang angle at

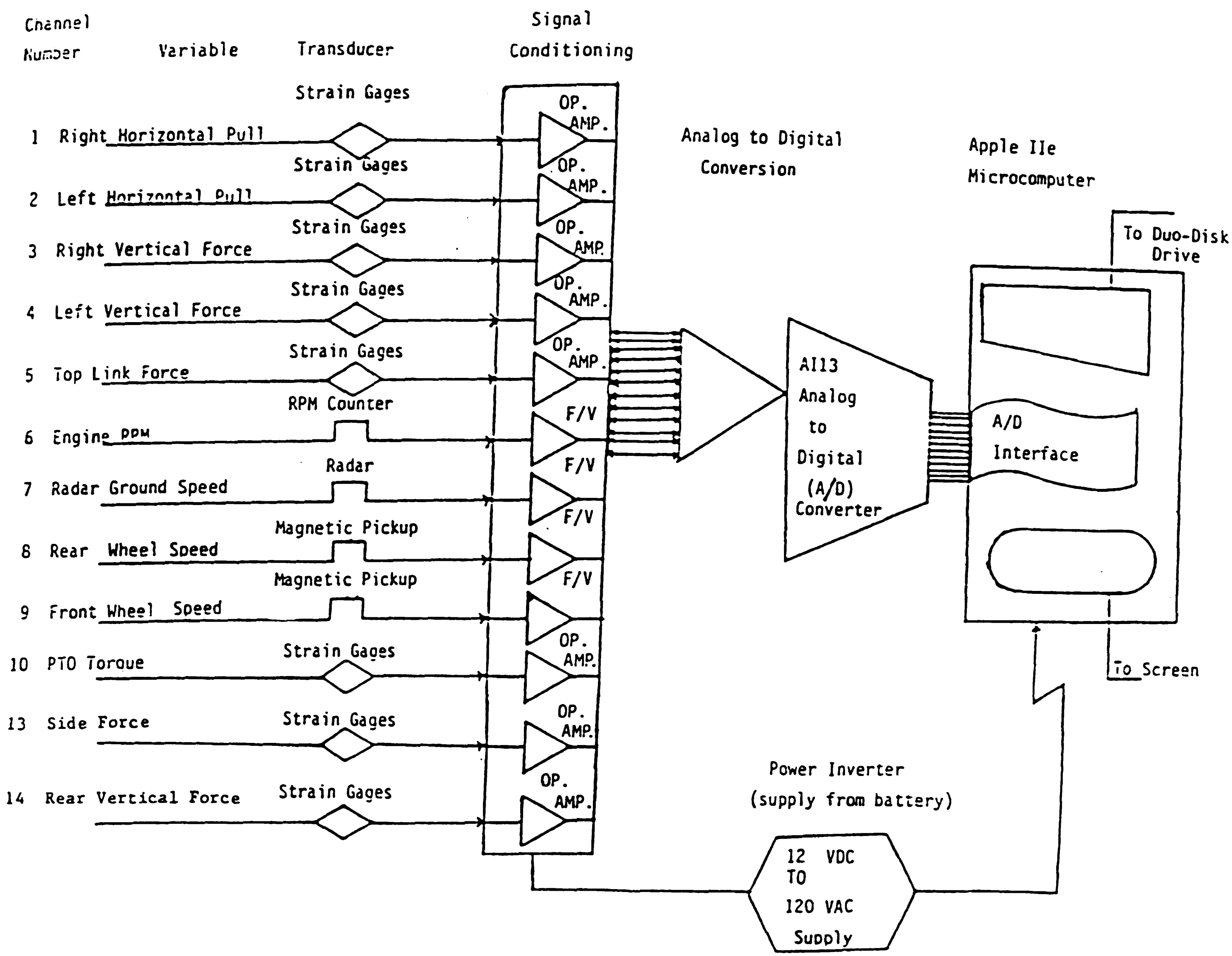

Figure 4.2.1 Instrumentation layout

Table 4.3.1 Layout of the field test

Test type	Gang angle degree	Ground speed kilometer per hour			
		2	4	6	8
Regular	26	x	x	x	x
	28	x	x	x	x
	30	x	x	x	x
	32	x	x	x	
	34	x	x		
Depth control	28		s d h		
	32		s d h		
Hard soil	28	x			
	32	x			
Unpowered	28	x		x	
	32	x		x	
Short top link	26	x	x	x	
	28		x		
	30	x x			
	32	x			

Notes: x--the test has been done for the maximum possible depth;
s--the test has been done for a shallow depth of 11 cm;
d--the test has been done for a deep depth of 17 cm;
h--the test has been done for the depth of 17 cm using hydraulic control.

8 km/hr and the 34 degree gang angle at 6 and 8 km/hr, the sway chain of the left lower link was very tight. This tensile force in the sway chain caused the side force reading in the rear wheel shaft to be erroneous. There was no tensile force in this chain for any of the other tests. Therefore seventeen field tests were conducted. These and the overall field test layout are represented in Table 4.3.1.

In a tillage operation, the depth control is usually expected to meet different crop requirements. Six tests were performed to investigate the variation of the drawbar power, PTO power and forces at two different depths (approximately 11 cm and 17 cm). Four out of six tests used the depth control wheel and the other two tests utilized the tractor hydraulic system to control the working depth.

Soil condition is another factor that affects the power disk behavior. Most of the tests were performed in the same field which had a soil type of sandy loam. Two tests were conducted on a heavy clay loam soil. It was assumed that the soil was homogeneous in the same site and the surface was flat, that is, there was no gradient effect.

When the powered and unpowered disk were compared, it was especially interesting to see the power requirements in both situations (Aiba, 1987). When the PTO shaft was disconnected from the power disk, the implement behaved like a regular unpowered disk. Four tests of this sort were conducted on 28 and 32 degree gang angles, each at 2 and 6 km/hr.

The first year, the field test was accomplished using a top link length of 715 mm. The next year 777 mm of the top link length was utilized and a deeper depth resulted. In 1987, seven tests were conducted in order to study the effect of the top link length on the working depth and other parameters using 715 mm of the top link.

4.3.2 EXPERIMENT PROCEDURE

Field tests were performed at the southwestern side of the Michigan State University campus farm. Soil was sandy loam with moisture content in the range of 10-20% (Appendix C).

During the field test, a front wheel assist tractor was used to pull the implement and the position control of the hydraulic system was employed to control the implement. The tractor operated on undisked soil (Figure 4.3.1), that is, no wheel was in the furrow. The implement hitching method with the tractor is shown in Figure 4.3.1. This hitching method avoided an excessively wide strip for the disk blade on the right side. Parameters measured were as follows:

1. engine speed;
2. ground speed;
3. tractor front and rear wheel rotation speeds;
4. lower link tension forces;
5. lower link vertical forces;
6. top link force;
7. side force;
8. vertical force on the rear wheel; and
9. PTO torque.

To collect one set of data, several steps were followed:

1. Established width measurement references (Figure 4.3.2). Three reference posts were set up before each test. The distance from the furrow wall to the posts was one meter, which was called "BEFORE" in Figure 4.3.2. The distances between posts in the direction of travel varied due to the different ground speeds, and as the ground speed increased, this distance should be longer.

2. Set the disk gang angle.

3. Activated the computer to collect data.

4. Selected the transmission gear speed for the appropriate ground speed.

5. Set the engine speed at aproximately 2000 rpm so that when the tractor was in operation, the engine rpm reduced to about 1900 rpm to give a correct PTO rpm of 540 and the expected ground speed. For higher ground speeds , the engine speed should be adjusted higher to maintain the engine working speed at around 1900 rpm.

6. When all settings described above were ready, disking was started. Once the tractor has worked at a stable ground speed after a short run, the RETURN key on the computer keyboard was pressed to start data collection. It took aproximately one minute to collect one set of data for 12 channels on the computer. The computer displayed menu options when it had finished the data collection. This set of data was saved onto a floppy disk by choosing the appropriate option. Steps 7, 8 and 9 were completed while the data file was being saved.

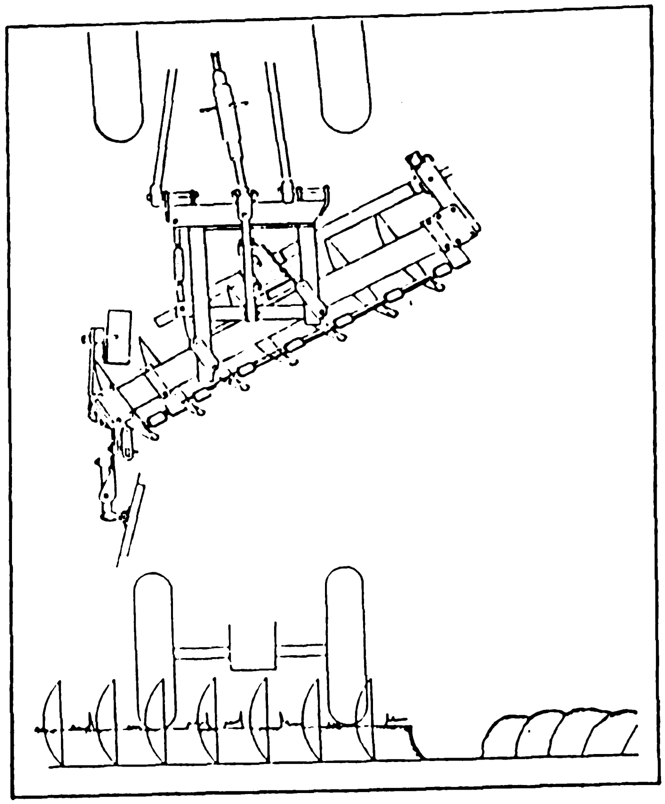

Figure 4.3.1 Hitching method

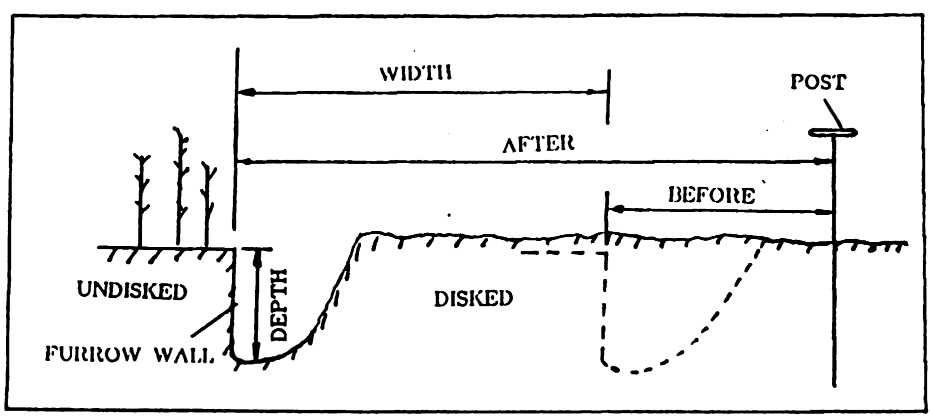

Figure 4.3.2 How to measure width and depth

7. Measured the width from the furrow wall to the posts again. This width was called "AFTER" in Figure 4.3.2. The actual working "WIDTH" was the "AFTER" minus the "BEFORE".

8. Measured the depth using a level and a tape.

9. Measured the hitch angles from the horizontal plane. These angles were used to compute the hitch draft and vertical forces.

Each time the data acquisition system was turned on, instruments were zeroed and the computer was initialized. After each half day field test, soil moisture samples, using cans and the soil sampler (Figure 4.3.3), were collcted. Also, the cone penetrometer was used to attain the soil cone index (Figure 4.3.4). The power disk field test record sheets are presented in Appendix B. They summarized what data needed to be recorded during the field test performance. The soil conditions that the field test was performed in are shown in Appendix C.

The field test data was recorded in the computer code. After field tests, work was needed to transfer the Apple II code to the Apple III code using a commercial program, SOSTRAN, and then to do calibration computation which utilized the program MASTER (Aiba, 1987) on the Apple III plus computer to get actual data.

Figure 4.3.3 Soil sampler and soil can

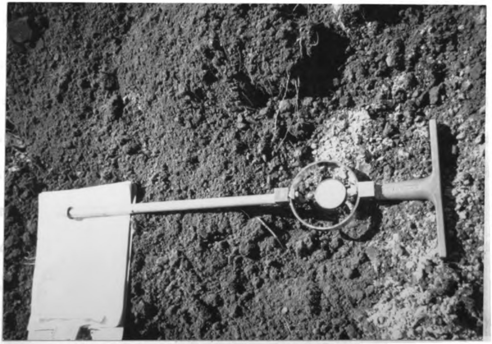

Figure 4.3.4 Cone penetrometer

CHAPTER 5

DYNAMIC SIMULATION OF DISK BLADE

The movement of each disk blade is in three dimensions. The computer simulation method was employed to study the disk motion characteristics. The simulation emphasized the disk with parameters of tilt angle (β) = 0°, disk diameter (D) = 710 mm, disk curvature (r) = 680 mm and PTO rotation speed (n) = 540 rpm. The disk blade was simulated on the circle with a diameter of 710 mm using various gang angles (α) and ground speeds (V).

5.1 REFERENCE SYSTEMS

Nartov (1985) defined three different coordinate systems to study the kinematics of a disk blade (Figure 5.1.1). The origin coincided with the center of the circular cutting edge of the disk. OX was in the direction of the assembly movement. OY was in the lateral direction, and OZ was in the vertical direction. By rotating OXYZ $+\alpha$ degrees about the Z axis, $OX_1Y_1Z_1$ resulted, and then rotating $OX_1Y_1Z_1$ $-\beta$ degrees about the X_1 axis, $OX_2Y_2Z_2$ resulted. OX_2 was in the horizontal direction of the disk motion as it rotated. OY_2 was along the disk axis and, OZ_2 was upward along the disk edge (Figure 5.1.2). Since the power

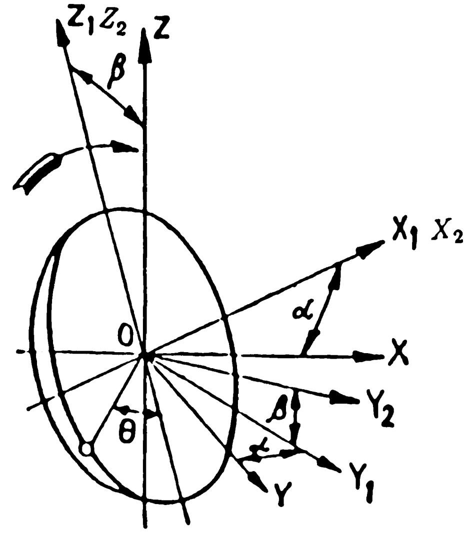

Figure 5.1.1 Reference coordinate systems

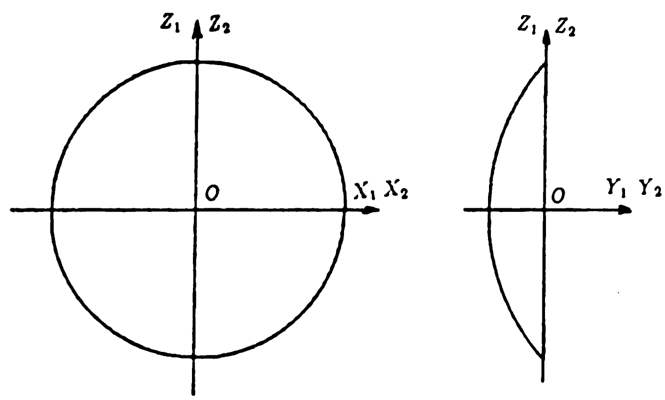

Figure 5.1.2 $OX_2Y_2Z_2/OX_1Y_1Z_1$ coordinate systems

disk used in the research had a tilt angle of $\beta = 0^0$, $OX_1Y_1Z_1$ was the same as $OX_2Y_2Z_2$.

The gang angle (α) was the angle between a horizontal diameter of the disk face and the travel direction of the assembly (Figure 5.1.3). As the disk rotated, it had a tendency to go in the X_1 direction which was the disk diameter direction. But the entire implement was hitched to the tractor. The disk movement from position I to position III could be divided into two parts (Figure 5.1.3). First, it moved to position II from position I along line I-II. Then it moved perpendicular to line I-II along line II-III to arrive at its final position III.

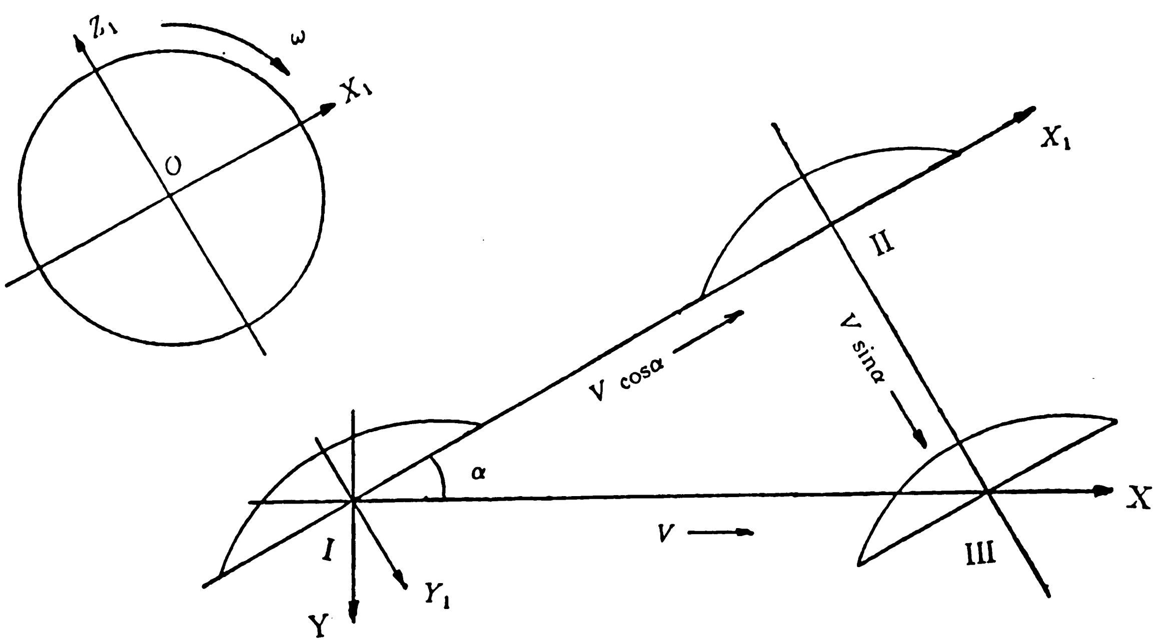

Figure 5.1.3 Disk movement

5.2 SLIPPING DISK

The movement of the disk blade was complicated. The blade rotated about its own axis while the implement moved along with the tractor at a certain speed. The blade movement was the combination of the angular rotation powered by the PTO shaft and the translation movement pulled by the tractor.

5.2.1 DEFINITION OF SLIPPAGE

In the $OX_1Y_1Z_1$ coordinate system along the line I-II in Figure 5.1.3, the disk had an angular velocity (ω) powered by the PTO drive and a forward translation speed (V_1) developed by the tractor pull in the X_1 direction

$$V_1 = V\cos\alpha \tag{5.2.1}$$

where

V -- assembly ground speed (km/hr);

α -- gang angle.

The angular velocity resulted in the maximum tangential peripheral velocity (V_1') on the disk edge

$$V_1' = R\omega \tag{5.2.2}$$

where

R -- disk radius (m);

ω -- disk angular velocity (rad/s).

The disk motion was a combination of the translatory motion and the rotary motion for any point on a disk edge. There were three possible combinations:

1. If the forward speed (V_1) was equal to the linear tangential speed (V_1'), that is,

$$V_1 = R\omega \tag{5.2.3}$$

the disk was pure rolling (Table 5.2.1);

2. If the forward speed was greater than the tangential speed,

$$V_1 > R\omega \tag{5.2.4}$$

the disk was skidding;

3. If the forward speed was less than the tangential speed,

$$V_1 < R\omega \tag{5.2.5}$$

the disk was slipping.

These could also be expressed as:

1. If the disk diameter (D) was equal to the disk rolling diameter (D'), the disk was pure rolling (Figure 5.2.1);

2. If the disk diameter (D) was less than the disk rolling diameter (D'), the disk was skidding. In this case, it was the same as that the disk was pure rolling with its rolling diameter (D');

3. If the disk diameter (D) was greater than the disk rolling diameter (D'), the disk was slipping. In this case, it was the same as that the disk was pure rolling with the rolling diameter (D').

Trajectories of a single point on the disk for these conditions are given in Figure 5.2.2.

conclution	condition	illustration
pure rolling	$V_1=R\omega$ or $D'=D$	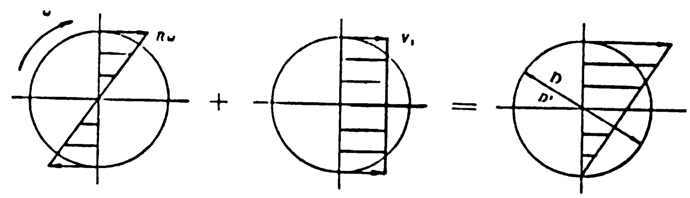
skidding	$V_1>R\omega$ or $D'>D$	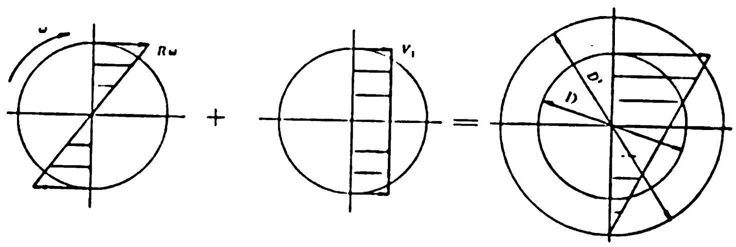
slipping	$V_1<R\omega$ or $D'<D$	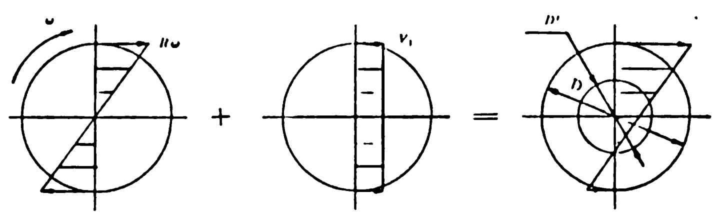

Figure 5.2.1 Disk working conditions

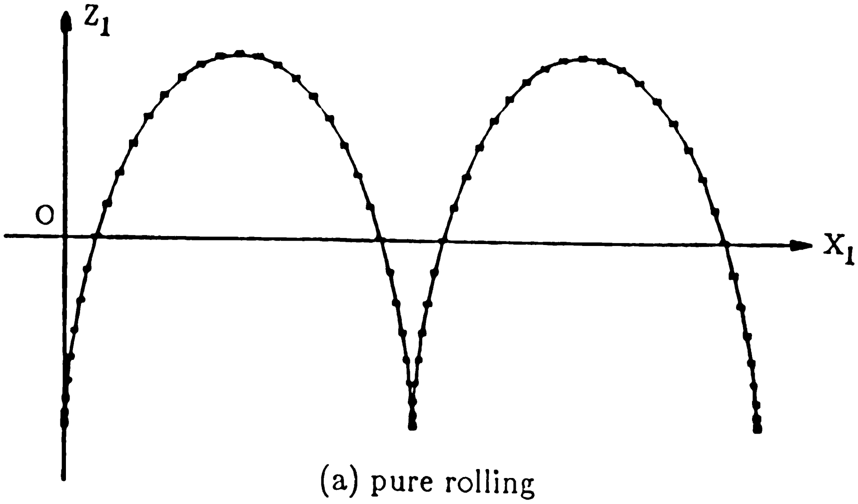

(a) pure rolling

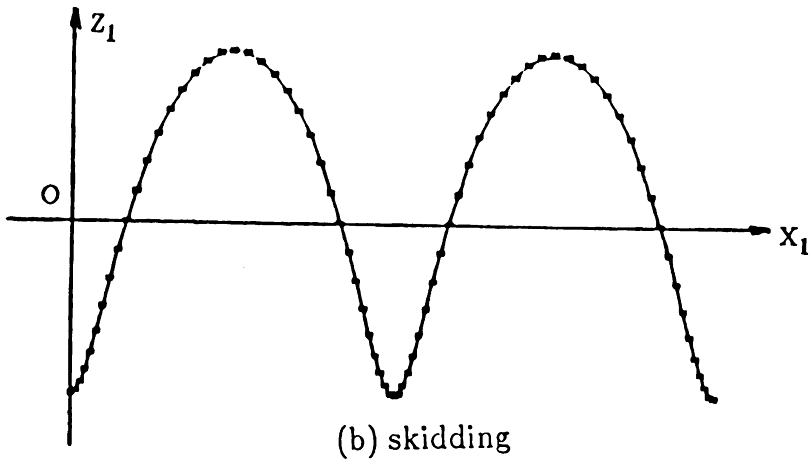

(b) skidding

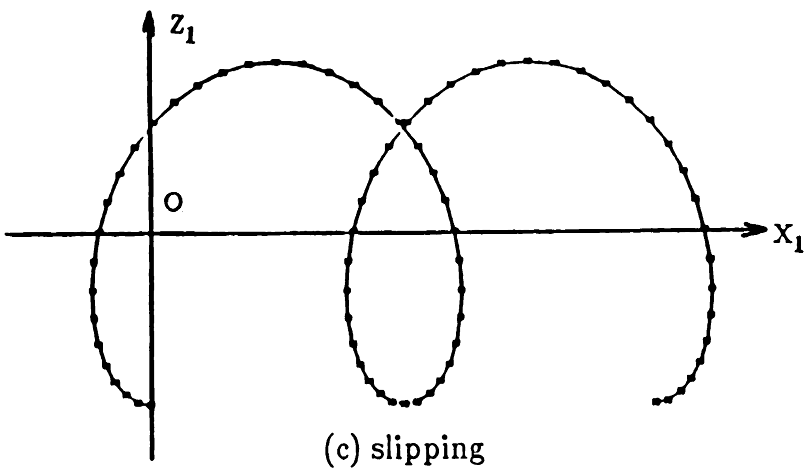

(c) slipping

Figure 5.2.2 Disk trajectories in three conditions

Given

PTO speed (n) = 540 rpm.

Gear ratio = $\frac{10}{29}\frac{11}{18}$ from PTO shaft to disk axis.

Disk diameter (D) = 710 mm.

Then the disk shaft speed is

$$n_1 = 540 \cdot \frac{10}{29} \cdot \frac{11}{18} = 113.8\ rpm$$

and the disk angular velocity is

$$\omega = \frac{2\pi n_1}{60} = \frac{2\pi 113.8}{60} = 11.917\ rad/s$$

The tangential speed of the disk cutting edge is

$$V_1' = R\omega = \frac{0.71}{2} \cdot 11.917 = 4.23\ m/s \tag{5.2.6}$$

On the other hand, Table 5.2.1 gives all possible V_1 values for our field tests in units of m/s. These ground speed were used not only in this research, but are reasonable for tillage operations. Therefore, it was true that Equation 5.2.5 was always satisfied when the tabular values were compared with 4.23 m/s, the result of Equation 5.2.6. Since this condition was met in all cases, the power disk worked in the slipping condition for all of our fielf tests.

Table 5.2.1 All possible speeds in X_1 direction

GROUND SPEED (km/hr)	2	4	6	8
GROUND SPEED (m/s)	0.5556	1.1111	1.6667	2.2222
GANG ANGLE (degree)	V1 SPEED (m/s)			
26	0.4993	0.9987	1.4980	1.9973
28	0.4905	0.9811	1.4716	1.9621
30	0.4811	0.9623	1.4434	1.9245
32	0.4711	0.9423	1.4134	1.8846
34	0.4606	0.9212	1.3817	1.8423

5.2.2 TRAJECTORIES OF MOTION OF DISK POINT

An interactive program, MOTION, written in FORTRAN (Appendix D), was used to simulate motion trajectories for a point on disk edge given different gang angles and ground speeds. Point coordinate equations for any point on a disk in the OXYZ system, given by Nartov (1985), were as follows

$$X = Vt + (\sqrt{r^2 - (D/2)^2} - \sqrt{r^2 - p^2})\cos\beta\sin\alpha + p\cos\theta\sin\beta\sin\alpha - p\sin\theta\cos\alpha \quad (5.2.7)$$

$$Y = (\sqrt{r^2 - (D/2)^2} - \sqrt{r^2 - p^2})\cos\beta\cos\alpha + p\cos\theta\sin\beta\cos\alpha + p\sin\theta\sin\alpha \quad (5.2.8)$$

$$Z = (\sqrt{r^2 - (D/2)^2} - \sqrt{r^2 - p^2})\sin\beta - p\cos\theta\cos\beta \quad (5.2.9)$$

where

t -- time (s);

r -- disk curvature (m);

p -- simulating point's radial distance form rotation axis (m);

θ -- simulating angle rotated from the bottom of the disk clockwise (rad) as shown in Figure 5.2.3; and

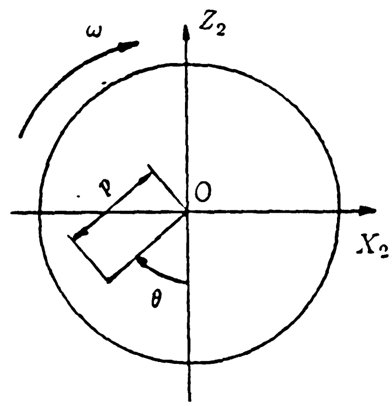

Figure 5.2.3 Illustration of p and θ

$$\theta=\omega t \tag{5.2.10}$$

The representation of the disk trajectories was in the $OX_1Y_1Z_1$ coordinate system (Figure 5.1.1 and Figure 5.1.3), where the disk was rotated in X_1 direction. The coordinate point equations in the $OX_1Y_1Z_1$ system were obtained by rotating XYZ $+\alpha$ degrees about the Z axis, that is, multiplying the vector [X Y Z] by the matrix operator (Rogers, 1976)

$$\begin{bmatrix} \cos\alpha & \sin\alpha & 0 \\ -\sin\alpha & \cos\alpha & 0 \\ 0 & 0 & 1 \end{bmatrix}$$

The resulting equations are

$$X_1 = Vt\cos\alpha - p\sin\theta \tag{5.2.11}$$

$$Y_1 = Vt\sin\alpha + (\sqrt{r^2-(D/2)^2} - \sqrt{r^2-p^2})\cos\beta + p\cos\theta\sin\beta \tag{5.2.12}$$

$$Z_1 = (\sqrt{r^2-(D/2)^2} - \sqrt{r^2-p^2})\sin\beta - p\cos\theta\cos\beta \tag{5.2.13}$$

Some simulation results are presented in Figure 5.2.4 through Figure 5.2.9 where the vertical movement is Z_1 of Equation 5.2.13 and the horizontal movement is X_1 of Equation 5.2.11. All of results are in the slipping condition. The more the disk point trajectory overlaps, the more the disk slips. The percentage of slippage varies with gang angle and ground speed. The percentage of slippage was defined (Zhou, 1980) as

$$SLIP\% = \frac{S_t - S}{S_t} 100 \tag{5.2.14}$$

where

S_t -- theoretical distance the disk moved;

S -- actual distance the disk moved.

As the disk was rotated one entire rotation in the X_1 direction and D = 0.71 m, the theoretical distance is

$$S_t = \pi D = \pi \cdot 0.71 = 2.23\ m \tag{5.2.15}$$

Since the disk implement was hitched to the tractor, it could move only along at the ground speed (V) of the tractor. The distance that the implement moved at speed (V) was the actual distance. This distance was simulated by using the program MOTION. Part of the simulation results are listed in Table 5.2.2. Disk trajectories with various slippages are shown in Figure 5.2.4 to Figure 5.2.9. In one rotation, the theoretical distance (S_t) was the same, and the actual distance (S) varied with gang angles and ground speeds. By using Equation 5.2.14, disk slippages were calculated. Table 5.2.2 showed that with a gang angle of 26° to 34° and ground speed of 2 to 8 km/hr, the disk slippages were varied from 52.79% to 89.11%.

As the slippage of the disk blade increased, the wear of the blade increased due to the friction between the soil and the disk blade. According to the simulations, a high ground speed resulted in low slippages which are benificial to the disk blade wear and also to the productivity. On the other hand, it was observed from the field tests that the disking quality was not good enough at the ground speed of 8 km/hr and the PTO speed of 540 rpm. The tillage quality was improved at lower ground speeds. Basically if the parameters of the ground speed, the gang angle setting and the PTO speed are considered, there will be a optimum combination among them to result in the less disk wear, good working quality and high productivity. This optimation needs more theoretical simulations and more field test evaluations.

Table 5.2.2 Slippage simulation results

Gang angle degree	Ground speed km/hr	Actual distance m	Theoretical distance m	Slip %
26	2	0.263283	2.2305308	88.20
	4	0.526567		76.39
	6	0.789850		64.59
	8	1.053133		52.79
30	2	0.253685	2.2305308	88.63
	4	0.507369		77.25
	6	0.761053		65.88
	8	1.014737		54.51
34	2	0.242850	2.2305308	89.11
	4	0.485699		78.22
	6	0.728548		67.34
	8	0.971398		56.45

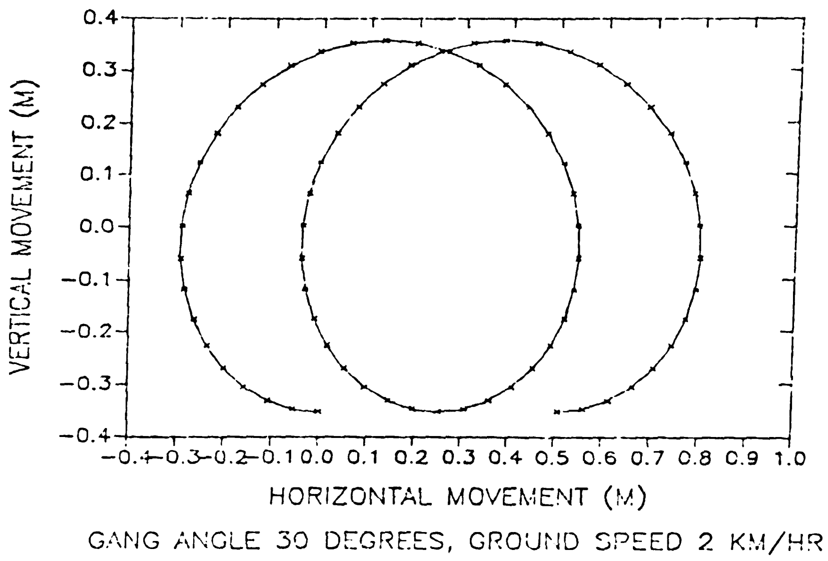

Figure 5.2.4 Disk trajectory with slippage of 88.63%

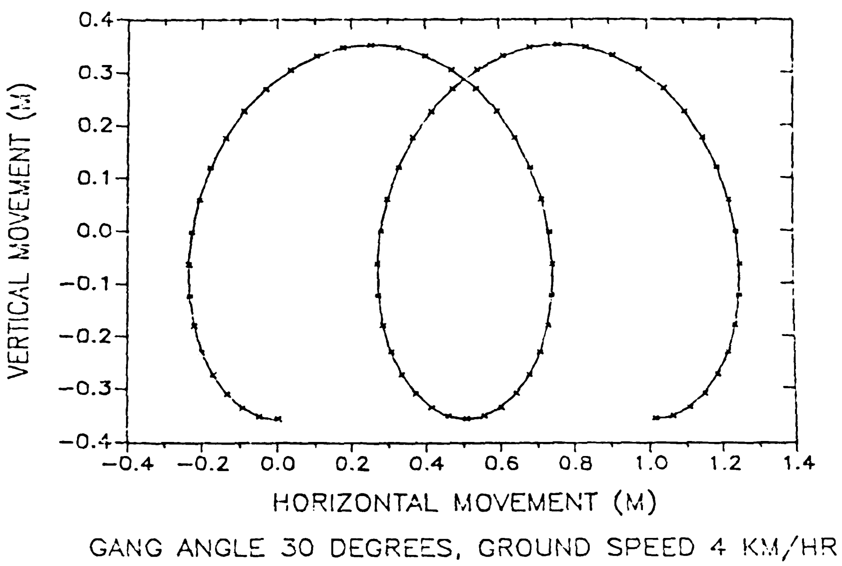

Figure 5.2.5 Dsik trajectory with slippage of 77.25%

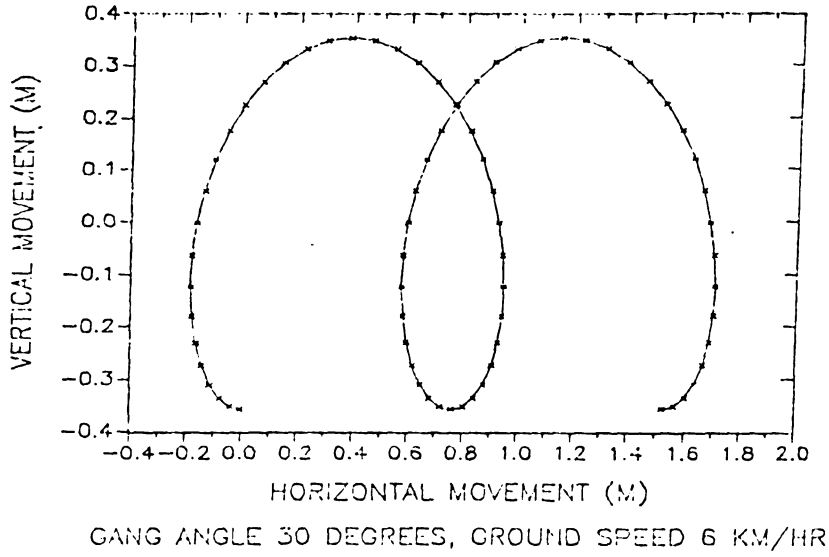

Figure 5.2.6 Disk trajectory with slippage of 65.88%

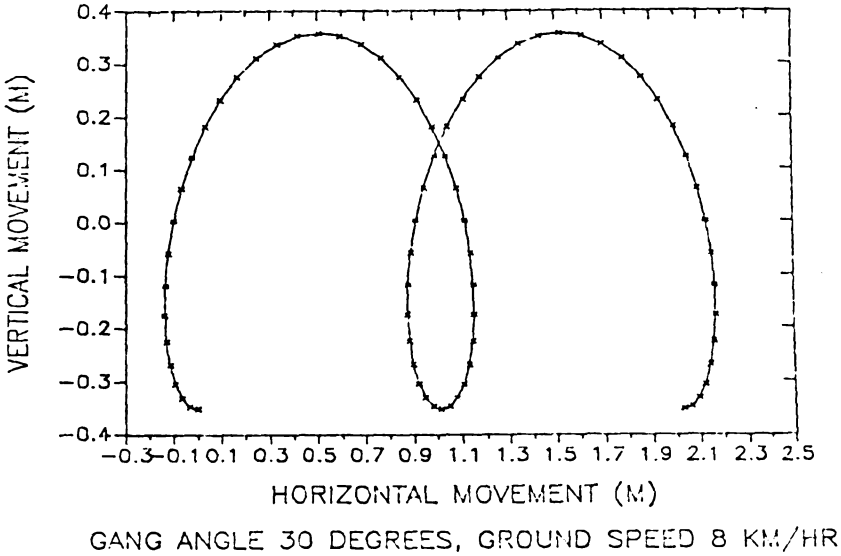

Figure 5.2.7 Disk trajectory with slippage of 54.51%

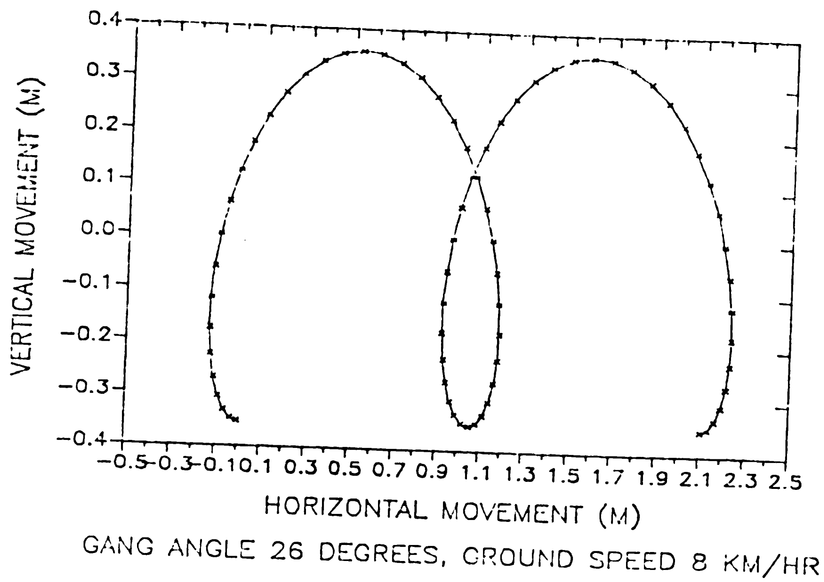

Figure 5.2.8 Disk trajectory with slippage of 52.79%

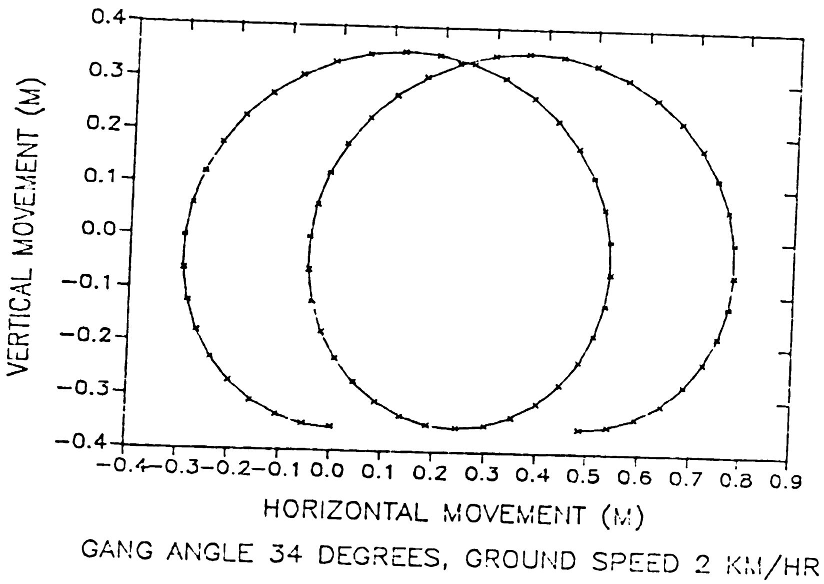

Figure 5.2.9 Disk trajectory with slippage of 89.11%

5.3 VELOCITY DISTRIBUTION SIMULATIONS

5.3.1 DERIVATION OF EQUATION

Any point on the rotating disk had an angular velocity (ω) and radius (p). Its linear tangential speed (V_t) was expresed as

$$V_t = p\,\omega \tag{5.3.1}$$

where

p -- radius of a disk point from the rotation axis (m);

ω -- disk angular velocity (rad/s).

By employing the reference systems described earlier, velocity components for a disk point in the $OX_2Y_2Z_2$ system (Figure 5.3.1) produced by ω were

$$V_{x2} = -p\,\omega\cos\theta \tag{5.3.2}$$

$$V_{y2} = 0 \tag{5.3.3}$$

$$V_{z2} = p\,\omega\sin\theta \tag{5.3.4}$$

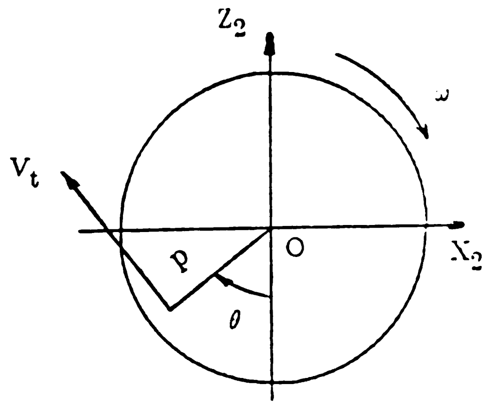

Figure 5.3.1 Disk tangential speed

Rotating the vector $[V_{x2}\ V_{y2}\ V_{z2}]$ β degrees about the X_2 axis (Figure 5.3.2), that is, multiplying the velocity vector in $OX_2Y_2Z_2$ reference by a matrix operator (Rogers,1976), V_{x1}, V_{y1}, V_{z1} resulted

$$[V_{x1}\ V_{y1}\ V_{z1}] = [V_{x2}\ V_{y2}\ V_{z2}]\begin{bmatrix}1 & 0 & 0\\ 0 & \cos\beta & \sin\beta\\ 0 & -\sin\beta & \cos\beta\end{bmatrix} \tag{5.3.5}$$

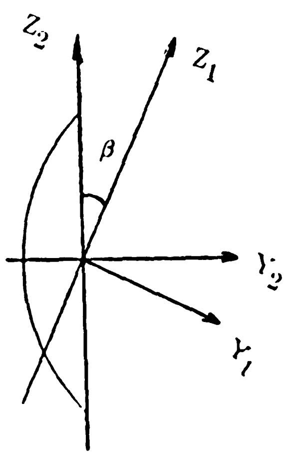

Figure 5.3.2 Coordinate rotation about X_2

Similarly, rotating the vector $[V_{x1}\ V_{y1}\ Vz1]$ $-\alpha$ degrees about the Z_1 axis (Figure 5.3.3), that is, multiplying the velocity vector in $OX_1Y_1Z_1$ reference by a matrix operator, V_{x1}, V_{y1}, V_{z1} resulted

$$[V_x\ V_y\ V_z] = [V_{x1}\ V_{y1}\ V_{z1}]\begin{bmatrix}\cos\alpha & -\sin\alpha & 0\\ \sin\alpha & \cos\alpha & 0\\ 0 & 0 & 1\end{bmatrix} \tag{5.3.6}$$

Replacing V_{x1}, V_{y1} and V_{z1} by using Equations 5.3.6, 5.3.5, 5.3.4, 5.3.3 and 5.3.2, Equation 5.3.6 became

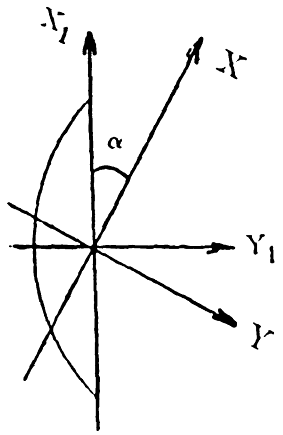

Figure 5.3.3 Coordinate rotation about Z_1

$$V_x = -p\,\omega(\sin\beta\sin\alpha\sin\theta + \cos\alpha\cos\theta) \tag{5.3.7}$$

$$V_y = p\,\omega(\sin\alpha\cos\theta - \sin\beta\cos\alpha\sin\theta) \tag{5.3.8}$$

$$V_z = p\,\omega\cos\beta\sin\theta \tag{5.3.9}$$

The above equations were resulted only from the disk blade rotations. The assembly ground speed (V) also contributed to the velocity vector $[V_x\ V_y\ V_z]$. Since V was in the X direction, it only increased the magnitude of the V_x. When both the linear speed and rotation velocity were considered, that is, add V into Equation 5.3.7, the equation became

$$V_x = V - p\,\omega(\sin\beta\sin\alpha\sin\theta + \cos\alpha\cos\theta) \tag{5.3.10}$$

Equations 5.3.10, 5.3.8 and 5.3.9 had a form similar to those derived by Nartov (1985).

5.3.2 VELOCITY DISTRIBUTION IN XY, XZ AND YZ PLANES

Equations 5.3.10, 5.3.8 and 5.3.9 describles the disk velocities in three dimensions. Using these equations, computer simulations were made with the program MOTION. A computer program PLOT3.VXYZ (Appendix E) was used to plot the simulation results in the planes. Figure 5.3.4 is a typical plot output from the computer. It showed that velocity distributions in both XZ and YZ planes were ellipses and in the XY plane the distribution was a straight line. The ellipse in the YZ plane was symetric about the origin, and the ellipse in the XZ plane was symetric about the X axis.

A disk blade was rotated clockwise starting at the lowest point A and went through points B, C, D, E, F and back to point A, as shown in the upper left corner of Figure 5.3.4. The velocity started with $V_x = 0$ at point A. When the blade rotated to point B, V_z became zero. At points C, D, E and F, V_y, V_x, V_y and V_z were equal to zero respectively. And finally the blade returned to its original position, point A, where $V_x = 0$. Table 5.3.1 shows that V_y and V_x are equal to zero at points A, C, D, and E. For point B in the table, its value is negative and the value just below it is positive. There is a transient point of zero between these two points where V_z is zero, which should be point B exactly. This can be seen from Figure 5.3.4 clearly. The same story is for point F where its values go from the positive to the negative.

A, C, D and E became the points of interest because they were located on axis. Point B and F were denoted because the component V_{Bz}/V_{Fz} of the disk tangential velocity $(R\omega)$ was equal to the assembly ground speed (V) (Figure 5.3.5).

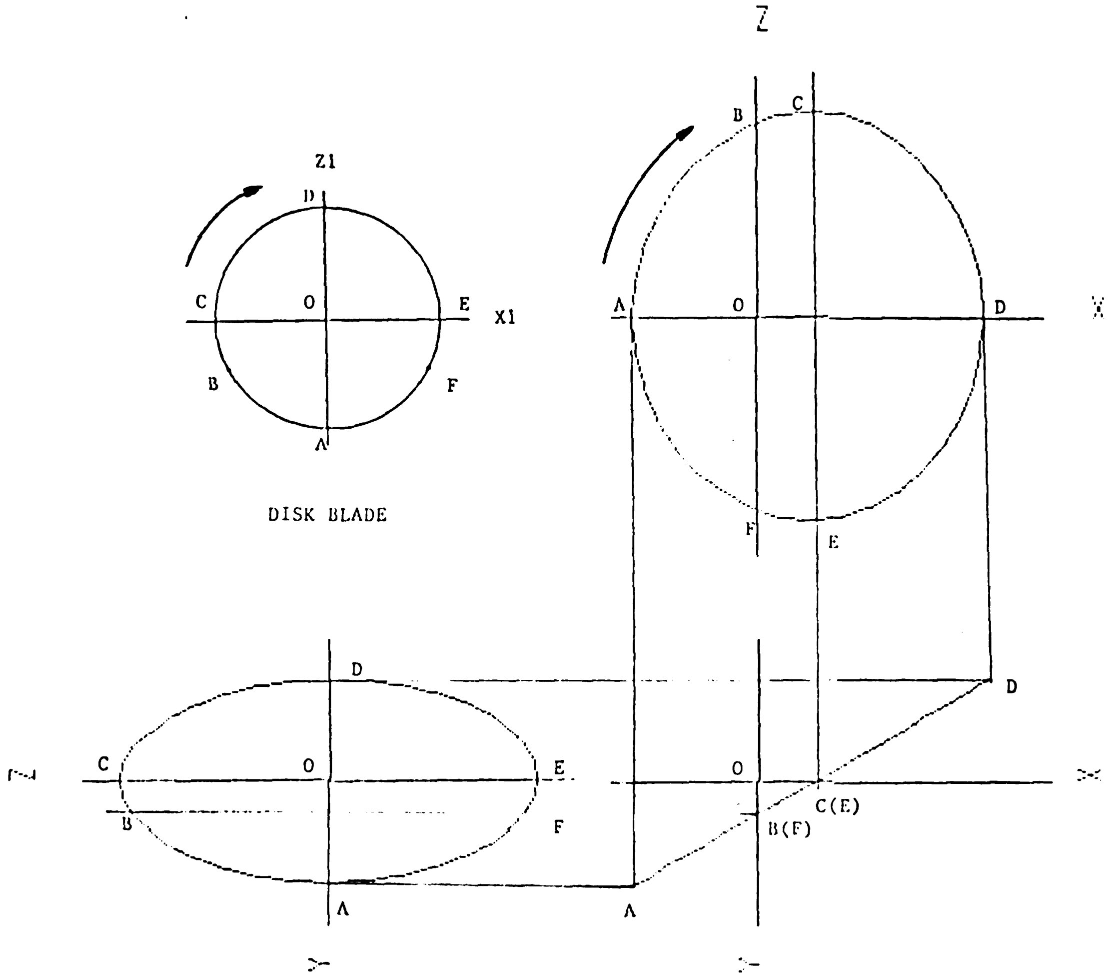

Figure 5.3.4 Velocity distributions in planes

Table 5.3.1 Velocity sumulation results

POINT	V_x	V_y	V_z	NOTE
A	-2.552450	2.115157	0.000000	$V_z=0$
	-2.538508	2.107108	0.368696	
	-2.496792	2.083023	0.734586	
	-2.427617	2.043085	1.094886	
	-2.331510	1.987598	1.446853	
	-2.209203	1.916984	1.787808	
	-2.061625	1.831780	2.115157	
	-1.889902	1.732635	2.426409	
	-1.695339	1.620305	2.719193	
	-1.479418	1.495642	2.991284	
	-1.243780	1.359597	3.240609	
	-0.990222	1.213205	3.465271	
	-0.720670	1.057579	3.663560	
	-0.437177	0.893905	3.833967	
B	-0.141901	0.723427	3.975195	$V_x=0$
	0.162911	0.547444	4.086170	
	0.474939	0.367294	4.166046	
	0.791810	0.184349	4.214217	
C	1.111110	0.000001	4.230314	$V_y=0$
	1.430410	-0.184347	4.214217	
	1.747281	-0.367293	4.166047	
	2.059309	-0.547442	4.086171	
	2.364121	-0.723426	3.975197	
	2.659398	-0.893903	3.833968	
	2.942890	-1.057578	3.663561	
	3.212442	-1.213204	3.465272	
	3.466002	-1.359596	3.240611	
	3.701639	-1.495642	2.991286	
	3.917561	-1.620304	2.719195	
	4.112123	-1.732635	2.426411	
	4.283847	-1.831780	2.115159	
	4.431424	-1.916983	1.787811	
	4.553732	-1.987598	1.446855	
	4.649839	-2.043086	1.094888	
	4.719014	-2.083024	0.734589	
	4.760731	-2.107109	0.368699	
D	4.774672	-2.115158	0.000003	$V_z=0$
	4.760732	-2.107109	-0.368694	
	4.719015	-2.083024	-0.734584	
	4.649840	-2.043086	-1.094884	
	4.553734	-1.987599	-1.446851	
	4.431426	-1.916985	-1.787806	
	4.283850	-1.831781	-2.115156	
	4.112126	-1.732637	-2.426407	
	3.917563	-1.620306	-2.719193	
	3.701641	-1.495643	-2.991284	
	3.466005	-1.359599	-3.240608	
	3.212445	-1.213205	-3.465271	
	2.942894	-1.057581	-3.663559	
	2.659400	-0.893905	-3.833968	
	2.364126	-0.723428	-3.975195	
	2.059312	-0.547444	-4.086171	
	1.747285	-0.367295	-4.166047	
	1.430413	-0.184349	-4.214218	
E	1.111114	-0.000002	-4.230316	$V_y=0$
	0.791812	0.184347	-4.214218	
	0.474944	0.367291	-4.166049	
F	0.162914	0.547442	-4.086172	$V_x=0$
	-0.141897	0.723424	-3.975199	
	-0.437175	0.893903	-3.833969	
	-0.720666	1.057577	-3.663563	
	-0.990219	1.213203	-3.465274	
	-1.243777	1.359595	-3.240613	
	-1.479416	1.495641	-2.991287	
	-1.695337	1.620303	-2.719199	
	-1.889901	1.732635	-2.426412	
	-2.061624	1.831779	-2.115162	
	-2.209202	1.916983	-1.787812	
	-2.331508	1.987597	-1.446858	
	-2.427616	2.043085	-1.094889	
	-2.496791	2.083023	-0.734592	
	-2.538508	2.107108	-0.368700	
A	-2.552450	2.115157	-0.000005	$V_z=0$

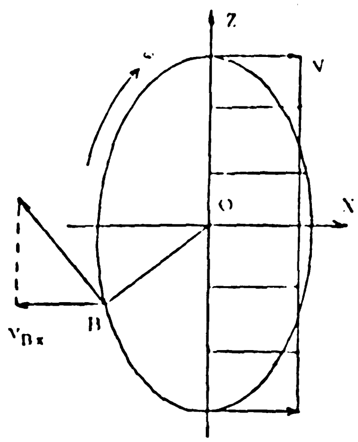

Figure 5.3.5 Tangential speed component in X direction

5.3.3 VELOCITY DISTRIBUTION IN ROTATION

Velocity distributions were affected by the change of the gang angle and ground speed. Since the disk tilt angle (β) was equal to zero in this research, the Equation 5.3.8 became

$$V_y = p\,\omega \sin\alpha \cos\theta \tag{5.3.11}$$

Similarly Equation 5.3.9 became

$$V_z = p\,\omega \sin\theta \tag{5.3.12}$$

The change of gang angle (α) did not affect V_z, and changing the ground speed had no effect on either V_y or V_z. For all of the tests, V_z had the same distributions in any one disk rotation (Figure 5.3.9). V_y remained the same distributions for the same gang angle even though the ground speeds varied (Figure 5.3.6). Increasing the gang angle increased the velocity in the Y axis for positive V_y and decreased the velocity for negative V_y. V_y remained at zero for $\theta = 90°$ and $\theta = 270°$ as demonstrated in Figure 5.3.6. Increasing the gang angle at a given ground speed decreased the velocity in the X axis for positive V_x and increased the velocity for negative V_x. V_x remained at zero for $\theta = 90°$ and $270°$ (Figure 5.3.7). The velocity in the X direction was also affected by the ground speed. When the the ground speed (V) was increased, V_x was increased (Figure 5.3.8).

Figure 5.3.9 gives the general distributions of V_x, V_y and V_z in two rotations of the disk blade. The working part of the disk was located on the lower part of the disk (the arc CBAFE of Figure 5.3.4) in between the angles $0°$ to $90°$ and $270°$ to $360°$. In Figure 5.3.9, the working part of the disk was between $360°$ to $450°$ and $270°$ to $360°$. The lower front part of the disk, at an angle of $270°$ to $360°$, cut and moved the soil, and the lower rear part at an angle of $0°$ to $90°$ moved and threw the soil. In Figure 5.3.6, it was demonstrated that V_y was always positive for the lower part of the blade. V_x was negative and became slightly positive as ground speed increased, and V_z was negative for the lower front part and positive for the lower rear part of the disk blade (Figure 5.3.9). Therefore, the lower front part of the disk cut the soil, moved it backward, to the right and some what lower. The lower rear part of the disk moved the cut soil upward, to the right and backward.

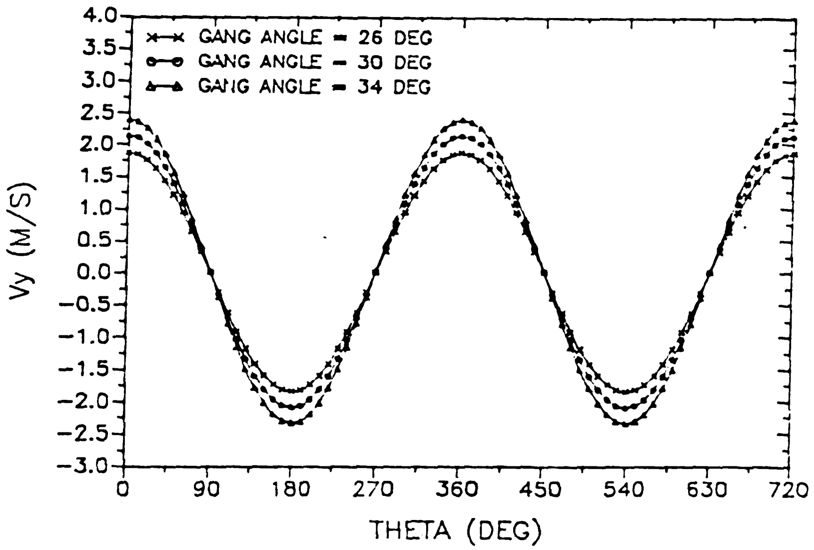

Figure 5.3.6 Effect of gang angle on V_y

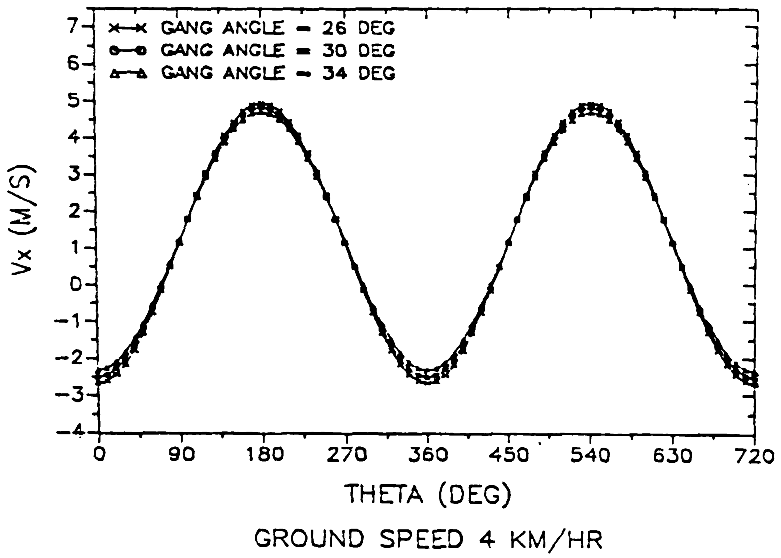

Figure 5.3.7 Effect of gang angle on V_x

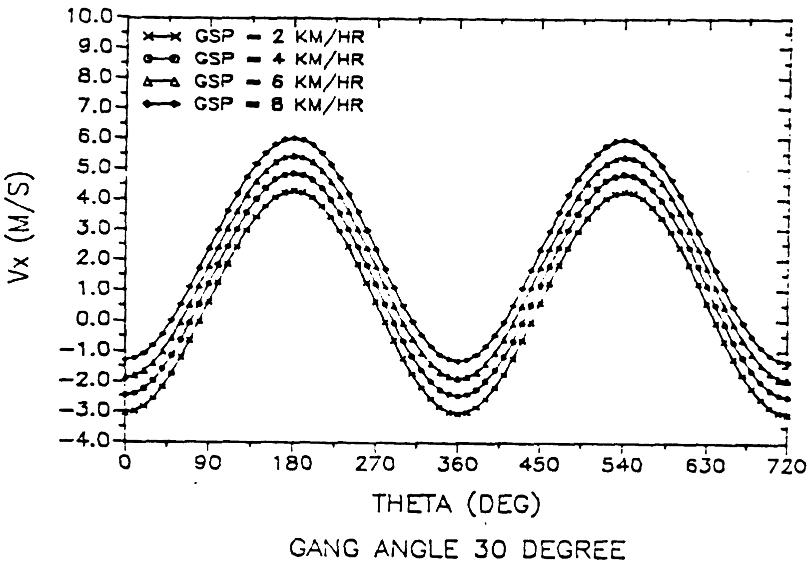

Figure 5.3.8 Effect of ground speed on V_x

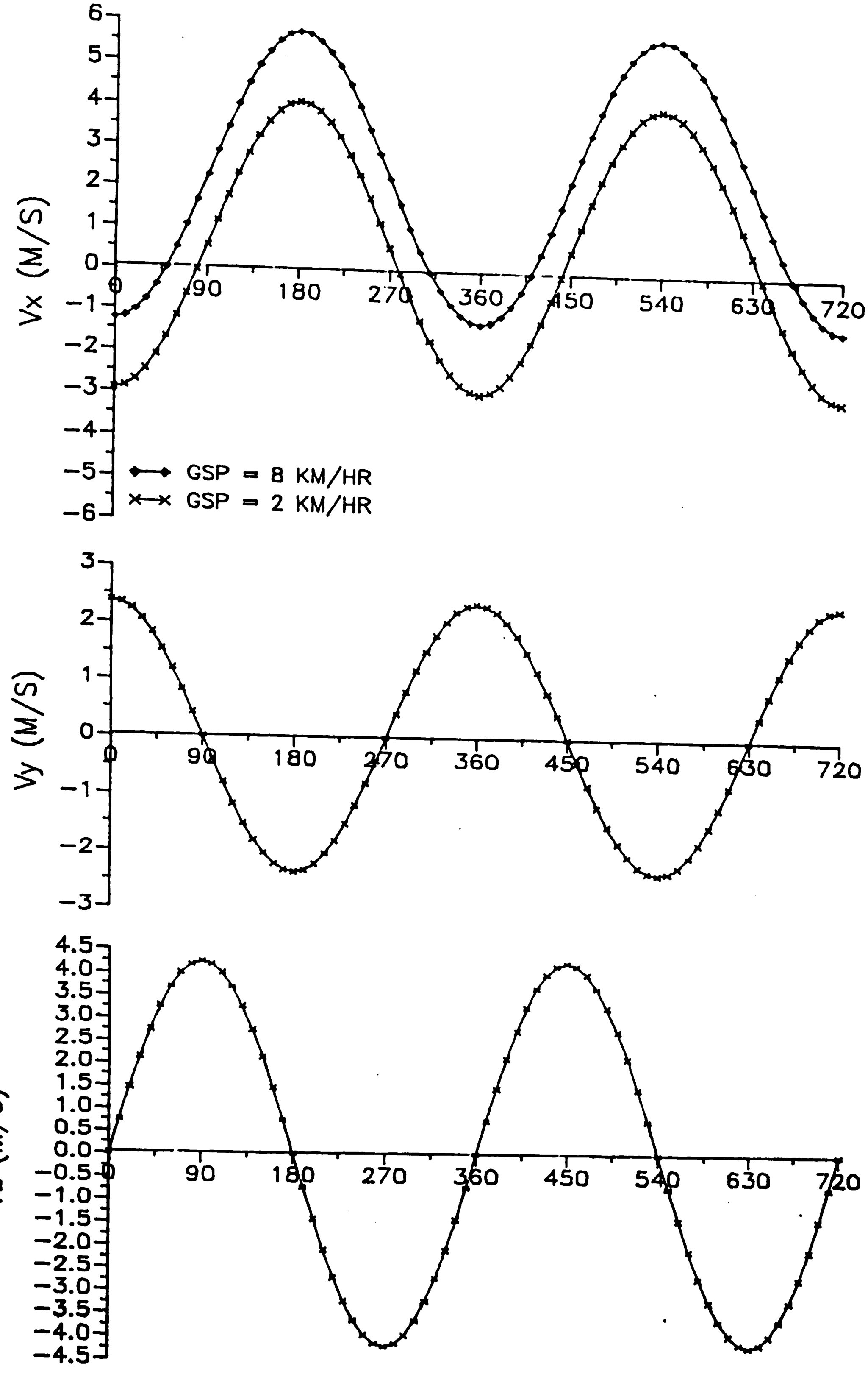

Figure 5.3.9 General velocity distribution in degrees of rotations

5.4 ABSOLUTE VELOCITY

Given Equations 5.3.10, 5.3.8 and 5.3.9, the magnitude of the absolute velocity vector of a disk point in three dimensional space is

$$V_{abs} = \sqrt{V_x^2+V_y^2+V_z^2} \tag{5.4.1}$$

Its direction can be determined from the direction cosines

$$\cos\lambda = \frac{V_x}{V_{abs}} \tag{5.4.2}$$

$$\cos\gamma = \frac{V_y}{V_{abs}} \tag{5.4.3}$$

$$\cos\delta = \frac{V_z}{V_{abs}} \tag{5.4.4}$$

where

λ -- angle between vecter V_{abs} and X axis (rad);

γ -- angle between vector V_{abs} and Y axis (rad);

δ -- angle between vectro V_{abs} and Z axis (rad).

The simulation using the above equations and the program MOTION, showed that the magnitude of the absolute velocity vector varied from 2.4 m/s up to 6.3 m/s. λ was in the range of 20° to 150°, γ was between 40° and 120°, and δ varied in the largest range from 5° to 180°. The results also proved that the variation of gang angle and ground speed had the influence on the vecter of absolute velocity.

From the simulation result plots in Figure 5.4.1 to Figure 5.4.4, the gang angle did not have much effect on the magnitude and the direction of the absolute velocity. The change of gang angle influenced the γ values slightly more than for the others.

The ground speed had more effect on both the magnitude and direction. Figure 5.4.5 shows that as the ground speed increased, the magnitude varied largely. When the ground speed was at 2 km/hr, the magnitude of the absolute velocity varied from 3.76 to 4.72 m/s. As the ground speed increased up to 8 km/hr, the manitude varied from 2.56 to 6.25 m/s, given the gang angle of 30°. The λ value shifted up when the ground speed went higher (Figure 5.4.6). The ground speed also affected γ and δ as indicated in Figure 5.4.7 and Figure 5.4.8.

Nartov (1985) reported that the maximum amplitude of the absolute velocity equalled 1.95V for the unpowered disk implement. In this study of the power disk, it proved that the absolute velocity, with the minimum amplitude of 1.098V and the maximum of 2.835V, was always greater than the ground speed given the range of gang angles between 26° and 34° and ground speeds between 2 km/hr and 8 km/hr.

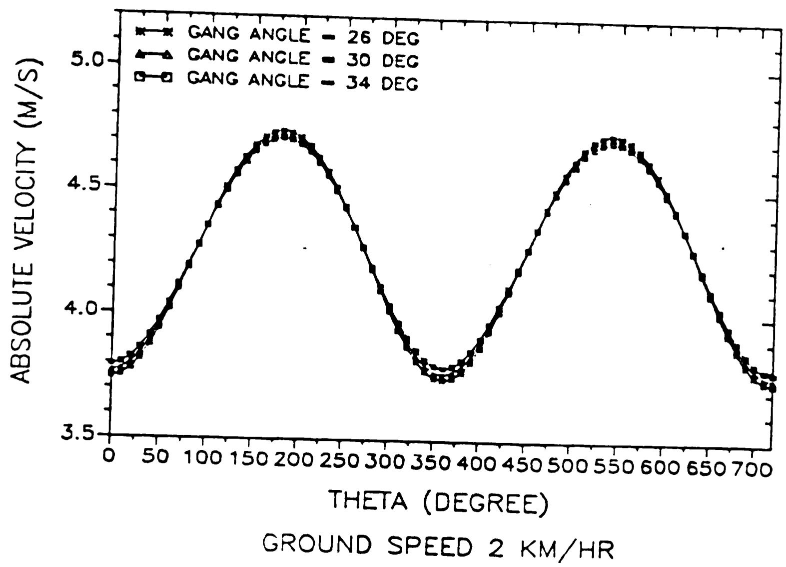

Figure 5.4.1 Effect of gang angle on magnitude of V_{abs}

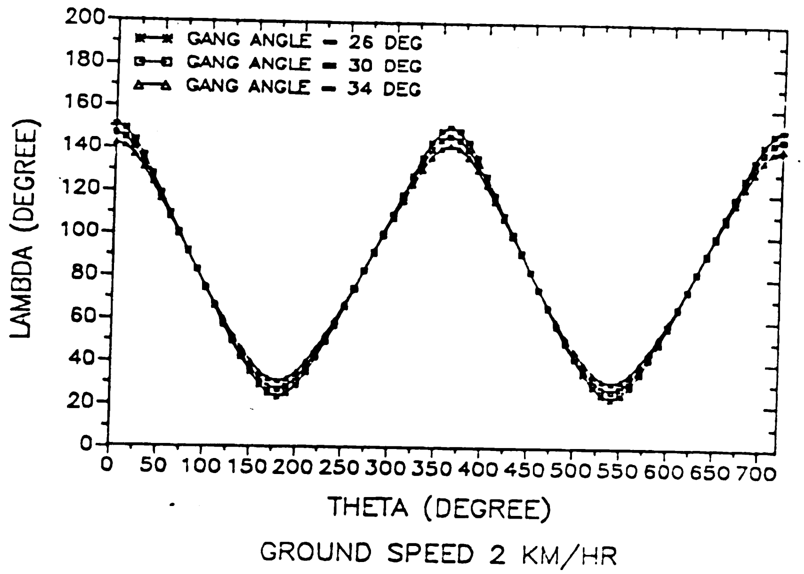

Figure 5.4.2 Effect of gang angle on λ

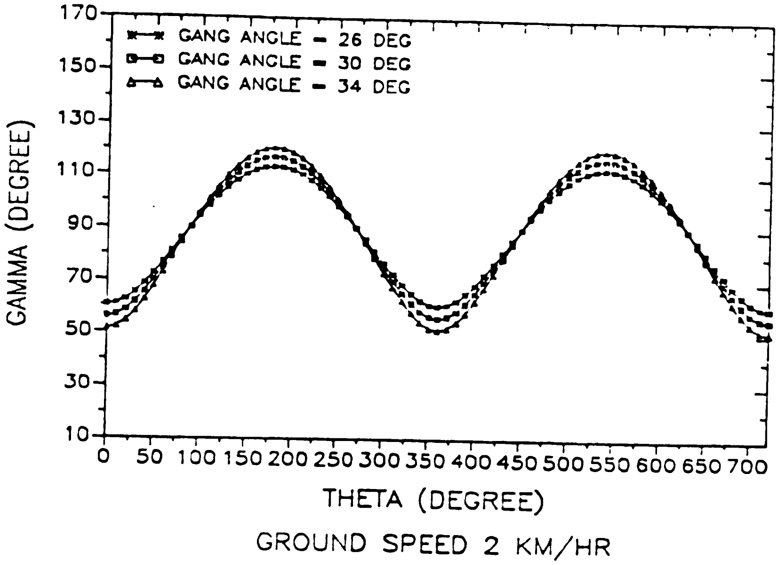

Figure 5.4.3 Effect of gang angle on γ

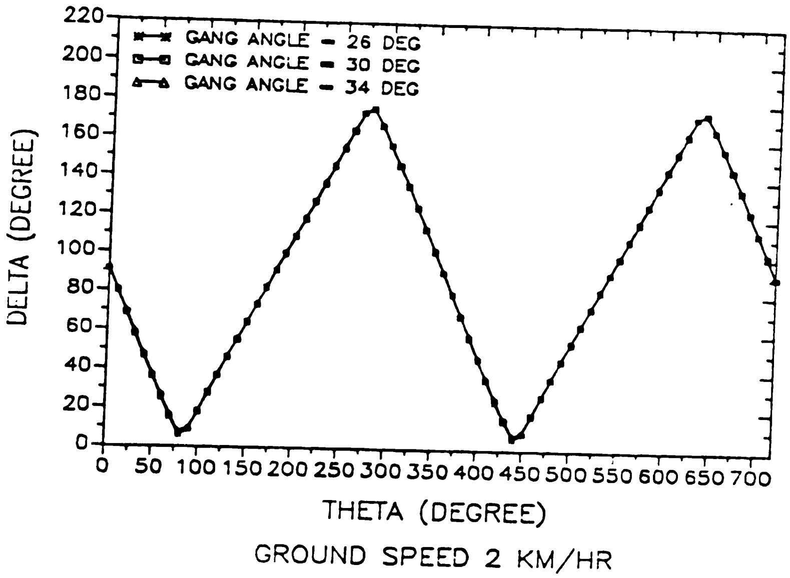

Figure 5.4.4 Effect of gang angle on δ

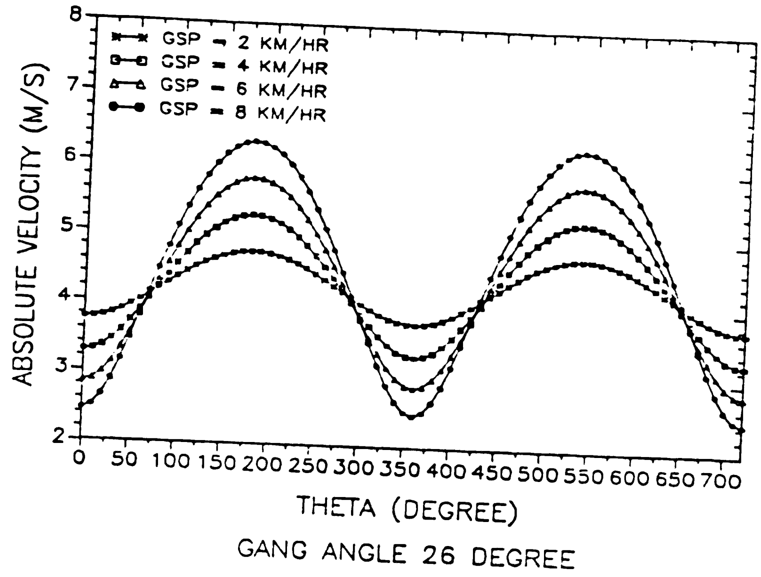

Figure 5.4.5 Effect of ground speed on magnitude of V_{abs}

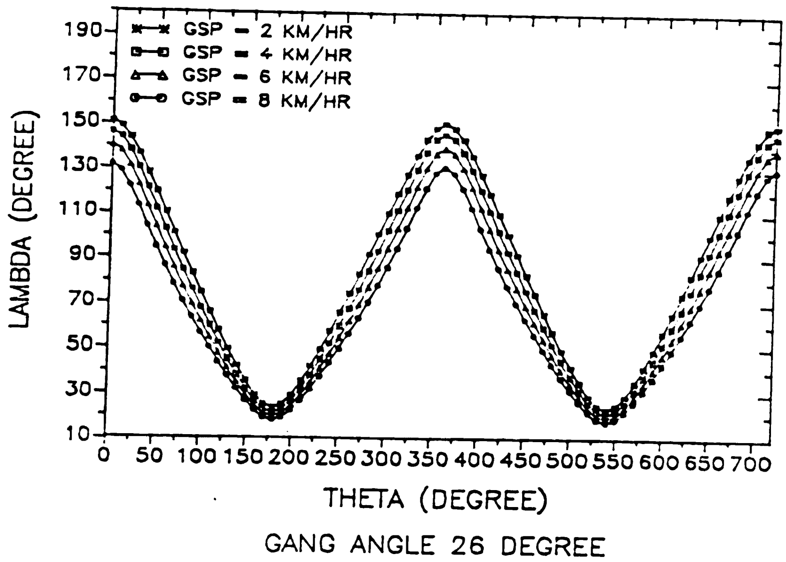

Figure 5.4.6 Effect of ground speed on λ

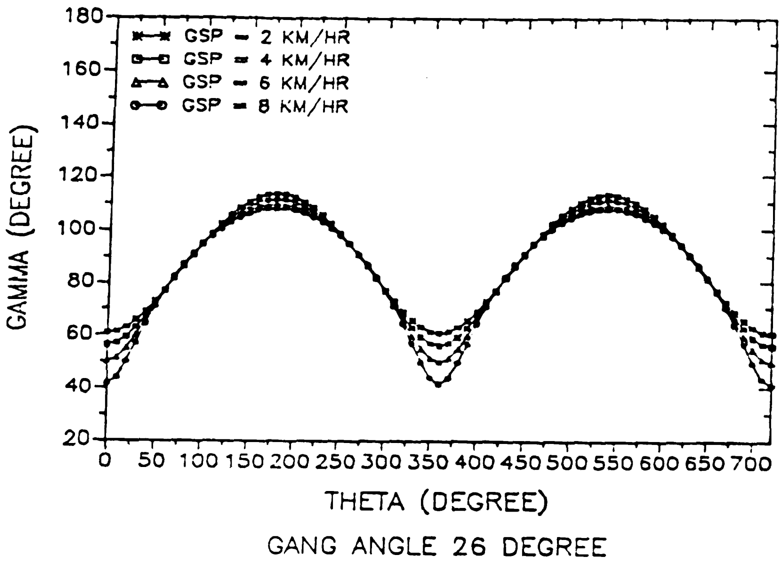

Figure 5.4.7 Effect of ground speed on γ

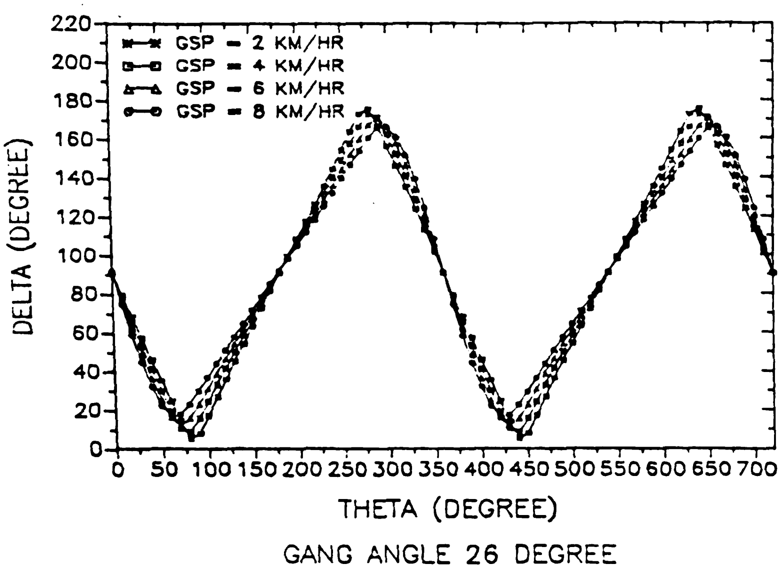

Figure 5.4.8 Effect of ground speed on δ

CHAPTER 6

SIDE FORCE STUDY

The side force is one of the key problems that should be considered during power disk design and study. It is generated by the reaction of the spherical disk in cutting the soil, deforming the slice, moving the soil along the disk and throwing it to one side.

6.1 SIDE FORCE MEASUREMENT

6.1.1 STRAIN GAUGE LOCATION AND WHEATSTONE BRIDGE

Previous researchers have developed many different kinds of equipment to study the reactions of a single disk blade, and a few of them have studied an entire commercial implement. In this research, an attempt was made to put strain gauges on the implement directly.

It was considered that the side force generated by the working disks was balanced by the rear furrow wheel. Therefore, two forces, the side force (SDF) and the vertical force (VTF), existed against the rear furrow wheel (Figure 6.1.1). Both forces were assumed to act on the the lowest point of the wheel's rim circle.

The side force and the vertical force produced tension and a bending moment on the shaft. The strain gauges were put on the rear furrow wheel shaft to measure these two forces. This shaft was manufactured with the length of 125 mm and was extended up to 270 mm (Figure 6.1.2) during the research. Therefore there was enough space for the strain gauges.

Two gauges were put on the top and the bottom of the shaft separately, and two on each side of the shaft. The top and bottom gauges formed a four arm wheatstone bridge to measured the bending moment and the side gauges formed the other bridge to measure the tension. The wheatstone bridge circuit and gauge arrangement are shown in Figure 6.1.3.

6.1.2 CALIBRATION

The calibration was carried out with two tractors. One of the tractors was hitched with the power disk so that the implement could be moved easily. The other tractor supplied a hydraulic power. The layout of the calibration is given in Figure 6.1.4. The rear furrow wheel shaft was affixed to a large post to prevent any movement of the power disk while external forces were applied. The horizontal force, which was produced mainly by the two way hydraulic cylinder, was read from the hyraulic dynamometer. The chain hoist gave the vertical force read from the 500 pound spring scale. Both forces applied to the bolt holes on the hub. The strain gauge responses were recorded by the computer in the data acquisition system. The calibration raw data and their computations are listed in Appendix F.

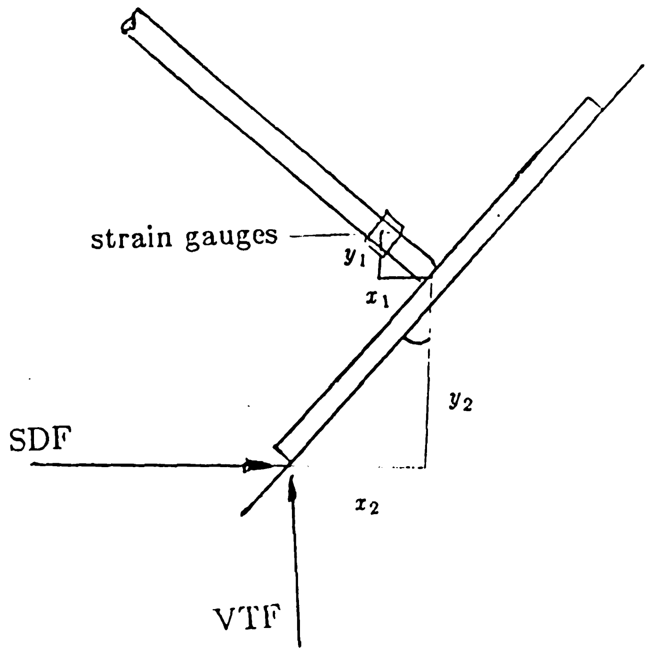

Figure 6.1.1 Rear view of the rear wheel showing side force and rear vertical force

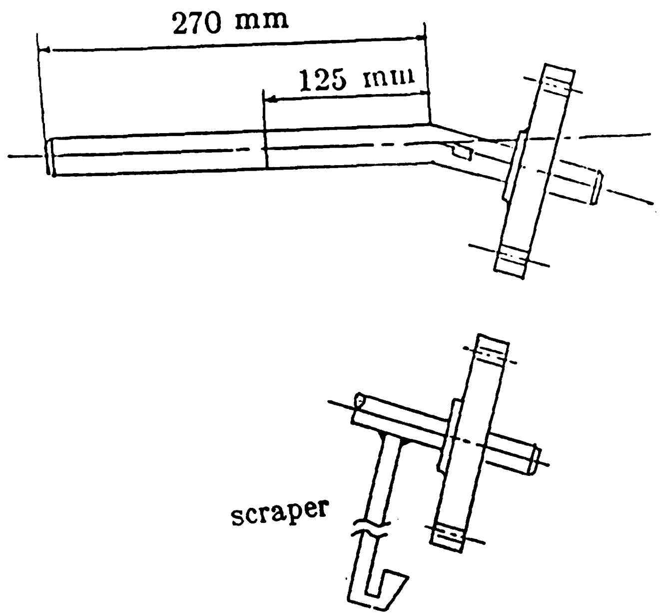

Figure 6.1.2 Top view of the rear wheel shaft and hub

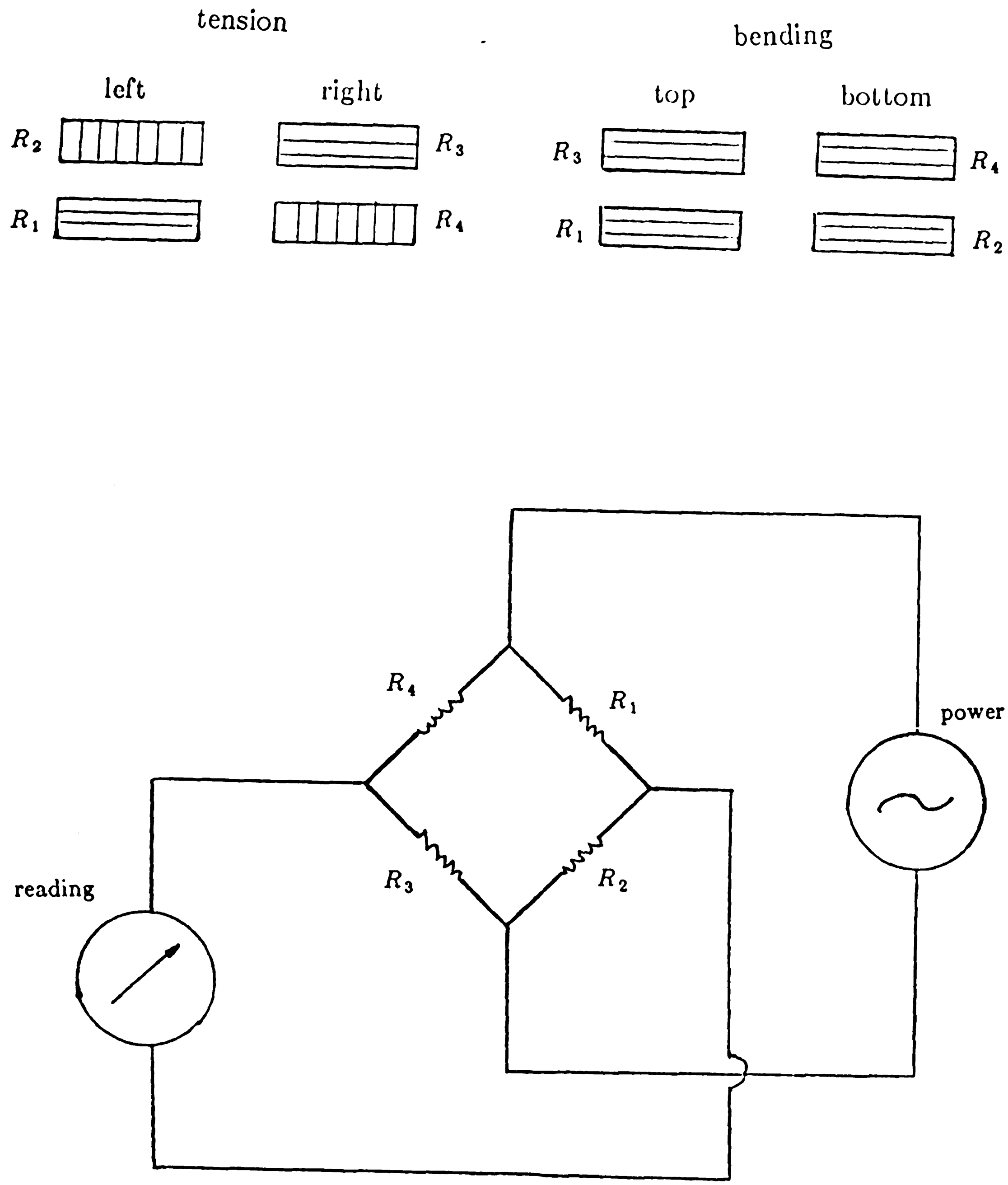

Figure 6.1.3 Strian gauge arrangement and Wheatstone bridge

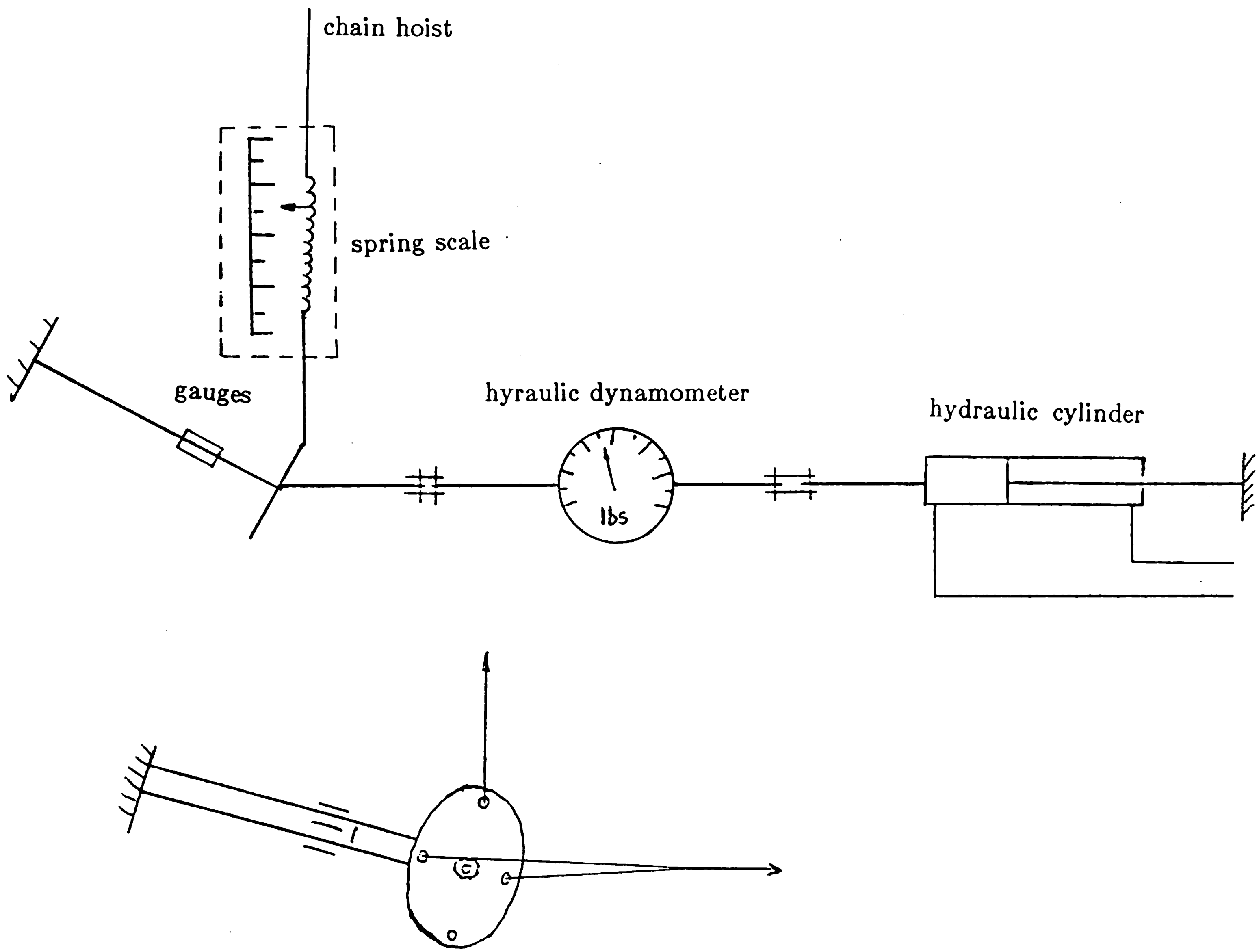

Figure 6.1.4 Calibration layout

To compute the calibration equations, the rear shaft free body diagram was considered (Figure 6.1.5). P_1 was split into two components, the vertical force (V_1) and the horizontal force (H_1) giving the angles of ϕ_1 and ϕ_2. Then the three forces of P_2, H_1 and V_1 were moved to the strain gauge point and combined as the vertical force (V), the horinzontal force (H) and the bending moment (M) when the dimensions of x's and y's were known (Figure 6.1.6). Therefore the bending gauges, that is, the top-bottom gauges, could only sense the moment (M) and the side gauges responsed to the forces of H and V. The first order linear equations were obtained

$$CH13 = -150.883+0.195621H+0.310272V \tag{6.1.1}$$

$$CH14 = 62.44379-7.99175M \tag{6.1.2}$$

where

CH13 -- channel 13 computer reading (mv);

CH14 -- channel 14 computer reading (mv);

H -- horizontal force (lbs);

V -- vertical force (lbs);

M -- bending moment (lbs-mm).

from statistical analysis. The cofficients of determination for each of the equations were 0.980 and 0.998, respectively.

In the field tests, it was assumed that the side force (SDF) and the vertical force (VTF) acted on the circle of the rear wheel rim (Figure 6.1.1). Given x_1, x_2, y_1 and y_2, the relationships between H, V and M and SDF and VTF were

$$H = SDF \tag{6.1.3}$$

$$V = VTF \tag{6.1.4}$$

$$M = 0.23456SDF - 0.13265VTF \tag{6.1.5}$$

where

SDF -- side force;

VTF -- vertical force.

Substituting the above equations into Equations 6.1.1 and 6.1.2, the strain gauge responses to the forces of SDF and VTF were determined

$$CH13 = -150.883 + 0.195621SDF + 0.310272VTF \tag{6.1.6}$$

$$CH14 = 62.44379 - 1.8745449SDF + 1.0601056VTF \tag{6.1.7}$$

where

SDF -- side force (lbs);

VTF -- vertical force (lbs).

These two equations could be expressed in a matrix form

$$\begin{bmatrix} CH13 \\ CH14 \end{bmatrix} = \begin{bmatrix} 0.195621 & 0.310272 \\ -1.8745449 & 1.0601056 \end{bmatrix} \begin{bmatrix} SDF \\ VTF \end{bmatrix} + \begin{bmatrix} -150.883 \\ 62.44379 \end{bmatrix} \tag{6.1.8}$$

Solved for SDF and VTF, and changed the force unit from pounds to Newtons

$$\begin{bmatrix} SDF \\ VTF \end{bmatrix} = \begin{bmatrix} 5.9912813 & -1.7535299 \\ 10.5941576 & 1.1055695 \end{bmatrix} \begin{bmatrix} CH13 + 150.883 \\ CH14 - 62.44379 \end{bmatrix} \tag{6.1.9}$$

where

SDF -- side force (N);

VTF -- vertical force (N).

Equation 6.1.9 was the one that was used in the program MASTER to do calibration computations (Aiba, 1987).

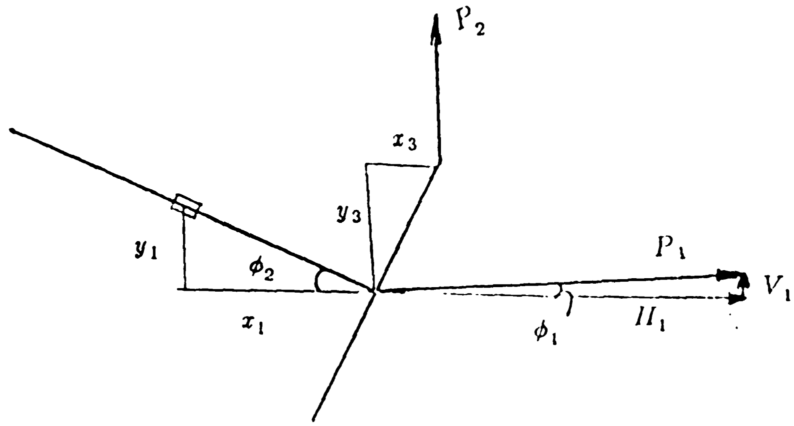

Figure 6.1.5 Rear shaft free body diagram

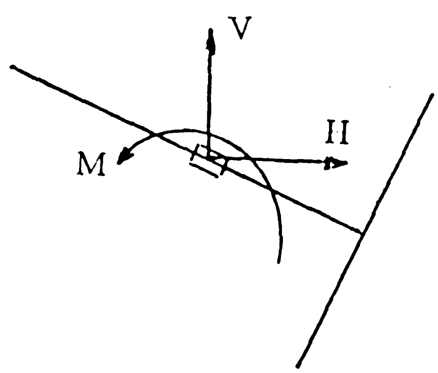

Figure 6.1.6 Three resultant forces

6.2 FIELD TEST RESULTS AND DISCUSSIONS

Using the method and the instrumentation just discussed, the side force and the vertical force were measured and calculated. Appendix G lists all side force data with their extremes (the minimum and the maximum) and Appendix H gives the rear vertical force data.

6.2.1 SIDE FORCE

Figure 6.2.1 ploted all side force data versus the ground speed. Each point of Figure 6.2.1 represents the average of 600 data points for a single test. Clearly there was a trend that as the ground speed increased, the side force also increased. For the regular tests where only gang angle and ground speed were varied, the results showed in Figure 6.2.1 were closely related. For the tests with additional variables, such as soil type and depth control, that is, where more than two variables were varied, the side force results were lower than the regular ones. This implied the new variables affected the side force. The results using the depth wheel to control the working depth were a lot lower than the regular results because the depth wheel absorbed part of the side force. The other variable effects were not clear because there was not enough data to investigate. Therefore only the regular results where the ground speed and the gang angle were varied are discussed in the rest of the chapter.

The regular test side force results versus the ground speed for different gang angles are shown in Figure 6.2.2. The side force was linear with the ground speed. At each gang angle setting, the linear relationship between the side force and the ground speed was slightly different from the others. The side force was highest at the 30° gang angle. Figure 6.2.3 presents the relationship between the side force and the gang angle for different ground speeds. For a given speed, the side force was almost constant as gang angle changed. The figure clearly indicated that the side force increased as the ground speed increased, but gang angle had little, if any, influence on side force.

6.2.2 ACCURACY IN SIDE FORCE MEASUREMENT

The data acquisition system worked well throughout the research. The system gave high linear responses which were indicated by the coefficients of determination (0.980 and 0.998) in calibration regressions.

There were two things about the implement gang angle settings realized after completing the field tests which resulted in inaccuracy in the side force measurement. One was that the relative positions of the implement about the tractor varied according to the gang angle settings and thereby the three point hitch may absorbed some of the side force. If the relative position between the tractor and the implement was ideal and the top link was parallel to the travel direction and the lower links contained the side force in the same magnitudes but the opposite directions (Figure 6.2.4), there would be no hitching effect. This relative implement position varied due to the change of the gang angle. When the implement swung to the left relatively (Figure 6.2.5), the hitch would absorb some side force. Therefore the measured side force from the rear shaft was less than the actual force. On the other hand, when the implement swung to the right (Figure 6.2.6), the hitch would produce some side force. The side force measured was larger than the actual side force. It was observed that the implement

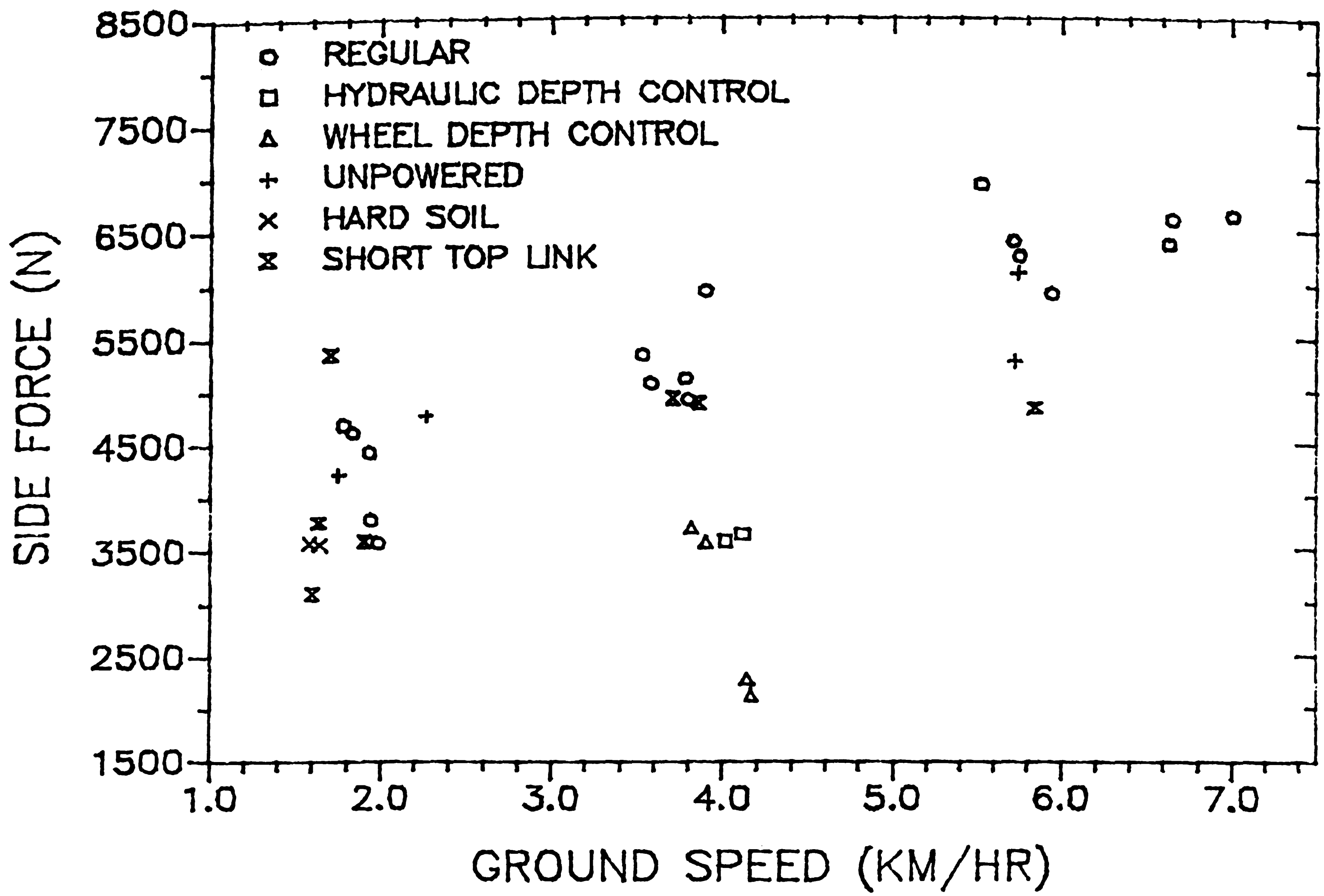

Figure 6.2.1 Relationship between side force and ground speed

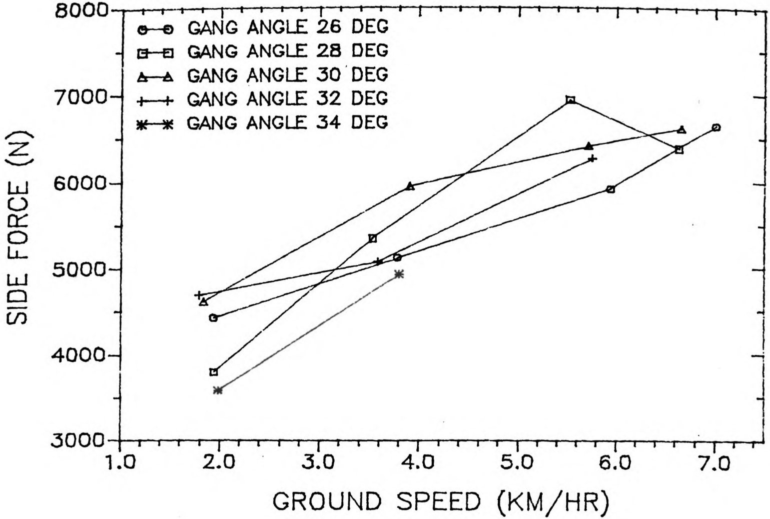

Figure 6.2.2 Relationship between regular side force and ground speed

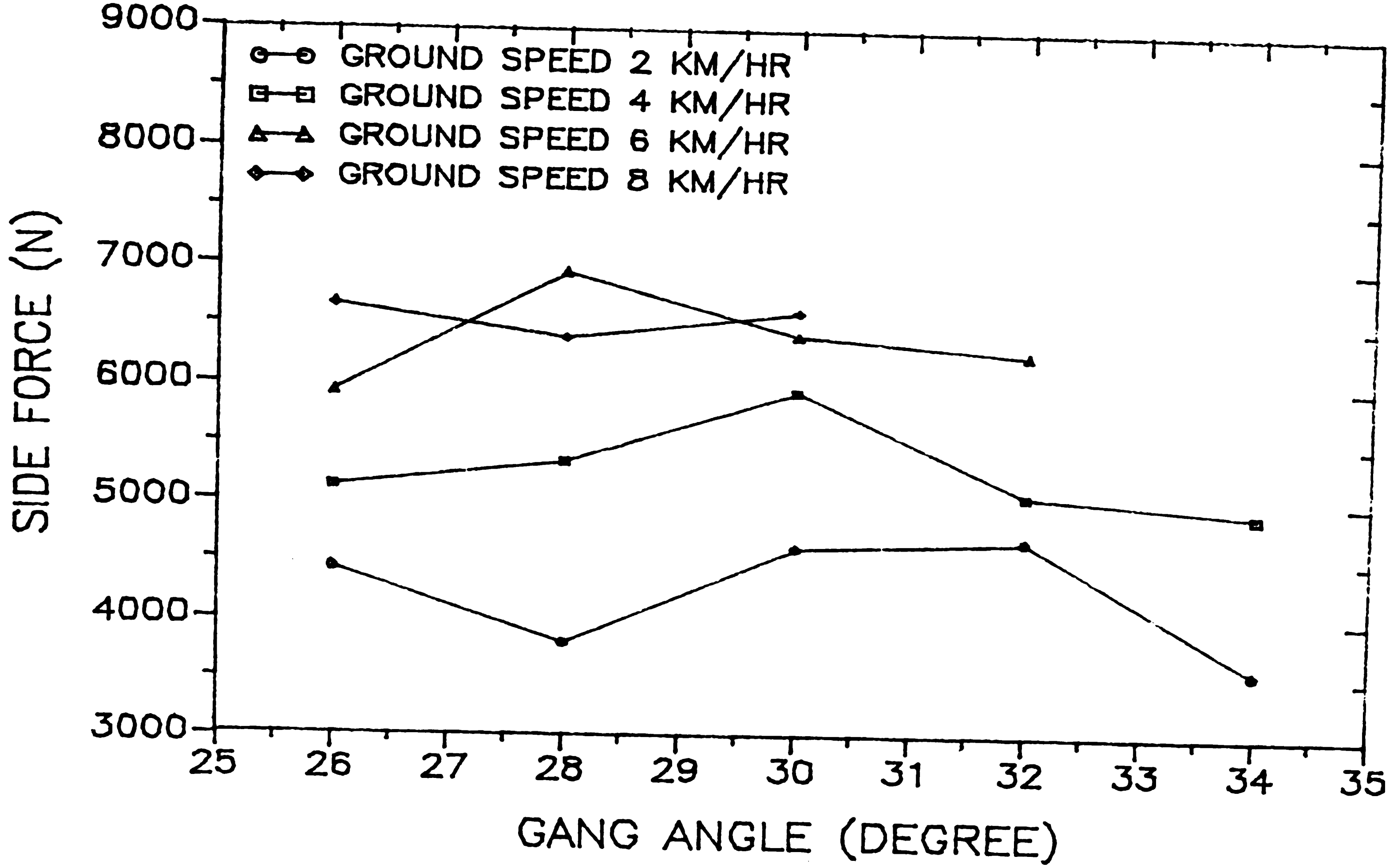

Figure 6.2.3 Relationship between regular side force and gang angle

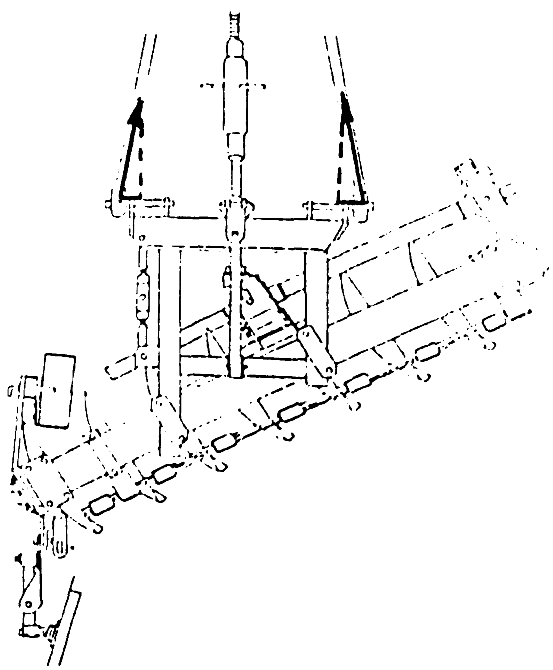

Figure 6.2.4 Ideal hitching

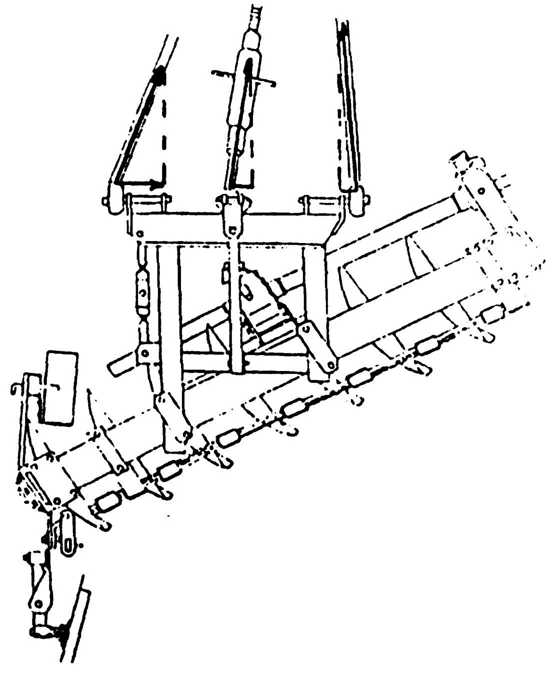

Figure 6.2.5 Hitch containing side force

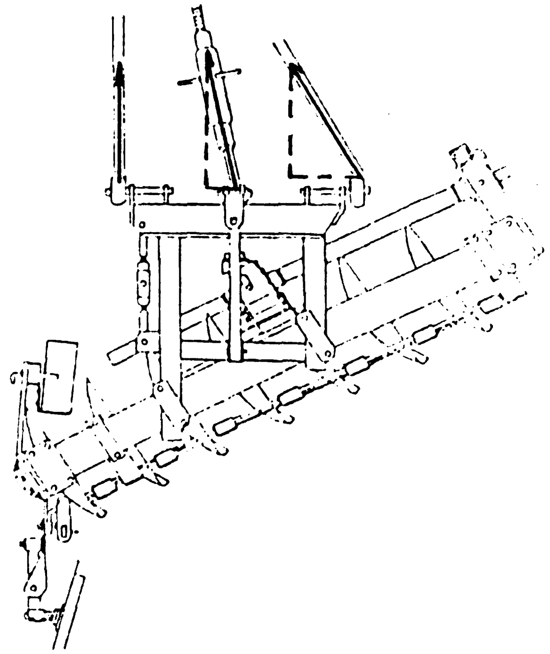

Figure 6.2.6 Hitch containing side force

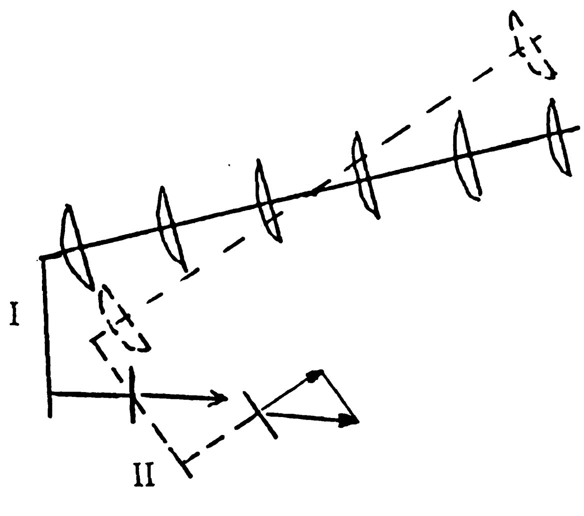

Figure 6.2.7 Rear shaft positions

rotated and the rear wheel moved to the right at low gang angle settings and to the left at high gang angle settings.

Second was the rear furrow wheel position. As the gang angle was changed, the rear shaft position varied also. In position I (Figure 6.2.7), the side force was measured more accurately. At another gang angle setting, the rear shaft was like position II. In this case, only part of the side force was measured.

6.2.3 REAR FURROW WHEEL SETTINGS

The rear furrow wheel is very important because its settings can influence the power disk behavior. Since the rear shaft was not straight (Figure 6.1.2), the rotations about the shaft center line and the furrow wheel arm resulted in dramatically different working depths, rear disk cutting paths and high rear vertical forces.

The relative position of the rear wheel settings was described by the wheel scraper welded on the shaft (Figure 6.1.2). Incorrect settings resulted in a shallow depth, a wrong rear disk path and a tight sway chain for the left lower link of the three point hitch. Figure 6.2.8 demonstrates one bad setting where the scraper is horizontal. The rear wheel cut the upper portion of the furrow wall which was not subjected to the total side force reaction and the maximum working depth was only about 10 cm. After many tests, another setting was found (Figure 6.2.9) where the scraper was in the vertical position and the rear wheel shaft was aproximately 50° from the horizontal plane. The rear wheel cut the lower corner of the furrow wall which would produce enough reaction to keep the sway chain loose. This setting also resulted in a deeper working depth with

Figure 6.2.8 Incorrect rear wheel setting

Figure 6.2.9 Correct rear wheel setting

the maximum of 30 cm. At this setting, the scraper did not function well and a large amount of soil fell onto the rear wheel. The scraper needed to be placed horizontally to avoid this soil accumulation.

6.2.4 DESIGN MODIFICATIONS

In order to set the rear furrow wheel properly, three design modifications were made. The first modification was that the rear shaft was extended from 125 mm up to 270 mm. The primary purpose of the extension was to make the rear wheel adjustable laterally to the left and the right. Later it was found that this extension also provided plenty of space to put strain gauges on the shaft.

A flange was put on the rear wheel arm to make the shaft rotation about the arm possible (Figures 6.2.8 and 6.2.10). This adjustment toward the rear wheel settings was as important as the rear wheel scraper rotation about the rear shaft center line. A good setting was a combination of these two rotations. For example, the rear wheel setting worked well while the scraper was rotated vertically and the rear shaft was rotated 50° from the horizontal plane.

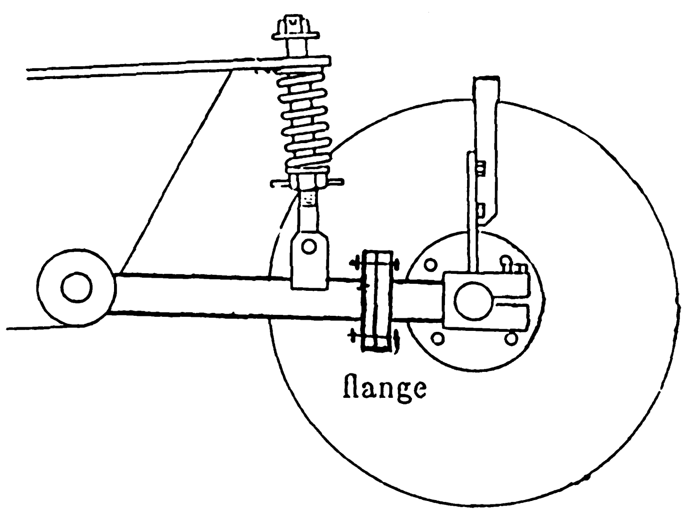

Figure 6.2.10 Flange on the rear wheel arm

The rear wheel rim was on the right hand side of the rear wheel as the power disk was manufactured. During the field tests, this rim position did not work well in reaction to the side force. Alternatively the rear wheel was rotated 180° and then put on so that the rim faced in the other direction as shown in Figure 6.1.1, and it worked better. This was the third modification.

6.2.5 REAR VERTICAL FORCE

While the side force information was collected, the rear vertical force was also measured. Figure 6.2.11 presents how the vertical force is related to the ground speed. It is obvious that the rear vertical force increased as the ground speed increased with two exceptions. The slope of the vertical force was less than that of the side force which meant the vertical force variation was less. The two high vertical force points at 2 km/hr with the gang angles of 26° and 28° resulted from another rear wheel setting. At these ground speed and gang angles, the sway chain of the right lower link of the three point hitch was tight. The rear wheel setting was readjusted as the rear shaft was aproximately 30° from the horizontal plane and the scraper was in the vertical position. At this rear wheel setting, the sway chain was loose. Figure 6.2.12 indicates that the vertical force was not related to the gang angle when the two high value points which resulted from another rear furrow wheel setting were removed.

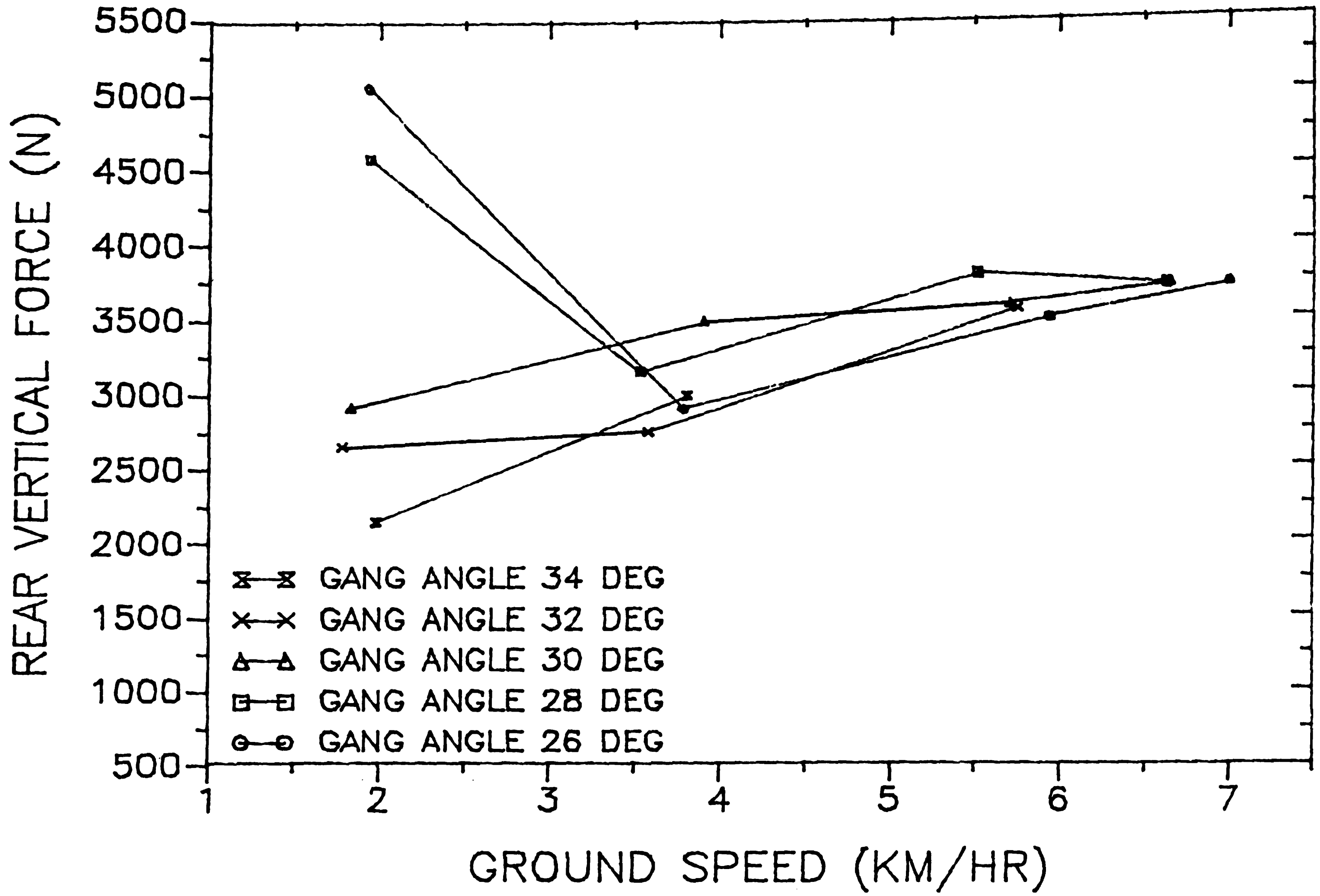

Figure 6.2.11 Relationship between vertical force and ground speed

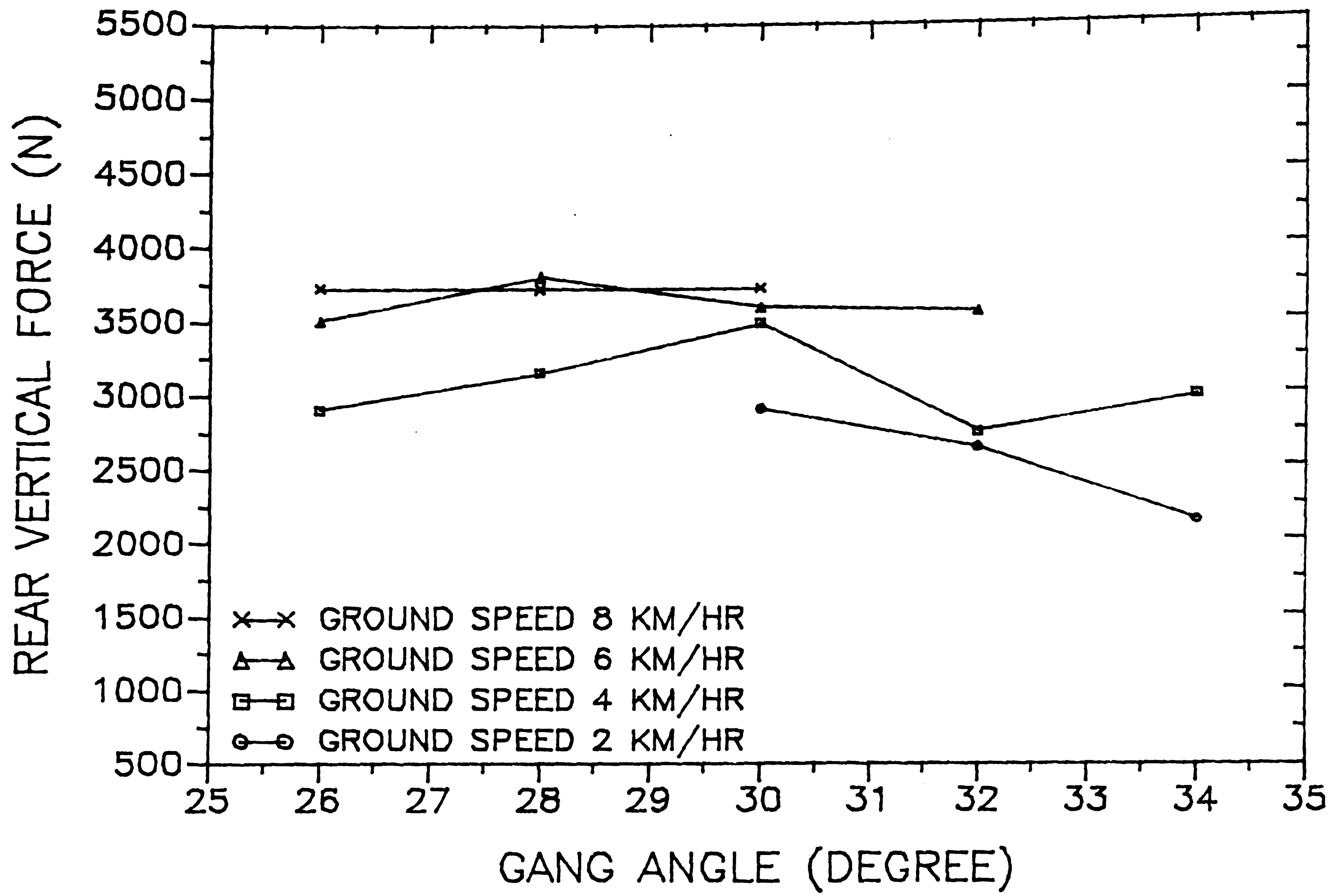

Figure 6.2.12 Relationship betwen vertical force and gang angle

6.3 REGRESSION ANALYSIS OF SIDE FORCE

Regression analysis is a modern technique that helps to study the relationship among variables more deeply and accurately. Based on the previous discussions, the regular side force test results had a linear relationship with the ground speed, which could be expressed using the model

$$Y = b_0 + b_1 X \tag{6.3.1}$$

where

Y -- side force;

X -- ground speed;

b_0, b_1 -- parameters to be estimated.

and the gang angle did not have much effect on the side force. Statistically it was interesting to investigate the linear relationship and use the statistical statement to comment on the ground speed and gang angle effects.

6.3.1 REGRESSION WITH BINARY VARIABLES

Since the side force data were obtained at various gang angles, these settings may affect the linear model 6.3.1 to have different paramenters as seen in Figure 6.2.2. Regression analysis was used to develop a linear relation between the side force and the ground speed. Binary variable were used to determine whether a single line would be sufficient or if a series of lines would be necessary because of different gang angle settings. The reason that the variables were called binary was that these variables contained binary numbers of 0 and 1. There were five gang angle settings (26°, 28°, 30°, 32°, and 34°) and four binary variables were employed. The following model was considered

$$Y = b_0 + b_1X + b_2Z_1 + b_3Z_2 + b_4Z_3 + b_5Z_4 \tag{6.3.2}$$

where

X -- ground speed;

b's -- parameters to be estimated;

Z's -- binary variables; where

$$Z_1=\begin{cases}1 & \text{if } gang \quad angle=26^\circ \\ 0 & others\end{cases}$$

$$Z_2=\begin{cases}1 & \text{if } gang \quad angle=28^\circ \\ 0 & others\end{cases}$$

$$Z_3=\begin{cases}1 & \text{if } gang \quad angle=30^\circ \\ 0 & others\end{cases}$$

$$Z_4=\begin{cases}1 & \text{if } gang \quad angle=32^\circ \\ 0 & others\end{cases}$$

The model 6.3.2 could be decomposed as a set of regression lines if Z's were substituted by their values

$$Y = (b_o + b_2) + b_1X \qquad \text{for } gang \quad angle=26^\circ\text{, } Z_1=1 \text{ and } Z_2=Z_3=Z_4=0 \tag{6.3.3}$$

$$Y = (b_o + b_3) + b_1X \qquad \text{for } gang \quad angle=28^\circ\text{, } Z_2=1 \text{ and } Z_1=Z_3=Z_4=0 \tag{6.3.4}$$

$$Y = (b_o + b_4) + b_1X \qquad \text{for } gang \quad angle=30^\circ\text{, } Z_3=1 \text{ and } Z_1=Z_2=Z_4=0 \tag{6.3.5}$$

$$Y = (b_o + b_5) + b_1X \qquad \text{for } gang \quad angle=32^\circ\text{, } Z_4=1 \text{ and } Z_1=Z_2=Z_3=0 \tag{6.3.6}$$

$$Y = b_0 + b_1X \qquad \text{for } gang \quad angle=34^\circ \text{ and } Z_1=Z_2=Z_3=Z_4=0 \tag{6.3.7}$$

The regression analysis was performed on an IBM PC computer using LOTUS spread sheet. The results and the ANOVA (ANalysis Of VAriance) table are given in Table 6.3.1. The coefficient of determination (R^2) was 0.902. The

Equations 6.3.3 to 6.3.7 became

$$Y = 3308.418 + 474.080X \quad \text{for } gang \ \ angle=26° \tag{6.3.8}$$

$$Y = 3511.296 + 474.080X \quad \text{for } gang \ \ angle=28° \tag{6.3.9}$$

$$Y = 3736.077 + 474.080X \quad \text{for } gang \ \ angle=30° \tag{6.3.10}$$

$$Y = 3569.583 + 474.080X \quad \text{for } gang \ \ angle=32° \tag{6.3.11}$$

$$Y = 2857.768 + 474.080X \quad \text{for } gang \ \ angle=34° \tag{6.3.12}$$

The above equations have the same slope of 474.080 and different Y axis intecepts. Therefore they are a set of parallel lines.

The F test

$$F=\frac{\dfrac{SSE(X)-SSE(X,Z_1,Z_2,Z_3,Z_4)}{4}}{\dfrac{SSE(X,Z_1,Z_2,Z_3,Z_4)}{11}} \tag{6.3.13}$$

where

$SSE(X)$ -- sum of square of errors using model 6.3.1;

$SSE(X,Z_1,Z_2,Z_3,Z_4)$ -- sum of square of errors using model 6.3.2.

tested whether there was the gang effect with hypothesis

$$H_o:\beta_2=\beta_2=\beta_3=\beta_4=0$$

$$H_a: \ not \ \ all \ \ \beta_k=0 \ (k=2, \ 3, \ 4)$$

Since

$$F=\frac{\dfrac{2796272.28-1670350.25}{4}}{\dfrac{1670350.25}{11}}=1.854$$

Table 6.3.1 Regression results with binary variables

Y	X	Z_1	Z_2	Z_3	Z_4	$\hat{Y}$	Errors
4414.62	1.93	1	0	0	0	4223.39	191.23
5107.53	3.78	1	0	0	0	5100.44	7.09
5911.06	5.94	1	0	0	0	6124.45	-213.39
6642.06	7.00	1	0	0	0	6626.98	15.08
3779.04	1.94	0	1	0	0	4431.01	-651.97
5324.65	3.53	0	1	0	0	5184.80	139.85
6924.14	5.52	0	1	0	0	6128.22	795.92
6370.65	6.63	0	1	0	0	6654.45	-283.80
4598.22	1.83	0	0	1	0	4603.64	-5.42
5924.63	3.90	0	0	1	0	5584.99	339.64
6396.28	5.71	0	0	1	0	6443.07	-46.79
6601.29	6.65	0	0	1	0	6888.71	-287.42
4668.67	1.78	0	0	0	1	4413.45	255.22
5053.51	3.58	0	0	0	1	5266.79	-213.28
6253.60	5.75	0	0	0	1	6295.54	-41.94
3554.85	1.98	0	0	0	0	3796.45	-241.60
4900.87	3.80	0	0	0	0	4659.27	241.60

Regression Output:	
Constant	2857.768
Std Err of Y Est	389.679
R Squared	0.902
No. of Observations	17
Degrees of Freedom	11
X Cofficient(s)	474.080 450.650 653.528 878.309 711.815
Std Err of Coef.	54.295 350.926 347.353 348.918 358.458

ANOVA Table

Source of variation	SS	df	MS
Regression	15456383.87	5	3091276.77
Error	1670350.25	11	151850.02
Total	17126734.12	16	

and

$$F_{table}(0.95, 4, 11)=3.36$$

given the significant level of α=0.05, then

$$F < F_{table}$$

It was concluded that there was no significant gang angle effect and the common line of model 6.3.1 was good enough to fit the test data.

6.3.2 SIMPLE LINEAR REGRESSION

Because statistical statement agreed with the earlier discussion that there was little gang angle effect, which was

$$\beta_2=\beta_3=\beta_4=\beta_5=0$$

the model 6.3.2 reduced as

$$Y = b_0 + b_1 X$$

The regression results using the above model plus the ANOVA table is given in Table 6.3.2. Substituting the estimated parameters, the above equation became

$$Y = 3337.507 + 500.88X \qquad (6.3.14)$$

with the $R^2 = 0.837$.

By performing the t test

$$t=\frac{b_1}{s(b_1)}=\frac{500.88}{57.128}=8.768$$

where

b_1 -- estimated parameter;

$s(b_1)$ -- estimated standard error of parameter b_1.

and

$$t_{table}(0.975,\ 15)=2.131$$

given the α level of 5% and

$$t_{tabel}(0.995,\ 15)=2.947$$

given the α level of 1%, it was proved that the linear relationship between the side force and the ground speed was highly significant since

$$t_1 > t_{table}(0.995,\ 15)$$

and this relationship was expressed by Equation 6.3.14. Figure 6.3.1 presented the raw data points, the regression line, the 95% confidence band and the error plots. The confidance band contains most of the data points so that the model 6.3.14 expresses the relationship bewteen the side force and the ground speed very well. The maxmum positive absolute error is 821.76 (N) and the maximum negative is -774.42 (N).

Table 6.3.2 Regression results with one variable

Y	X	$\hat{Y}$	Errors
4414.62	1.93	4304.23	110.39
5107.53	3.78	5230.85	-123.32
5911.06	5.94	6312.75	-401.69
6642.06	7.00	6843.69	-201.63
3779.04	1.94	4309.23	-530.19
5324.65	3.53	5105.63	219.02
6924.14	5.52	6102.38	821.76
6370.65	6.63	6658.36	-287.71
4598.22	1.83	4254.14	344.08
5924.63	3.90	5290.96	633.67
6396.28	5.71	6197.55	198.73
6601.29	6.65	6668.38	-67.09
4668.67	1.78	4229.09	439.58
5053.51	3.58	5130.68	-77.17
6253.60	5.75	6217.59	36.01
3554.85	1.98	4329.27	-774.42
4900.87	3.80	5240.87	-340.00

Regression Output:	
Constant	3337.527
Std Err of Y Est	431.762
R Squared	0.837
No. of Observations	17
Degrees of Freedom	15
X Cofficient(s)	500.880
Std Err of Coef.	57.128

ANOVA Table			
Source of variation	SS	df	MS
Regression	14330461.85	1	14330461.85
Error	2796272.28	15	186418.15
Total	17126734.12	16	

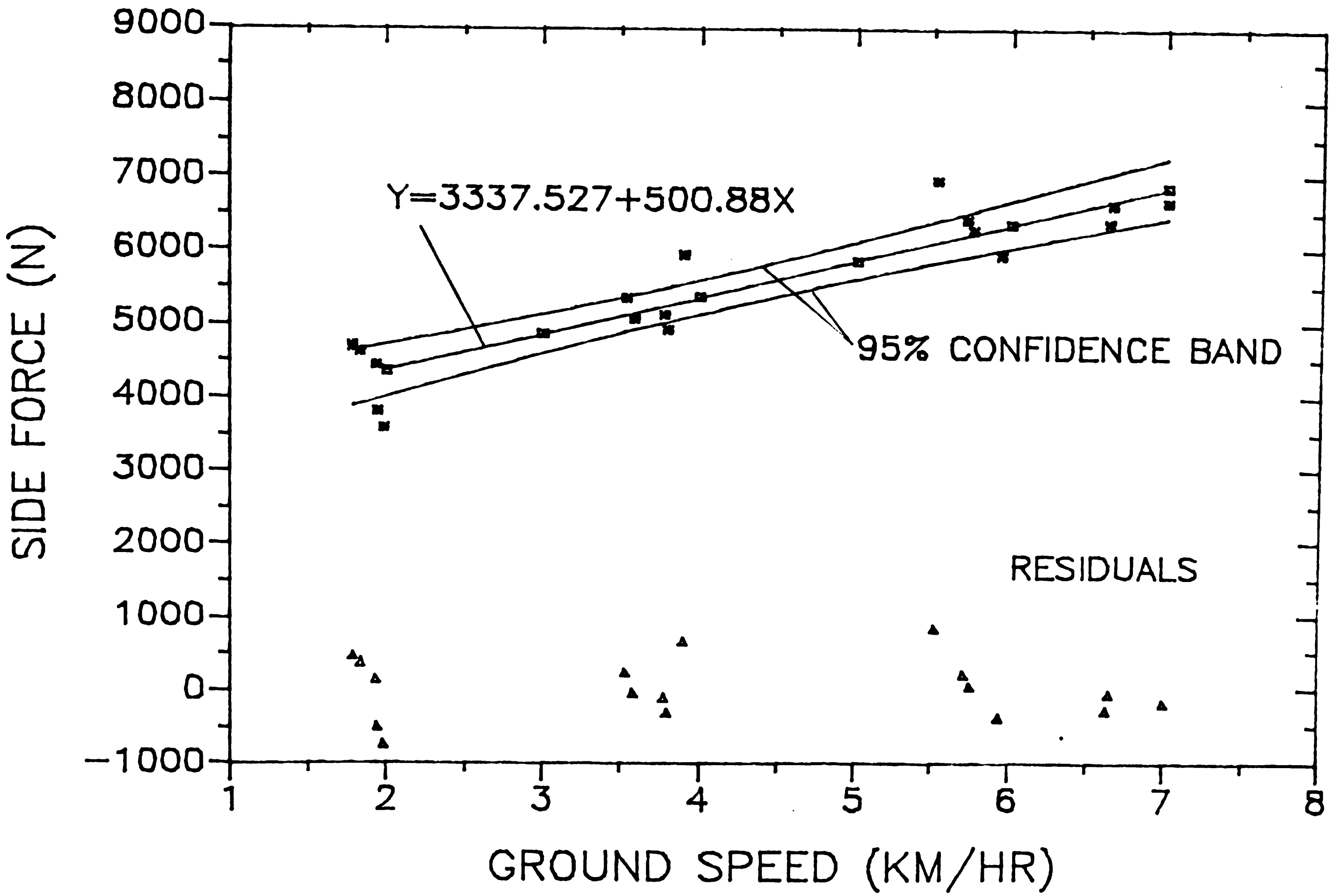

Figure 6.3.1 Linear regression analysis plot

CHAPTER 7

CONCLUSIONS AND RECOMMENDATIONS

7.1 CONCLUSIONS

Based on the theoretical, experimental and statistical studies, the following conclusions can be drawn:

1. The power disk worked in the slipping condition. Given the gang angles of 26° to 34° and the ground speeds of 2 to 8 km/hr, the disk slippages were between 52.79% and 89.11%.

2. The disk velocity distributions were ellipses in the XZ and YZ planes and a straight line in the XY plane. The distributions were affected by the ground speed and gang angle.

3. The absolute velocity of the disk blade, with the amplitudes between 1.098V and 2.835V, was always greater than the implement ground speed.

4. The gang angle settings had little, if any, effect on the vertical force.

5. According to Figure 6.2.3, little influence of gang angle settings on the side force was observed. As discussed in Section 6.2.2, the side force for large gang angles was underestimated and the side force for small gang angles was overestimated. Consequently additional tests which fix the power disk

position relative to the tractor are necessary to determine the effect of gang angle on the side force.

6. The linear relationship between the side force and the ground speed was established through the experimental and statistical analyses. The statistical test indicated that this relationship was highly significant and could be expressed using a simple linear model 6.3.14.

7. The rear furrow wheel setting was important, and it affected the power disk behavior dramatically.

8. The rear vertical force increased as the ground speed increased.

7.2 RECOMMENDATIONS

Further advanced studies of the power disk are necessary. Several topics are suggested for the future research projects:

1. Theoretical study of the power disk. A modern computer modeling and simulation method can be employed to study the power disk, such as disk blade motion, power requirement and furrow width, at various gang angles, ground speeds, tilt angles, disk curvatures and PTO speeds.

2. Further field tests are needed to investigate the gang angle effect on side force and other factors. The relative position of the implement about the tractor needs to be fixed in order to detect the gang angle effects.

3. Full understanding of the rear furrow wheel is a interesting and important aspect in the power disk research.

4. The side force needs to be studied with more variables besides the ground speed and the gang angle, such as the working depth and soil condition.

APPENDICES

APPENDIX A

POWER DISK SPECIFICATIONS

MODEL	F 2806
DIMENSSIONS	
OVERALL LENGTH	2770 mm
OVERALL WIDTH	2200 mm
OVERALL HEIGHT	1450 mm
MASS	875 kg
NUMBER OF DISK BLADE	6
DRIVING SYSTEM	BEVEL GEAR AND ROLLER CHAIN
DISK BLADE DIAMETER	710 mm
DISK CURVATURE	680 mm
DISKING DEPTH	150--300 mm
DISKING WIDTH	1750 mm
GANG ANGLE	25-- 35 DEGREES
WORKING SPEED	3-- 5 km/hr
APPLICABLE TRACTOR	100--130 HP
PTO REVELOTION	540 rpm
HITCHING	THREE POINT HITCH

APPENDIX B

POWER DISK FIELD TEST RECORD SHEETS

The following two sheets summarized the data needed during the field test. The test data sheet was filled out for each test run and the soil condition data was collected for each half day period.

POWER DISK FIELD TEST

DATA SHEET

DATE:_______________1987

FLOPPY DISK NO.:_______

FILENAME:______________

GEAR/G.SPEED:_____/____

WIDTH & DEPTH (cm)

NO.	WORKING WIDTH			WORKING DEPTH	FORROW WIDTH		
	before	after	width		top	middle	bottom
1							
2							
3							
4							
5							
MEAN							

ANGLES (degrees)

GANG ANGLE	REAR DISK ANGLE	3-POINT HITCH		
		top link	lower left	lower right

NOTES: 1.THIS RUN IS UP/DOWN HILL/FLAT;
2.THE CHAIN IS LOOSE/TIGHT;
3.WORKING QUALITY: GOOD/AVERAGE/BAD,
IF ANY, PICTURE NO.:___/___/___/___/____;
4:RESIDUAL CONDITION: NO/SOME/A LOT,
IF ANY, PICTURE NO.:___/___/___/___/___;
5:TOP LINK LENGTH:_______CM;
6:LOWER LINK LENGTH: LEFT______CM, RIGHT_____CM;
7.OTHERS.

POWER DISK FIELD TEST

SOIL CONDITION

DATE:________________1987

WEATHER:________________

NO.	LAYER	CONE INDEX	SOIL MOISTURES			
			CAN NO.	GROSS WEIGHT	DRY WEIGHT	MOISTURE
1	SURFACE					
2						
3						
4						
5						
6	MIDDLE					
7						
8						
9						
10						
MEAN						

NOTES: 1.DISK DIAMETERS:

1.____CM, 2.____CM, 3.____CM, 4.____CM, 5.____CM, 6.____CM

REAR DISK.____CM;

2.OTHERS.

APPENDIX C

SOIL DATA

The soil samples and the soil cone index were collected for each half day period. The soil samples were put in soil cans for the use of determining soil moisture contents. The cone index was recorded in the soil condition data sheet shown in Appendix B. Six to ten data were collected for each test day. The data shown in the following page were the averaged data for each test day.

Table C.1 Soil data

Date	Location	Average moisture %	Average cone index (top layer) N/cm^2
9/1/87	Collins	16.72	26.67
9/2/87	Collins	12.43	38.42
9/3/87	Collins	12.67	33.17
9/3/87	Dairy barn	13.88	70.68
9/9/87	Collins	14.19	33.17
9/21/87	Collins	No data collected	due to sudden rain
10/5/87	Collins	16.54	29.98

Note: Soil at Dairy barn is hard soil.
Its cone index is twice higher than that at Collins.

APPENDIX D

COMPUTER PROGRAM - MOTION

This interactive computer program written in FORTRAN was used to study the dynamics of the power disk. Simulations were done on the Prime 750 computer. The disk trajectories and velocity distributions were simulated by using this program. The flowchart of the program is given on the following page and the list of the program follows.

PROGRAM FLOWCHART

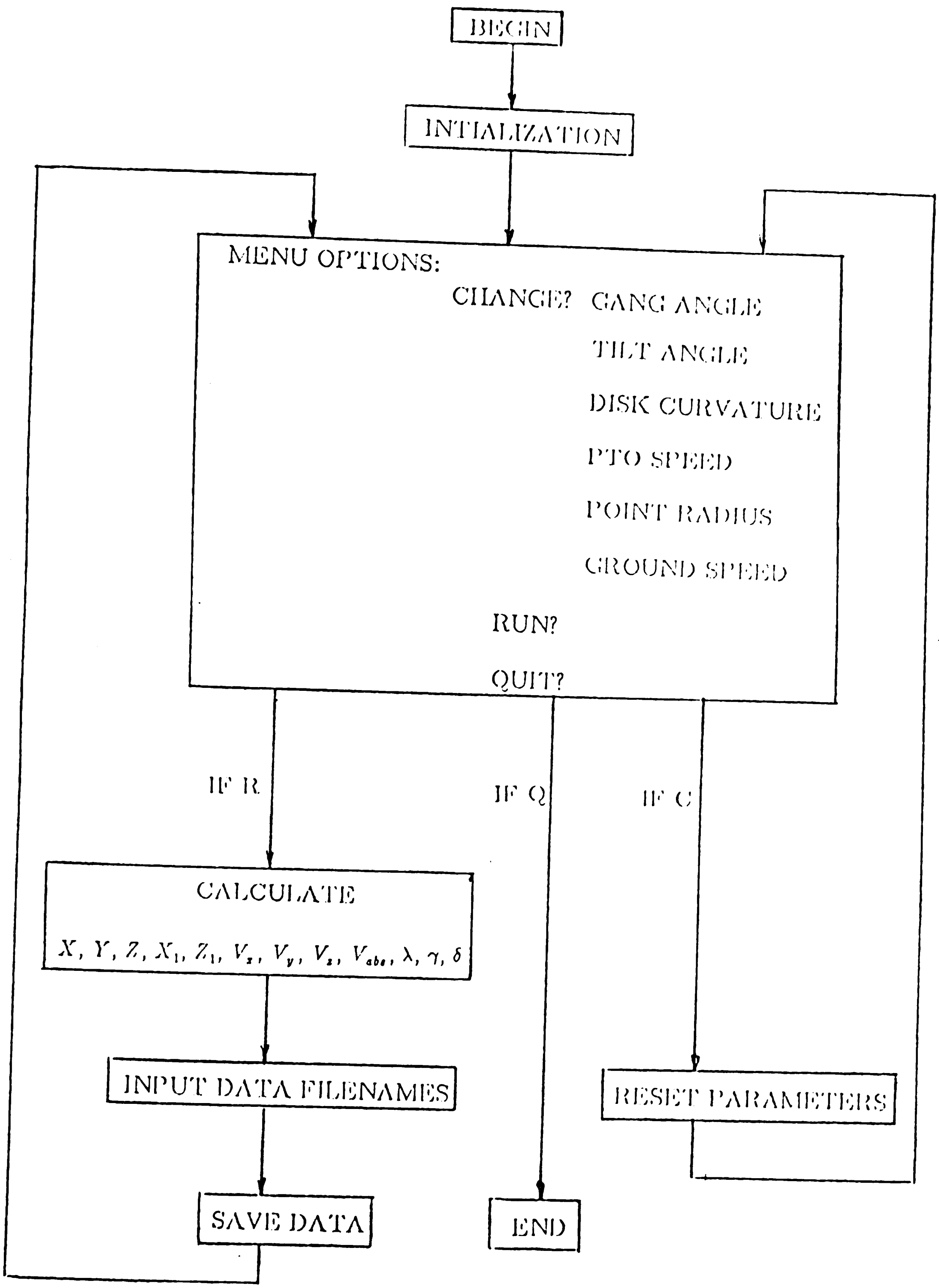

```
C
CCCCCCCCCCCCCCCCCCCCCCCC  PROGRAM DESCRIPTION  CCCCCCCCCCCCCCCCCCCCCCCC
C
C       THIS PROGRAM SIMULATES THE KINEMICS OF POWER DISK
C
CCCCCCCCCCCCCCCCCCCCCCCCCCCCCCCCCCCCCCCCCCCCCCCCCCCCCCCCCCCCCCCCCCCCCC
C
C
CCCCCCCCCCCCCCCCCCCCCCCCCCC  VARIABLE IDENTIFICATION  CCCCCCCCCCCCCCCCCC
C
C ALPHA     DISK GANG ANGLE
C BETA      TILT ANGLE
C P         SIMULATING POINT ON DISK
C R         DISK CURVETURE
C D         DISK DIAMETER
C GSPEED    DISK GROUND SPEED
C NPTO      PTO RPM
C THETA     ANGLE OF DISK ROTATION
C X,Y,Z     COORDINATES OD X,Y,Z AXES
C VX,VY,VZ  VELOCITIES IN X,Y,Z,DIRECTIONS
C VABS      ABSOLUTE VELOCITY
C UPLIMIT   UPPER LIMIT OF SIMULATION
C
CCCCCCCCCCCCCCCCCCCCCCCCCCCCCCCCCCCCCCCCCCCCCCCCCCCCCCCCCCCCCCCCCCCCC
C
C
CCCCCCCCCCCCCCCCCCCCCCCCCCCCC  VARIABLE DIMENSSIONS  CCCCCCCCCCCCCCCCCCC
C
      REAL ALPHA,BETA,P,GSPEED,NPTO,R
      INTEGER UPLIMIT
      CHARACTER*1 OPT
      COMMON ALPHA,BETA,P,NPTO,GSPEED,R,UPLIMIT
C
CCCCCCCCCCCCCCCCCCCCCCCCCCCCCCCCCCCCCCCCCCCCCCCCCCCCCCCCCCCCCCCCCCCCCCCCCC
C
C
CCCCCCCCCCCCCCCCCCCCCCCCCCCC   INITIALIZATION   CCCCCCCCCCCCCCCCCCCCCCCCCC
C
      ALPHA=26.*3.1415926/180
      BETA=0.
      NPTO=540.
      GSPEED=4.*1000./3600.
      P=355./1000.
      R=680./1000.
      UPLIMIT=72
C
CCCCCCCCCCCCCCCCCCCCCCCCCCCCCCCCCCCCCCCCCCCCCCCCCCCCCCCCCCCCCCCCCCCCCC
C
C
10    PRINT*,'  '
      PRINT*,'MENU OPTIONS......'
      PRINT*,'  '
      PRINT*,'     A  CHANGE DISK GANG ANGLE ALPHA'
      PRINT*,'     B  CHANGE DISK TILT ANGLE BETA'
      PRINT*,'     C  CHANGE DISK CURVETURE'
      PRINT*,'     N  CHANGE PTO RPM 540/1000'
```



```
      PRINT*,'     P  CHANGE SIMULATING POINT ON DISK'
      PRINT*,'     R  RUN WITH NEW DATA SETTING'
      PRINT*,'     U  CHANGE UPPER LIMIT OF SIMULATION LOOP'
      PRINT*,'     V  CHANGE GROUND SPEED'
      PRINT*,'     Q  QUIT THE PROGRAM'
      PRINT*,'     '
C
C READ OPTION
C
      READ(1,'(A)')OPT
      CALL UPCASE(OPT)
C
C GOTO SUBROUTINE
C
      IF(OPT.EQ.'A') THEN
        CALL DANGLE
      ELSEIF(OPT.EQ.'B') THEN
        CALL TANGLE
      ELSEIF(OPT.EQ.'C') THEN
        CALL CURVTURE
      ELSEIF(OPT.EQ.'N') THEN
        CALL PTORPM
      ELSEIF(OPT.EQ.'P') THEN
        CALL POINT
      ELSEIF(OPT.EQ.'R') THEN
        CALL RUNNING
      ELSEIF(OPT.EQ.'U') THEN
        CALL UPPLIMIT
      ELSEIF(OPT.EQ.'V')THEN
        CALL SPEED
      ELSEIF(CPT.EQ.'Q') THEN
        GOTO 99
      ELSE
        PRINT*,' CHOOSE YOUR OPTION, PLEASE'
      ENDIF
        GOTO 10
C
C
99    CONTINUE
      STOP
      END
C
C
CCCCCCCCCCCCCCCCCCCCCCCCCCCCCCCCCCCCCCCCCCCCCCCCCCCCCCCCCCCCCCCCCCCCCCCCCC
C
C
CCCCCCCCCCCCCCCCCCCCCCCCC SUBROUTINE DANGLE  CCCCCCCCCCCCCCCCCCCCCCCCCC
C
      SUBROUTINE DANGLE
      REAL ALPHA
      COMMON ALPHA,BETA,P,NPTO,GSPEED,R,UPLIMIT
C
      ALPHA=ALPHA*180./3.1415926
      WRITE(*,'(5X,10H  ALPHA  = ,F13.6)')ALPHA
      PRINT*,'  '
      PRINT*,'ENTER NEEW ALPHA IN DEGREES'
```

```
      READ(*,*)ALPHA
      ALPHA=ALPHA*3.1415926/180.
      RETURN
      END
C
CCCCCCCCCCCCCCCCCCCCCCCCCCCCCCCCCCCCCCCCCCCCCCCCCCCCCCCCCCCCCCCCCCCCCC
C
C
CCCCCCCCCCCCCCCCCCCCCCCCCCCC  SUBROUTINE TANGLE  CCCCCCCCCCCCCCCCCCCCCC
C
      SUBROUTINE TANGLE
      REAL BETA
      COMMON ALPHA,BETA,P,NPTO,GSPEED,R,UPLIMIT
C
      BETA=BETA*180./3.1415926
      PRINT*,'    BETA  = ',BETA
      PRINT*,' '
      PRINT*,'    ENTER NEW BETA IN DEGREES'
      READ(*,*)BETA
      BETA=BETA*3.1415926/180.
      RETURN
      END
C
CCCCCCCCCCCCCCCCCCCCCCCCCCCCCCCCCCCCCCCCCCCCCCCCCCCCCCCCCCCCCCCCCCCCC
C
C
CCCCCCCCCCCCCCCCCCCCCCCCCCC SUBROUTINE PTORPM  CCCCCCCCCCCCCCCCCCCCCCCC
C
      SUBROUTINE PTORPM
      REAL NPTO
      COMMON ALPHA,BETA,P,NPTO,GSPEED,R,UPLIMIT
C
      PRINT*,' PTO RPM  = ',NPTO
      PRINT*,' '
      PRINT*,' ENTER NEW PTO RPM'
      READ(*,*)NPTO
      RETURN
      END
C
CCCCCCCCCCCCCCCCCCCCCCCCCCCCCCCCCCCCCCCCCCCCCCCCCCCCCCCCCCCCCCCCCCC
C
C
CCCCCCCCCCCCCCCCCCCCCCCCCCC SUBROUTINE POINT CCCCCCCCCCCCCCCCCCCCCCCCCC
C
      SUBROUTINE POINT
      REAL P
      COMMON ALPHA,BETA,P,NPTO,GSPEED,R,UPLIMIT
C
      P=P*1000.
      PRINT*,' P VALUE = ',P
      PRINT*,' '
      PRINT*,' ENTER NEW P IN MM'
      READ(*,*)P
      P=P/1000.
      RETURN
      END
```



```
C
CCCCCCCCCCCCCCCCCCCCCCCCCCCCCCCCCCCCCCCCCCCCCCCCCCCCCCCCCCCCCCCCCCCCCC
C
C
CCCCCCCCCCCCCCCCCCCCCCCCC  SUBROUTINE SPEED  CCCCCCCCCCCCCCCCCCCCCCCCCCC
C
      SUBROUTINE SPEED
      REAL GSPEED
      COMMON ALPHA,BETA,P,NPTO,GSPEED,R,UPLIMIT
C
      GSPEED=GSPEED*3600./1000.
      PRINT*,' GROUND SPEED  = ',GSPEED
      PRINT*,' '
      PRINT*,' ENTER NEW GROUND SPEED IN Km/Hr'
      READ(*,*)GSPEED
      GSPEED=GSPEED*1000./3600.
      RETURN
      END
C
CCCCCCCCCCCCCCCCCCCCCCCCCCCCCCCCCCCCCCCCCCCCCCCCCCCCCCCCCCCCCCCCCCCC
C
C
CCCCCCCCCCCCCCCCCCCCCCCC   SUBROUTINE CURVTURE  CCCCCCCCCCCCCCCCCCCCCCCCC
C
      SUBROUTINE CURVTURE
      REAL R
      COMMON ALPHA,BETA,P,NPTO,GSPEED,R,UPLIMIT
C
      R=R*1000.
      PRINT*,' R VALUE = ',R
      PRINT*,' '
      PRINT*,' ENTER NEW R IN MM'
      READ(*,*)R
      R=R/1000.
      RETURN
      END
C
CCCCCCCCCCCCCCCCCCCCCCCCCCCCCCCCCCCCCCCCCCCCCCCCCCCCCCCCCCCCCCCCCCCCCC
C
C
CCCCCCCCCCCCCCCCCCCCCCCCCC    SUBROUTINE UPPLIMIT  CCCCCCCCCCCCCCCCCCCCC
C
      SUBROUTINE UPPLIMIT
      INTEGER UPLIMIT
      COMMON ALPHA,BETA,P,NPTO,GSPEED,R,UPLIMIT
C
      PRINT*,' UPPER LIMIT OF SIMULATION IS ',UPLIMIT
      PRINT*,' '
      PRINT*,' ENTER NEW UPPER LIMIT (INTEGER)'
      READ(*,*)UPLIMIT
      RETURN
      END
C
CCCCCCCCCCCCCCCCCCCCCCCCCCCCCCCCCCCCCCCCCCCCCCCCCCCCCCCCCCCCCCCCCCCCCC
C
C
```

```
CCCCCCCCCCCCCCCCCCCCCCCCCCC   SUBROUTINE RUNNING   CCCCCCCCCCCCCCCCCCCCCCCC
C
      SUBROUTINE RUNNING
      REAL ALPHA,BETA,P,R,D,NPTO,NDISK,NK,J,W
      REAL ALPHA1,BETA1,P1,R1,GSPEED1,X1,Z1
      REAL X,Y,Z,VX,VY,VZ,VABS
      REAL LAMBDA,GAMMA,DELTA,THETA
      INTEGER UPLIMIT
      CHARACTER*20 XYZFILE,XZFILE,VXYZFILE,VPFILE,VABSFILE
      CHARACTER*20 TLFILE,TGFILE,TDFILE
      COMMON ALPHA,BETA,P,NPTO,GSPEED,R,UPLIMIT
C
C
      D=710./1000.
      NDISK=NPTO*10./29.*11./18.
      W=2.*3.1415926*NDISK/60.
      NK=SQRT(R*R-(D/2)**2)-SQRT(R*R-P*P)
C
C
      ALPHA1=ALPHA*180/3.1415926
      BETA1=BETA*180/3.1415926
      R1=R*1000
      P1=P*1000
      GSPEED1=GSPEED*3600/1000
C
C
C COMPUTE X,Y,Z
C
      PRINT*,'ENTER COORDINATE DATA FILENAME—XYZ..(THETA,X,Y,Z)'
        READ(1,'(A)')XYZFILE
        OPEN(8,FILE=XYZFILE)
      PRINT*,'ENTER COORDINATE DATA FILENAME—XZ..(X1,Z1)'
        READ(1,'(A)')XZFILE
        OPEN(9,FILE=XZFILE)
C
C
      WRITE(8,'(/,5X,17H  DISK ANGLE    = ,F13.4)')ALPHA1
      WRITE(8,'(/,5X,17H  TILT ANGLE    = ,F13.4)')BETA1
      WRITE(8,'(/,5X,17H    PTO RPM     = ,F13.4)')NPTO
      WRITE(8,'(/,5X,17H  GROUND SPEED  = ,F13.4)')GSPEED1
      WRITE(8,'(/,5X,17HDISK CURVETURE  = ,F13.4)')R1
      WRITE(8,'(/,5X,17HSIMULATE POINT  = ,F13.4)')P1
C
      WRITE(8,'(/,10X,''THETA'',10X,''X'',10X,''Y'',10X,''Z'',/)')
C
C
      DO 101 I=0,UPLIMIT
        J=I*5*3.1415926/180
        THETA=I*5
        X=NK*COS(BETA)*SIN(ALPHA)+P*COS(J)*SIN(BETA)*SIN(ALPHA)
     +    -P*SIN(J)*COS(ALPHA)+GSPEED*J/W
        Y=NK*COS(BETA)*COS(ALPHA)+P*COS(J)*SIN(BETA)*COS(ALPHA)
     +    +P*SIN(J)*SIN(ALPHA)
        Z=NK*SIN(BETA)-P*COS(J)*COS(BETA)
C
        WRITE(8,'(5X,4F13.6)')THETA,X,Y,Z
```



```
C
C COMPUTE X1,Z1
C
        X1=GSPEED*J/W*COS(ALPHA)-P*SIN(J)
        Z1=NK*SIN(BETA)-P*COS(J)*COS(BETA)
C
        WRITE(9,'(5X,2F13.6)')X1,Z1
101   CONTINUE
      CLOSE(8)
      CLOSE(9)
C
C
      PRINT*,'ENTER VELOCITY FILENAME—VELO...(THETA,VX,VY,VZ)'
        READ(1,'(A)')VXYZFILE
        OPEN(8,FILE=VXYZFILE)
      PRINT*,'ENTER VELOCITY FILENAME—VXYZ..FOR PLOT (VX,VY,VZ)'
        READ(1,'(A)')VPFILE
        OPEN(9,FILE=VPFILE)
      PRINT*,'ENTER ABSOLUTE VELOCITY FILENAME-VABS.(THETA,VABS)'
        READ(1,'(A)')VABSFILE
        OPEN(10,FILE=VABSFILE)
      PRINT*,'ENTER THETA-LAMBDA FILENAME—TL..(THETA,VX)'
        READ(1,'(A)')TLFILE
        OPEN(11,FILE=TLFILE)
      PRINT*,'ENTER THETA-GAMMA FILENAME—TG..(THETA,VY)'
        READ(1,'(A)')TGFILE
        OPEN(12,FILE=TGFILE)
      PRINT*,'ENTER THETA-DELTA FILENAME—TD..(THETA,VZ)'
        READ(1,'(A)')TDFILE
        OPEN(13,FILE=TDFILE)
C
C COMPUTE VX,VY,VZ
C
      DO 111 I=0,UPLIMIT
        J=I*5*3.1415926/180
        THETA=I*5
        VX=GSPEED-P*W*(SIN(BETA)*SIN(ALPHA)*SIN(J)
     +      +COS(ALPHA)*COS(J))
        VY=P*W*(SIN(ALPHA)*COS(J)-SIN(BETA)*COS(ALPHA)*SIN(J))
        VZ=P*W*COS(BETA)*SIN(J)
        WRITE(8,'(5X,4F13.6)')THETA,VX,VY,VZ
        WRITE(9,'(5X,3F13.6)')VX,VY,VZ
C
C COMPUTE VABS
C
        VABS=SQRT(VX**2+VY**2+VZ**2)
        WRITE(10,'(5X,2F13.6)')THETA,VABS
C
C COMPUTE ANGLES
C
        LAMBDA=ACOS(VX/VABS)*180/3.1415926
        GAMMA=ACOS(VY/VABS)*180/3.1415926
        DELTA=ACOS(VZ/VABS)*180/3.1415926
        WRITE(11,'(5X,2F13.6)')THETA,LAMBDA
        WRITE(12,'(5X,2F13.6)')THETA,GAMMA
        WRITE(13,'(5X,2F13.6)')THETA,DELTA
```

```
C
111     CONTINUE
        CLOSE(8)
        CLOSE(9)
        CLOSE(10)
        CLOSE(11)
        CLOSE(12)
        CLOSE(13)
        RETURN
        END
C
CCCCCCCCCCCCCCCCCCCCCCCCCCCCCCCCCCCCCCCCCCCCCCCCCCCCCCCCCCCCCCCCCCCCCCCC
```

APPENDIX E

COMPUTER PROGRAM - PLOT3.VXYZ

An interactive computer program written in FORTRAN was used to plot three dimensional curves and figures on the Prime 750 computer. The plot can be translated and rotated as desired. Figure 5.3.4 was plotted by using this program. The program flowchart and the program list are given as follows:

PROGRAM FLOWCHART

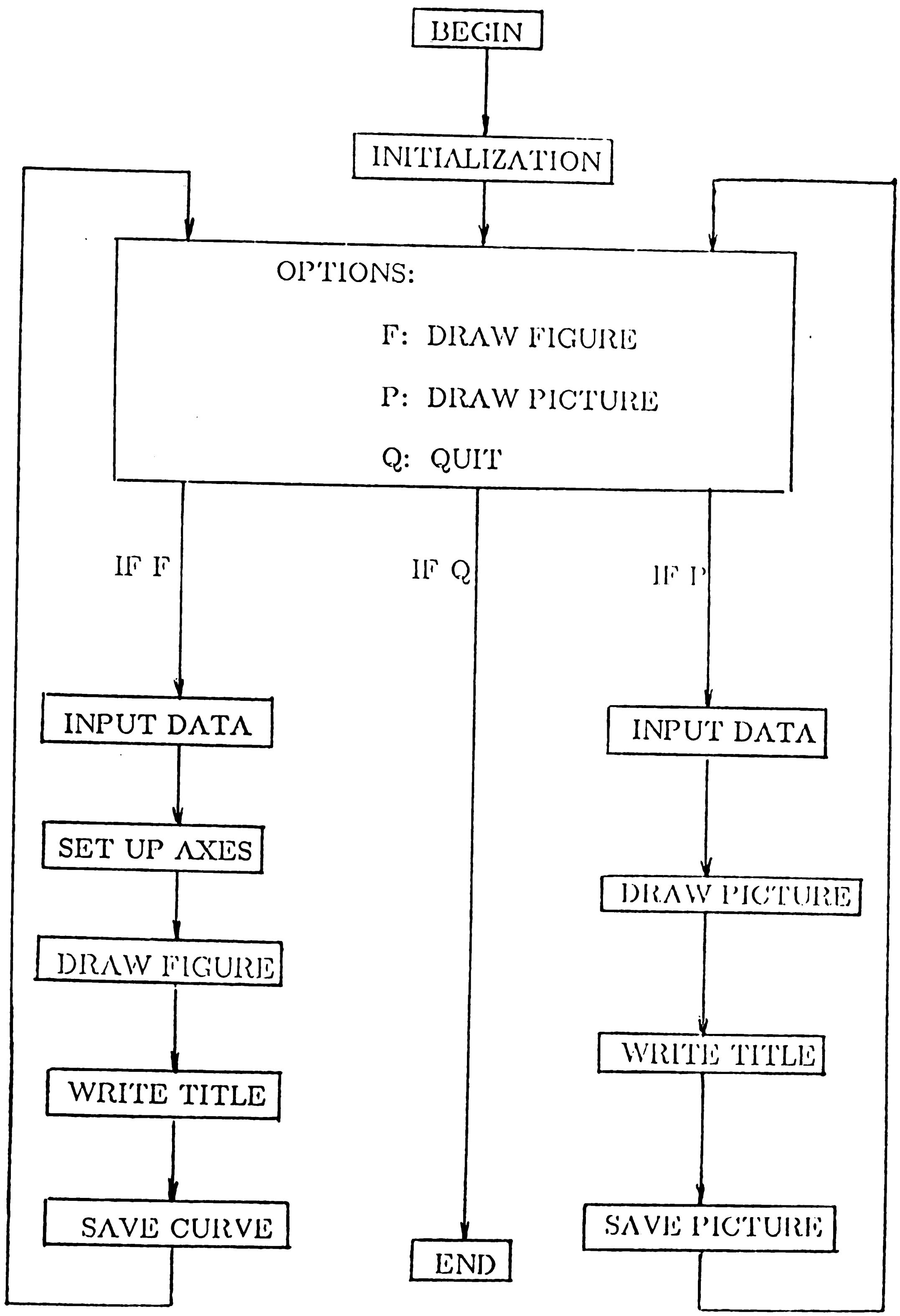

```
C
C THE FOLLOWING PROGRAM MAIN.3D DRAWS A 3-DIMENSIONAL PICTURE
C GIVEN A COORDINATE POINT DATA FILE AND A MOVE/DRAW SEQUENCE
C DATA FILE. IT CAN ALSO TRANSFORMATE THE PICTURE.
C
C
C VARIABLE LIST
C     PT—COODINATE DATE POINTS. PT(N,1)=X, PT(N,2)=Y,PT(N,3)=Z
C     SEQ—MOVE/DRAW SEQUENCE. SEQ(N,1)=0 FOR MOVE,=1 FOR DRAW.
C          SEQ(N,2)=DATE POINT NUMBER
C     NP—TOTAL NUMBER OF MOVES AND DRAWS
C     OPT—MENU OPTION
C
C
      REAL PT(300,3),VX,VY,VZ
      REAL XMIN,XMAX,YMIN,YMAX,ZMIN,ZMAX
      COMMON XMIN,XMAX,YMIN,YMAX,ZMIN,ZMAX,VX,VY,VZ
      INTEGER SEQ(300,2),NP
      CHARACTER*1 OPT
C
C INITIALIZE GRAPHICS
C
      CALL INITT3(960)
      CALL ANMODE
      CALL ZUP
      CALL CARTVP(10.,10.,10.)
      CALL LOOKAT(0.,0.,0.)
      CALL MAGNFY(9.)
      CALL PERSPT(.FALSE.)
C
C MENU
C
10    CONTINUE
        PRINT*,' '
        PRINT*,'MENU OPTIONS'
        PRINT*,'    C—CLOSE GRAPHIC FILE'
        PRINT*,'    D—DRAW PICTURE'
        PRINT*,'    E—ENTER DATA (NO.,X,Y,Z)'
        PRINT*,'    F—PLOT FIGURES'
        PRINT*,'    I—INPUT DATA (X,Y,Z)'
        PRINT*,'    L—SET LOOKAT POINT'
        PRINT*,'    M—SET MAGNIFY FACTOR'
        PRINT*,'    O—OPEN GRAPHIC FILE'
        PRINT*,'    P—PERSPECTIVE DRAW'
        PRINT*,'    Q—QUIT'
        PRINT*,'    R—ROTATION'
        PRINT*,'    T—TRANSLATION'
        PRINT*,'    U—SET X, Y OR Z UP'
        PRINT*,'    V—SET VIEW POINT'
        PRINT*,' '
C
C READ OPTION,CONVERT TO UPPER CASE IF LOWER
C
      READ(1,'(A)')CPT
      CALL UPCASE(OPT)
C
```



```
C GO TO APPROPRIATE SUBROUTINE GIVEN OPTION CHOICE
C
      IF(OPT.EQ.'E')THEN
        CALL DATA(PT,SEQ,NP)
      ELSEIF(CPT.EQ.'D')THEN
        CALL NEWPAG
        CALL DRWFIG(PT,SEQ,NP)
      ELSEIF(OPT.EQ.'O')THEN
        CALL OPNGFL
      ELSEIF(OPT.EQ.'T')THEN
        CALL TRANSLAT(PT,NP)
      ELSEIF(CPT.EQ.'R')THEN
        CALL ROTATION(PT,NP)
      ELSEIF(OPT.EQ.'P')THEN
        CALL PERSPT(.TRUE.)
        CALL NEWPAG
        CALL DRWFIG(PT,SEQ,NP)
        CALL PERSPT(.FALSE.)
      ELSEIF(OPT.EQ.'L')THEN
        CALL LPOINT
      ELSEIF(OPT.EQ.'V')THEN
          CALL VPOINT
      ELSEIF(OPT.EQ.'M')THEN
        CALL MAGNIFY
      ELSEIF(CPT.EQ.'C')THEN
        CALL CLOSTK(IER)
      ELSEIF(OPT.EQ.'F')THEN
        CALL NEWPAG
        CALL PLOT(PT,NP)
      ELSEIF(CPT.EQ.'I')THEN
        CALL IDATA(PT,NP)
      ELSEIF(OPT.EQ.'U')THEN
        CALL XYZUP
      ELSEIF(CPT.EQ.'Q')THEN
        GO TO 99
      ELSE
        PRINT*,'CHOOSE YOUR OPTION PLEASE'
        ENDIF
C
C REPRINT MENE
C
      GO TO 10
C
C QUIT
C
99    CONTINUE
      CALL EXIT
      END
C
CCCCCCCCCCCCCCCCCCCCCCCCCCCCCCCCCCCCCCCCCCCCCCCCCCCCCCCCCCCCCCCCCCC
C
CCCCCCCCCCCCCCCCCCCCCCCCCCCCCCCCCCCCCCCCCCCCCCCCCCCCCCCCCCCCCCCCCCC
C
C
C                SUBROUTIN DATA
C
```

```
C
CCCCCCCCCCCCCCCCCCCCCCCCCCCCCCCCCCCCCCCCCCCCCCCCCCCCCCCCCCCCCCCCCC
C
C SUBROUTINE DATA ASKS THE USER FOR THE NAMES OF THE FILES THAT CONT
C THE COORDINATES OF THE DATE POINTS AND THE MOVE/DRAW SEQUENCE,OPEN
C THEM UP AND READ THEM.
C
C FILOP-FILENAME THAT HAS COODINATES IN IT
C FILSQ-FILENAME THAT HAS MOVE/DRAW SEQUENCE IN IT.
C NP------FINAL VALUE--NUMBER OF DATA POINTS, INTERIAL VALUE--COUNTER
C NC------COUNTER VALUE FOR DATA NUMBER OF MOVES AND DRAWS.
C
      SUBROUTINE DATA( PT,SEQ,NP)
      REAL PT(300,3)
      INTEGER SEQ(300,2),NP,NC
      CHARACTER*32 FILDP,FILSQ
C
C OPEN FILE WITH COODINATE DATA
C
      PRINT*,'ENTER NAME OF DATA POINT FILE'
      READ(1,'(A)')FILDP
      OPEN(12,FILE=FILDP)
C
C READ COODINATES FROM DILE
C
10    CONTINUE
      READ(12,*,END=20)NP,PT(NP,1),PT(NP,2),PT(NP,3)
      GO TO 10
20    CLOSE(12)
C
C
C OPEN FILE WITH DRAW SEQUENCE DATA'
C
C
C
      PRINT*,'ENTER NAME OF SEQUENCE FILE'
      READ(1,'(A)')FILSQ
      OPEN(13,FILE=FILSQ)
C
C READ SEQUENCE
C
      NC=0
30    CONTINUE
        NC=NC+1
        READ(13,*,END=40)SEQ(NC,1),SEQ(NC,2)
      GO TO 30
40    CLOSE(13)
      RETURN
      END
C
CCCCCCCCCCCCCCCCCCCCCCCCCCCCCCCCCCCCCCCCCCCCCCCCCCCCCCCCCCCCCCCCCCCCCCCC
C
CCCCCCCCCCCCCCCCCCCCCCCCCCCCCCCCCCCCCCCCCCCCCCCCCCCCCCCCCCCCCCCCCCCCCCCC
C
C
C                   SUBROUTINE DRAW FIGURE
```



```
C
CCCCCCCCCCCCCCCCCCCCCCCCCCCCCCCCCCCCCCCCCCCCCCCCCCCCCCCCCCCCCCCCCCCCCCCCCCCC
C
C
C SUBROUTINE DRWFIG DRAWS THE PICTURE AND X-Y-Z COORDINATES.
C
C N-------COORDINATE POINT NUMBER
C X,Y,Z---STARTING POINT TO WRITE TITLE
C STRING-VARIABLE CONTAING THE TITLE
C SF------CHARACTOR SCALING FACTOR
C A-------OPTION
C
C
      SUBROUTINE DRWFIG(PT,SEQ,NP)
      REAL PT(300,3)
      INTEGER SEQ(300,2),NP,N
      REAL X,Y,Z,SF
      CHARACTER*70 STRING
      CHARACTER*1 A
C
C
C ENTER GRAPHICS MODE
C
      CALL RECOVR
C
C
C SET PICTURE TITLE
C
C
      PRINT*,'DO YOU WANT TO WRITE TITRE FOR PICTURE Y/N'
      READ(1,'(A)')A
      IF(A.EQ.'N')THEN
C
C SET DEFAULT
C
           STRING='     '
           X=1.
           Y=0.
           Z=20.
           SF=1
           GO TO 20
C
C WRITE THE TITLE FROM KEYBOARD
C
      ELSEIF(A.EQ.'Y')THEN
           PRINT*,'INPUT PICTURE TITLE'
           READ(1,'(A)')STRING
C
           PRINT*,'INPUT STARTING POINT OF TITLE--X,Y,Z'
           READ(*,*)X,Y,Z
C
           PRINT*,'INPUT CHARACTER SCALING FACTCR--SF'
           READ(*,*)SF
      ENDIF
C
C
```

```
C DRAW
C
20      DO 10 I=1,NP
          N=SEQ(I,2)
          IF(SEQ(I,1).EQ.0)THEN
            CALL MOVEA3(PT(N,1),PT(N,2),PT(N,3))
          ELSE
            CALL DRAWA3(PT(N,1),PT(N,2),PT(N,3))
          ENDIF
10    CONTINUE
C
C DRAW COODNATES-X,Y,Z
C
      CALL MOVEA3(0.,0.,0.)
      CALL DRAWA3(12.,0.,0.)
      CALL MOVEA3(13.,0.,0.)
      CALL CHARTK('X',1.)
C
      CALL MOVEA3(0.,0.,0.)
      CALL DRAWA3(0.,12.,0.)
      CALL MOVEA3(0.,13.,0.)
      CALL CHARTK('Y',1.)
C
      CALL MOVEA3(0.,0.,0.)
      CALL DRAWA3(0.,0.,12.)
      CALL MOVEA3(0.,0.,13.)
      CALL CHARTK('Z',1.)
C
C
C WRITE TITLE
C
      CALL MOVEA3(X,Y,Z)
      CALL CHARTK(STRING,SF)
C
C
C
C RETURN TO ALPHANUMBERIC MODE
C
      CALL ANMODE
      RETURN
      END
C
CCCCCCCCCCCCCCCCCCCCCCCCCCCCCCCCCCCCCCCCCCCCCCCCCCCCCCCCCCCCCCCCCCC
C
CCCCCCCCCCCCCCCCCCCCCCCCCCCCCCCCCCCCCCCCCCCCCCCCCCCCCCCCCCCCCCCCCCC
C
C
C                    SUBROUTINE OPEN G FILE
C
C
CCCCCCCCCCCCCCCCCCCCCCCCCCCCCCCCCCCCCCCCCCCCCCCCCCCCCCCCCCCCCCCCCCC
C
C SUBROUTINE OPNGFL ASKS THE USER FOR A FILENAME AND OPENS A GRAPHIC
C
C GFILEN— FILENAME OF GRAPHICS
C IER———INTEGER VARIABLE FOR ERROR CODE
```



```
C
      SUBROUTINE OPNGFL
      CHARACTER*32 GFILEN
C
C
      PRINT*,' '
      PRINT*,'ENTER NAME FOR GRAPHIC FILE'
      READ(1,'(A)')GFILEN
      CALL OPENTK(GFILEN,IER)
      RETURN
      END
C
CCCCCCCCCCCCCCCCCCCCCCCCCCCCCCCCCCCCCCCCCCCCCCCCCCCCCCCCCCCCCCCCCCC
C
CCCCCCCCCCCCCCCCCCCCCCCCCCCCCCCCCCCCCCCCCCCCCCCCCCCCCCCCCCCCCCCCCCC
C
C
C                    SUBROUTINE TRNSLATION
C
CCCCCCCCCCCCCCCCCCCCCCCCCCCCCCCCCCCCCCCCCCCCCCCCCCCCCCCCCCCCCCCCCCC
C
C
C SUBROUTINE TRANSLAT HELP USER TO TRANSLATE HIS ORIGINAL PICTURE TO
C
C
C NP———NUMBER OF DATAS
C T1———IDENTITY 3 BY 3 MATRICES
C PT———ORIGINAL COORDINATE POINTS ADDING ALWAYS PT(NP,4)=1
C HPT———FINAL MATRIX OF DALCULATION
C
C
      SUBROUTINE TRANSLAT(PT,NP)
      REAL T1(4,4)
      REAL PT(300,3),HPT(300,4),PPT(300,4)
      INTEGER NP
C
C SET IDENTITY MATRICES
C
      CALL MIDN(T1,4)
C
C
C SET NEW ORIGIN COORDINATE BASED ON ORIGINAL
C
      PRINT*,'INPUT COORDINATE TO BE NEW ORIGIN——X,Y,Z'
      READ(*,*)T1(4,1),T1(4,2),T1(4,3)
        T1(4,1)=-T1(4,1)
        T1(4,2)=-T1(4,2)
        T1(4,3)=-T1(4,3)
C
      DO 40 I=1,NP
         PPT(I,1)=PT(I,1)
         PPT(I,2)=PT(I,2)
         PPT(I,3)=PT(I,3)
         PPT(I,4)=1.
40    CONTINUE
C
```

```
C
C  TRANSLATING CALCULATIONS
C
      CALL MMLT(HPT,PPT,T1,100,4,4)
C
C
C
      DO 50 I=1,NP
        PT(I,1)=HPT(I,1)
        PT(I,2)=HPT(I,2)
        PT(I,3)=HPT(I,3)
50    CONTINUE
C
C
      RETURN
      END
C
C
CCCCCCCCCCCCCCCCCCCCCCCCCCCCCCCCCCCCCCCCCCCCCCCCCCCCCCCCCCCCCCCCCCCCCC
C
CCCCCCCCCCCCCCCCCCCCCCCCCCCCCCCCCCCCCCCCCCCCCCCCCCCCCCCCCCCCCCCCCCCCCC
C
C
CC                          SUBROUTINE LOOKAT POINT
C
CCCCCCCCCCCCCCCCCCCCCCCCCCCCCCCCCCCCCCCCCCCCCCCCCCCCCCCCCCCCCCCCCCCCCC
C
C
C SUBROUTINE LPOINT SET UP LOOKAT POINT—X,Y,Z
C
C
      SUBROUTINE LPOINT
        REAL X,Y,Z
        PRINT*,' ENTER LOOKAT POINT—X,Y,Z'
        READ(*,*)X,Y,Z
        CALL LOOKAT(X,Y,Z)
      RETURN
      END
C
CCCCCCCCCCCCCCCCCCCCCCCCCCCCCCCCCCCCCCCCCCCCCCCCCCCCCCCCCCCCCCCCCCCCCC
C
CCCCCCCCCCCCCCCCCCCCCCCCCCCCCCCCCCCCCCCCCCCCCCCCCCCCCCCCCCCCCCCCCCCCCC
C
C
C                          SUBROUTINE VIEW POINT
C
CCCCCCCCCCCCCCCCCCCCCCCCCCCCCCCCCCCCCCCCCCCCCCCCCCCCCCCCCCCCCCCCCCCCCC
C
C
C SUBROUTINE VPOINT SET UP VIEWPOINT—VX,VY,VZ
C
C
        SUBROUTINE VPOINT
        REAL VX,VY,VZ
        COMMON XMIN,XMAX,YMIN,YMAX,ZMIN,ZMAX,VX,VY,VZ
        PRINT*,' ENTER VIEW POINT - VX,VY,VZ  (INTEGER)'
```



```
        READ(*,*)VX,VY,VZ
        CALL CARTVP(VX,VY,VZ)
        RETURN
        END
C
CCCCCCCCCCCCCCCCCCCCCCCCCCCCCCCCCCCCCCCCCCCCCCCCCCCCCCCCCCCCCCCCCCCCCC
C
CCCCCCCCCCCCCCCCCCCCCCCCCCCCCCCCCCCCCCCCCCCCCCCCCCCCCCCCCCCCCCCCCCCCCC
C
C
C                          SUBROUTINE MAGNIGY
C
CCCCCCCCCCCCCCCCCCCCCCCCCCCCCCCCCCCCCCCCCCCCCCCCCCCCCCCCCCCCCCCCCCCCCC
C
C
C SUBROUTINE MAGNIGY SET UP MAGNIGY FACTOR——MF
C
C
      SUBROUTINE MAGNIFY
        REAL MF
        PRINT*,' ENTER MAGNIFY FACTOR—MF'
        READ(*,*)MF
        CALL MAGNFY(MF)
      RETURN
      END
C
CCCCCCCCCCCCCCCCCCCCCCCCCCCCCCCCCCCCCCCCCCCCCCCCCCCCCCCCCCCCCCCCCCCCCC
C
CCCCCCCCCCCCCCCCCCCCCCCCCCCCCCCCCCCCCCCCCCCCCCCCCCCCCCCCCCCCCCCCCCCCCC
C
C
C                          SUBROUTINE ROTATION
C
CCCCCCCCCCCCCCCCCCCCCCCCCCCCCCCCCCCCCCCCCCCCCCCCCCCCCCCCCCCCCCCCCCCCCC
C
C
C SUBROUTINE ROTATION HELP THE USER TO ROTATE HIS PICTURE ABOUT X,Y
C
C DEG,RAD——ROTATING ANGLE IN DEGREES AND RADIAN RESPECTIVERY
C NP———NUMBER OF DATA
C RT———ORIGINAL COODINATE DATA POINTS WITH PT(NP,4)=1
C HPT——FINAL MATRIX OF CALCULATION
C T1———IDENTITY MATRIX
C A————ROTATING AXIS OPTION
C
C
      SUBROUTINE ROTATION(PT,NP)
      REAL R1,R2,DEG,RAD
      REAL PT(300,3),HPT(300,4),PPT(300,4)
      INTEGER NP
      REAL T1(4,4)
      CHARACTER*1 A
C
C
C SET 4X4 IDENTITY MATRIX
      CALL MIDN(T1,4)
```

```
C
      PRINT*,'  ROTATE ABOUT WITCH AXIS—X,Y OR Z'
      READ(1,'(A)')A
C
      PRINT*,'  HOW MANY DEGREES IT WILL ROTATE'
      READ(*,*)DEG
        RAD=DEG*3.1415926/180
        R1=COS(RAD)
        R2=SIN(RAD)
C
C
      DO 70 I=1,NP
         PPT(I,1)=PT(I,1)
         PPT(I,2)=PT(I,2)
         PPT(I,3)=PT(I,3)
         PPT(I,4)=1.
70    CONTINUE
C
C
      IF(A.EQ.'Y')THEN
           GO TO 10
      ELSEIF(A.EQ.'Z')THEN
           GO TO 20
      ENDIF
C
C ROTATING ABOUT X AXIS
C
      T1(2,2)=R1
      T1(2,3)=R2
      T1(3,2)=-R2
      T1(3,3)=R1
      GO TO 30
C
C ROTATING ABOUT Y AXIS
C
10    T1(1,1)=R1
      T1(1,3)=-R2
      T1(3,1)=R2
      T1(3,3)=R1
      GO TO 30
C
C ROTATING ABOUT Z AXIS
C
20    T1(1,1)=R1
      T1(1,2)=R2
      T1(2,1)=-R2
      T1(2,2)=R1
C
C ROTATION CALCURATION
C
30    CALL MMLT(HPT,PPT,T1,100,4,4)
C
      DO 60 I=1,NP
         PT(I,1)=HPT(I,1)
         PT(I,2)=HPT(I,2)
         PT(I,3)=HPT(I,3)
```



```
60    CONTINUE
      RETURN
      END
C
CCCCCCCCCCCCCCCCCCCCCCCCCCCCCCCCCCCCCCCCCCCCCCCCCCCCCCCCCCCCCCCCCCCCCCCCC
C
CCCCCCCCCCCCCCCCCCCCCCCCCCCCCCCCCCCCCCCCCCCCCCCCCCCCCCCCCCCCCCCCCCCCCCCCC
C
C
C                     SUBROUTINE X Y Z UP
C
CCCCCCCCCCCCCCCCCCCCCCCCCCCCCCCCCCCCCCCCCCCCCCCCCCCCCCCCCCCCCCCCCCCCCCCCC
C
C
      SUBROUTINE XYZUP
      CHARACTER*1 XYZ
C
      PRINT*,' ENTER X, Y OR Z, THE AXIS WILL BE UP'
      READ(1,'(A)')XYZ
C
      IF(XYZ.EQ.'X')THEN
         CALL XUP
      ELSEIF(XYZ.EQ.'Y')THEN
         CALL YUP
      ELSE
         CALL ZUP
      ENDIF
C
C
      RETURN
      END
C
CCCCCCCCCCCCCCCCCCCCCCCCCCCCCCCCCCCCCCCCCCCCCCCCCCCCCCCCCCCCCCCCCCCCCCCCC
C
C
CCCCCCCCCCCCCCCCCCCCCCCCCCCCCCCCCCCCCCCCCCCCCCCCCCCCCCCCCCCCCCCCCCCCCCCCC
C
C
C
C                          SUBROUTINE INPUT DATA
C
CCCCCCCCCCCCCCCCCCCCCCCCCCCCCCCCCCCCCCCCCCCCCCCCCCCCCCCCCCCCCCCCCCCCCCCCC
C
C THIS SUBROUTINE IS FOR INPUTING COORDINATE DATA TO DO CURVE/SURFACE
C PLOTING
C
      SUBROUTINE IDATA(PT,NP)
      REAL XMIN,XMAX,YMIN,YMAX,ZMIN,ZMAX
      COMMON XMIN,XMAX,YMIN,YMAX,ZMIN,ZMAX,VX,VY,VZ
      REAL PT(300,3)
      INTEGER NP,NC
      CHARACTER*39 FILIP
C
C OPEN FILE
C
      PRINT*,' ENTER NAME OF DATA FILE'
```

```
      READ(1,'(A)')FILIP
      OPEN(12,FILE=FILIP)
C
C READ FILE
C
      NC=0
10    CONTINUE
      NC=NC+1
      READ(12,*,END=20)PT(NC,1),PT(NC,2),PT(NC,3)
      GOTO 10
20    CLOSE(12)
C
      NP=NC-1
C
C SET UP COORDINATES
C
      XMIN=PT(1,1)
      XMAX=PT(1,1)
      YMIN=PT(1,2)
      YMAX=PT(1,2)
      ZMIN=PT(1,3)
      ZMAX=PT(1,3)
C
      DO 25 I=2,NP
         XMIN=AMIN1(XMIN,PT(I,1))
         XMAX=AMAX1(XMAX,PT(I,1))
         YMIN=AMIN1(YMIN,PT(I,2))
         YMAX=AMAX1(YMAX,PT(I,2))
         ZMIN=AMIN1(ZMIN,PT(I,3))
         ZMAX=AMAX1(ZMAX,PT(I,3))
25    CONTINUE
C
C  PRINT ON SCREEN
C
      WRITE(*,'(5X,2F13.2)')XMIN,XMAX
      WRITE(*,'(5X,2F13.2)')YMIN,YMAX
      WRITE(*,'(5X,2F13.2)')ZMIN,ZMAX
C
C SET UP
C
      PRINT*,'ENTER X AXIS LIMITS--XMIN,XMAX'
      READ(*,*)XMIN,XMAX
      PRINT*,'ENTER Y AXIS LIMITS--YMIN,YMAX'
      READ(*,*)YMIN,YMAX
      PRINT*,'ENTER Z AXIS LIMITS--ZMIN,ZMAX'
      READ(*,*)ZMIN,ZMAX
C
      RETURN
      END
C
CCCCCCCCCCCCCCCCCCCCCCCCCCCCCCCCCCCCCCCCCCCCCCCCCCCCCCCCCCCCCCCCCCCCCCCC
C
CCCCCCCCCCCCCCCCCCCCCCCCCCCCCCCCCCCCCCCCCCCCCCCCCCCCCCCCCCCCCCCCCCCCCCCC
C
C
C                  SUBROUTINE PLOTING CURV/SURFACE
```



```
C
CCCCCCCCCCCCCCCCCCCCCCCCCCCCCCCCCCCCCCCCCCCCCCCCCCCCCCCCCCCCCCCCCCCCCCCC
C
C
      SUBROUTINE  PLOT(PT,NP)
      REAL PT(300,3)
      INTEGER NP
      REAL XMIN,XMAX,YMIN,YMAX,ZMIN,ZMAX,X,Y,Z,SF
      REAL XXMAX,YYMAX,ZZMAX,VX,VY,VZ,AB
      COMMON XMIN,XMAX,YMIN,YMAX,ZMIN,ZMAX,VX,VY,VZ
      CHARACTER*70 STRING
      CHARACTER*1 A
C
C ENTER GRAPHIC MODE
C
      CALL RECOVR
C
C SET PLOTING TITLE
C
      PRINT*,'DO YOU WANT TO WRITE A TITLE FOR PLOTING Y/N'
      READ(1,'(A)')A
      IF(A.EQ.'N')THEN
C
C SET DEFAULT
C
         STRING='     '
         X=1.
         Y=1.
         Z=1.
        SF=1.
         GO TO 20
C
C WRITE THE TITLE
C
      ELSEIF(A.EQ.'Y')THEN
         PRINT*,'INPUT PLOTING TITLE'
         READ(1,'(A)')STRING
C
         PRINT*,'INPUT STARTING POINT OF TITLE --X,Y,Z'
         READ(*,*)X,Y,Z
C
         PRINT*,'INPUT CHARACTER SCALING FACTOR --SF'
         READ(*,*)SF
      ENDIF
C
C DRAW THE X,Y,Z
C
20    CONTINUE
       XXMAX=XMAX+1.
       CALL MOVEA3(XMIN,0.,0.)
       CALL DRAWA3(XMAX,0.,0.)
       AB=ABS(VX)
       IF(AB.GT.1.) GOTO 30
       CALL MOVEA3(XXMAX,0.,0.)
       CALL CHARTK('X',1.)
C
```

```
30        YYMAX=YMAX+1.
          CALL MOVEA3(0.,YMIN,0.)
          CALL DRAWA3(0.,YMAX,0.)
          AB=ABS(VY)
          IF(AB.GT.1.) GOTO 40
          CALL MOVEA3(0.,YYMAX,0.)
          CALL CHARTK('Y',1.)
C
40        ZZMAX=ZMAX+1.
          CALL MOVEA3(0.,0.,ZMIN)
          CALL DRAWA3(0.,0.,ZMAX)
          AB=ABS(VZ)
          IF(AB.GT.1.) GOTO 50
          CALL MOVEA3(0.,0.,ZZMAX)
          CALL CHARTK('Z',1.)
C
C
C DRAW PLOT
C
C
50        CALL MOVEA3(PT(1,1),PT(1,2),PT(1,3))
          DO 91 I=2,NP
             CALL DRAWA3(PT(I,1),PT(I,2),PT(I,3))
91        CONTINUE
C
C WRITE THE PLOT TITLE
C
          CALL MOVEA3(X,Y,Z)
          CALL CHARTK(STRING,SF)
C
C
          CALL ANMODE
          RETURN
          END
cccccccccccccccccccccccccccccccccccccccccccccccccccccccccccccccccccccccc
```

APPENDIX F

CALIBRATION RAW DATA AND COMPUTATIONS

The calibration of channel 13 and channel 14 was carried out successfully in August 24, 1987. The raw data, their computation results and regression outputs are given in the following page. The computations were based on the discussions in Chapter 6. The regressions were carried out by using LOTUS software.

Table F.1 Calibration raw data and computations

RAW DATA				COMPUTATIONS				
CH 13 reading	CH 14 reading	P_1 lbs	P_2 lbs	H_1 lbs	V_1 lbs	H lbs	V lbs	M lbs-m
55	-482	330	385	329.548	17.271	329.548	402.271	67.928
134	-702	720	380	719.013	37.682	719.013	417.682	95.007
187	-857	1000	377	998.630	52.336	998.630	429.336	114.517
237	-1015	1280	375	1278.246	66.990	1278.246	441.990	134.143
276	-1135	1520	375	1517.917	79.551	1517.917	454.551	151.163
191	-937	1150	380	1148.424	60.186	1148.424	440.186	125.502
141	-791	890	385	888.780	46.579	888.780	431.579	107.642
109	-678	690	387	689.054	36.112	689.054	423.112	93.690
67	-585	500	390	499.315	26.168	499.315	416.168	80.562
35	-471	330	375	329.548	17.271	329.548	392.271	66.771
72	-586	440	405	439.397	23.028	439.397	428.028	78.042
141	-728	710	405	709.027	37.159	709.027	442.159	97.190
212	-927	1050	401	1048.561	54.953	1048.561	455.953	120.839
266	-1040	1260	400	1258.273	65.943	1258.273	465.943	135.616
339	-1239	1660	393	1657.725	86.878	1657.725	479.878	163.173
240	-1042	1310	398	1308.205	68.560	1308.205	466.560	138.930
168	-880	1010	401	1008.616	52.859	1008.616	453.859	118.002
123	-729	730	405	729.000	38.205	729.000	443.205	98.608
91	-624	550	405	549.246	28.785	549.246	433.785	85.843
31	-498	350	406	349.520	18.318	349.520	424.318	71.775
107	-667	530	457	529.274	27.738	529.734	484.738	90.438
171	-846	850	454	848.835	44.486	848.835	498.486	112.785
207	-949	1040	450	1038.579	54.429	1038.575	504.429	125.797
268	-1100	1320	447	1318.191	69.083	1318.191	516.083	145.306
329	-1254	1610	443	1607.794	84.261	1607.794	527.261	165.410
225	-1025	1220	445	1218.328	63.850	1218.328	508.850	137.983
187	-857	910	448	908.753	47.626	908.753	495.626	116.346
122	-700	630	450	629.137	32.972	629.137	482.972	96.720
88	-590	440	450	439.397	23.028	439.397	473.028	83.246
35	-467	230	453	229.685	12.037	229.685	465.037	68.700

CH 13 Regression Output:		
Constant	-150.883	
Std Err of Y Est	12.63132	
R Squared	0.980038	
No. of Observations	30	
Degrees of Freedom	27	
X Coefficient(s)	0.195621	0.310272
Std Err of Coef.	0.006862	0.079461

CH 14 Regression output:	
Constant	62.44379
Std Err of Y Est	11.07110
R Squared	0.997744
No. of Observations	30
Degrees of Freedom	28
X Coefficient(s)	-7.99175
Std Err of Coef.	0.071801

APPENDIX G

SIDE FORCE DATA

The side force was measured throughout the field tests. Each type of test was explained in Chapter 4. The gang angle was set before each field test. The ground speed and the side forces were averaged from 600 data points for each test. The minimum and the maximum side forces were the extreme points within the 600 data points. The tillage depth was averaged based on three measurements for each test.

Most of the tests were free depth control, that is, the implement cut as deep as possible. In the depth control tests, the depth was controlled by using the depth wheel or the tractor hydraulic system.

The tests using the depth wheel control and two regular tests for the 26 and 28 degree gang angles at 2 km/hr used a different rear furrow wheel setting. The rear wheel shaft was 32 degrees from the horizontal plane and the scraper was at the vertical position, while in the other tests the shaft was 50 degrees.

Two tests were conducted on the hard soil with the cone indix was two times of that in the other soil condition to investigate the soil type effect.

The rest of two kinds of tests were explained in chapter 4.

Table G.1 Side force data

Type	Gang gangle (degree)	Ground speed (km/hr)	Depth (cm)	Side force (N) average	minimum	maximum
Regular	26	1.93	22.90	4414.62	3199.63	5586.69
		3.78	29.97	5107.53	3872.39	6499.35
		5.94	28.13	5911.06	4718.29	7398.75
		7.00	23.97	6642.06	3941.83	8807.46
	28	1.94	26.77	3779.06	2951.36	4956.76
		3.53	23.80	5324.65	3740.04	7269.79
		5.52	28.20	6924.14	4573.45	8532.72
		6.63	28.40	6370.65	5094.44	8624.53
	30	1.83	28.60	4598.22	2135.83	6909.93
		3.90	26.10	5924.63	4300.88	7807.15
		5.71	28.30	6396.28	4830.73	8644.13
		6.65	28.43	6601.29	5169.16	8020.65
	32	1.78	28.70	4668.67	2952.13	5792.26
		3.58	28.80	5053.51	1349.39	6853.42
		5.75	27.23	6253.60	4530.36	8384.36
	34	1.98	30.10	3554.85	2437.22	5198.80
		3.80	29.87	4900.87	3499.11	6529.03
Depth wheel control	28	4.17	11.23	2096.25	854.19	3437.61
		3.82	17.77	3682.80	2589.50	4823.89
	32	4.15	11.27	2249.97	1297.53	3300.12
		3.90	17.67	3547.65	2052.36	4571.78
Hydraulic depth control	28	4.02	14.77	3564.07	2053.99	5011.92
	32	4.12	17.27	3630.45	1889.24	5702.40
Hard soil	28	1.58	13.80	3537.10	966.82	5685.51
	32	1.64	16.03	3519.47	558.68	7620.69
Unpowered	28	1.75	23.47	4192.02	3062.13	5189.46
		5.72	20.10	5265.31	2952.84	7301.46
	32	2.26	24.73	4737.71	3434.35	6997.05
		5.74	26.10	6095.35	4005.17	7618.93
Short top link	26	1.60	21.95	3050.91	1413.10	4401.23
		3.71	21.47	4897.34	1756.14	8212.83
		5.84	21.63	4819.71	2210.22	7411.77
	28	3.86	24.03	4856.54	2084.95	8472.06
	30	1.90	22.70	3553.56	2500.22	5228.59
		1.63	20.30	3724.62	1857.94	6401.53
	32	1.70	28.67	5312.71	4029.35	6992.21

APPENDIX H

REAR VERTICAL FORCE DATA

The rear furrow wheel vertical force was measured in the same tests where the side force was measured. The data explainations are the same as the side force in Appendix G.

Table H.1 Rear vertical force data

Type	Gang angle (degree)	Ground speed (km/hr)	Depth (cm)	Vertical force (N)		
				average	minimum	maximum
Regular	26	1.93	22.90	5039.83	3812.67	6512.33
		3.78	29.97	2895.57	1996.83	3704.56
		5.94	28.13	3491.86	2130.84	6388.87
		7.00	23.97	3712.41	2399.57	5255.00
	28	1.94	26.77	4565.41	3161.97	6312.15
		3.53	23.80	3144.46	1901.94	7542.08
		5.52	28.20	3791.36	2624.86	5424.60
		6.63	28.40	3933.25	2945.50	4965.09
	30	1.83	28.60	2902.70	1541.98	4307.21
		3.90	26.10	3477.41	2188.70	4591.31
		5.71	28.30	3586.65	2687.69	4915.30
		6.65	28.43	3710.40	2819.63	5196.86
	32	1.78	28.70	2636.67	1093.30	3847.00
		3.58	28.80	2742.53	1321.56	4160.26
		5.75	27.23	3557.25	2177.03	4997.43
	34	1.98	30.10	2135.72	1287.80	4905.74
		3.80	29.87	2981.76	1785.73	5957.16
Depth wheel control	28	4.17	11.23	3123.92	1938.73	7308.63
		3.82	17.77	4630.99	3380.02	5847.73
	32	4.15	11.27	3230.12	1750.64	4645.27
		3.90	17.67	4225.09	2941.82	5409.52
Hydraulic depth control	28	4.02	14.77	2577.40	1792.59	4364.35
	32	4.12	17.27	2622.88	516.18	6093.31
Hard soil	28	1.58	13.80	2325.83	853.58	3446.96
	32	1.64	16.03	2412.02	959.96	4582.26
Unpowered	28	1.75	23.47	2779.73	2034.95	3945.46
		5.72	20.10	3017.41	1456.53	4179.80
	32	2.26	24.73	3099.09	2308.00	7307.17
		5.74	26.10	3775.91	2754.36	4954.99
Short top link	26	1.60	21.95	2439.67	1167.26	5714.74
		3.71	21.47	3090.50	1685.99	5103.54
		5.84	21.63	2873.84	1876.50	4211.20
	28	3.86	24.03	3120.54	1875.17	7672.27
	30	1.90	22.70	2344.15	1316.08	3206.88
		1.63	20.30	2874.79	1538.83	4287.46
	32	1.70	28.67	3079.87	2111.30	4912.06

BIBLIOGRAPHY

BIBLIOGRPHY

Abernathy, G. H. 1976. Draft Requirements of a Self-powered Disk. ASAE Paper No. 76-1021. ASAE, St. Joseph, MI 49085.

Aiba, K. 1987. The Performance Evaluation of The Power Disk. Unpulished M.S. Thesis. Michigan State University.

Clyde, A. W. 1937. Load Studies on Tillage Tools. Agricultural Engineering 18(3):117-121.

Culpin, C. 1981. Farm Machinery. Tenth Edition. Granada Publishing Ltd.

Doeblin, E. O. 1983. Measurement Systems: Application and Design. Third Edition. McGraw-Hill Book company.

Draper, N. R. and H. Smith. 1981. Applied Regression Analysis. Second Edition. John Wiley & Sons Inc.

Dwyer, M. J. 1985. Power Requirements For Field Machines. Agricultural Engineer 40(2):50-59.

Finnery, J. B. 1982. The Role of Discs in Primary Cultivation. Agricultural Engineer 37(1):15-19.

Gill, W. R. and J. G. Hendrick. 1976. The Irregularity of Soil Disturbance Depth by Circular and Rotating Tillage Tools. Transactions of ASAE 19(2):230-233.

Gill, W. R., C. A. Reaves and A. C. Bailey. 1980. The Effect of Geometric Parameters on Disk Forces. Transaction of ASAE 23(2):266-269.

Gill, W. R., C. A. Reaves and A. C. Bailey. 1980. The Influence of Velocity and Disk Angle on the Kinematic Parameter λ of Disks. Transactions of ASAE 23(6):1344-1348.

Gill, W. R., C. A. Reaves and A. C. Bailey. 1981. The Influence of Harrow Disk Curvature on Forces. Transaction of ASAE 24(3):579-583.

Gill, W. R., A. C. Bailey and C. A. Reaves. 1982. Harrow Disk Curvature - Influence on Soil Penetration. Transactions of ASAE 25(5):1173-1180.

Gordon, E. D. 1941. Physical Reactions of Soil on Plow Disks. Agricultural Engineering 22(6):205-208.

Harrison, H. P. 1975. Instrumentation of Multicomponent Sensor. Transactions of ASAE 18(4):765-769.

Harrison, H. P. and T. Thivavarnvongs. 1976. Soil Reacting Forces From Lab Measurements. Canadian Agricultural Engineering 18(1):49-53.

Harrison, H. P. 1977. Soil Reacting Forces for Disks From Field Measurements. Transactions of ASAE 20(5):836-838.

Hoki. M., T. H. Burkhardt, R. H. Wilkinson and T. Tanoue. 1985. Study of Power Disk Driven by Tractor PTO. ASAE Paper No. 85-1018. ASAE, St. Joseph, MI 49085.

Kepner, R. A., R. Bainer and E. L. Barger. 1978. Principles of Farm Machinery. Third Edition. AVI Publishing Company Inc., Westport, Connecticut.

Klenin. N. I., I. F. Popov and V. A. Sakun. 1985. Agricultural Machines, Theory of Operation, Computation of Controlling Parameters and Condition of Operation. Amerind Publishing Co. PVT Ltd.

Kushwaha, R. L., A. S. Vaishnav and G. C. Zoerb. 1986. Performance of Powered-disc Coulters Under No-till Crop Residue in the Soil Bin. Canadian Agricultural Engineering 28(2):85-90.

Nartov, P. S. 1966. Method of Calculation of Basic Paramenters and Kinematics of Disk Working Tools of Forest Soil Working Implements. NAL Translation No. 25690.

Nartov, P. S. 1967. Basics of Parameters of Working Tools of Forest Disk Implements. NAL Translation No. 25681.

Nartov, P. S. 1967. Study of Working Tools of Disk Plows. NAL Translation No. 23846.

Nartov, P. S. 1985. Disk Soil-working Implements. Voronezh University Press, Voronezh.

Neter, J., W. Wasserman and M. H. Kutner. 1985. Applied Linear Statistical Models. Second Edition. Richard D. Irwin Inc.

Power Disk Manual - F 2806 (in Japanese). 1986. Toyosha Company Ltd, Japan.

Reaves, C. A., W. R. Gill and A. C. Bailey. 1981. Influence of Width and Depth of Cut on Disk Forces. Transactions of ASAE 24(3):572-578.

Rogers, D. F. and J. A. Adams. 1976. Mathematical Elements for Computer Graphics. McGraw-Hill Book Company.

Soehne, W. H. 1963. Aspects of Tillage. Canadian Agricultural Engineering 5(1):2-3,8.

Taylor, P. A. 1967. Field Measurement of Forces and Moments on Wheatland Plow Disks. Transactions of ASAE 10(6):762-768,770.

Tembo, S., T. H. Burkhardt, R. H. Wilkinson and M. Hoki. 1986. Performance of the PTO Power Disk Tiller. ASAE Paper No. 86-1010. ASAE, St. Joseph, MI 49085.

Tembo, S. 1986. Performance Evaluation of the Power Disk - a PTO Driven Disk Tiller. Unpublished M. S. Thesis. Michigan State University.

Traulsen, H. 1982. The Role of the Mouldboard Plough. Agricultural Engineer 37(1):12-14.

Young, P. E. 1976. A Machine to Increase Productivity of a Tillage Operation. Transactions of ASAE 19(6):1055-1061.

Zhou, Yiming. 1980. The Tractor Mechanics (in Chinese). Beijing Agricultural Engineering University Press, Beijing, People's Republic of China.